IOSUD – "DUNĂREA DE JOS" UNIVERSITY OF GALAȚI

Doctoral School for Mechanical and Industrial Engineering

PhD THESIS

Summary

STUDIES AND RESEARCH REGARDING THE GENERATION AND TRANSMISSION OF THE ENERGY IN THE COASTAL AREAS OF THE BLACK SEA

PhD Student,

Eng. Alexandra-Ionelia DIACONIȚĂ (MANOLACHE)

PhD Supervisor,

Prof. Gabriel ANDREI

Series I 6: Mechanical Engineering No. 74

GALAȚI

2023

IOSUD – "DUNĂREA DE JOS" UNIVERSITY OF GALAȚI

Doctoral School for Mechanical and Industrial Engineering

PhD THESIS

Summary

STUDIES AND RESEARCH REGARDING THE GENERATION AND TRANSMISSION OF THE ENERGY IN THE COASTAL AREAS OF THE BLACK SEA

PhD Student

Eng. Diaconiță Alexandra-Ionelia (Manolache)

Chair	Prof. Elena SCUTELNICU
	"Dunărea de Jos" University of Galați
PhD Supervisor,	Prof. Eng. Gabriel ANDREI
	"Dunărea de Jos" University of Galați
	Prof. Eng. Anton HADĂR
	National University of Science and Technology "Politehnica", Bucharest
Committee:	Prof. Dan Mihai CONSTANTINESCU
	National University of Science and Technology "Politehnica", Bucharest
	Prof. Liliana Celia RUSU
	"Dunărea de Jos" University of Galați

Series I 6: Mechanical Engineering No. 74

GALAȚI

2023

The series of doctoral theses defended publicly in UDJG starting on October 1, 2013, are:

Field ENGINEERING SCIENCES

Series I 1**:** **Biotechnologies**
Series I 2**:** **Computers and information**
Series I 3: **Electrical engineering**
Series I 4**:** **Industrial engineering**
Series I 5: **Material engineering**
Series I 6**:** **Mechanical engineering**
Series I 7**:** **Food Engineering**
Series I 8: **Systems Engineering**
Series I 9**:** **Engineering and management in agriculture and rural development**

Field ECONOMICS

Series E 1: **Economy**
Series E 2: **Management**
Series E 3: **Marketing**
Series SSEF: **Science of Sport and Physical Education**
Series SJ: **Law**

Field HUMANITIES

Series U 1: **Philology-English**
Series U 2: **Philology-Romanian**
Series U 3**:** **History**
Series U 4: **Philology-French**

Field MATHEMATICS AND NATURE SCIENCES

Series C: **Chemistry**

Field BIOMEDICAL SCIENCES

Series M: **Medicine**
Series F: **Pharmacy**

Acknowledgment

On the occasion of completing this remarkable stage in my academic journey, I wish to express my profound and special gratitude to those who have been by my side in the realization of my doctoral thesis. This journey would not have been possible without the support and remarkable contribution of exceptional individuals.

First and foremost, I would like to extend my sincerest thanks to my doctoral advisor, Prof. Gabriel Andrei, who not only guided me in my research but also inspired me in a unique way. With his wisdom and dedication to our field, he has been a constant source of motivation and support throughout this scientific journey. With a particular passion for detail and a keen eye for the scientific method, Prof. Gabriel Andrei taught me that research is not only about discovering answers but also about formulating the right questions. This was a valuable and crucial lesson that I learned from him. He always encouraged me to delve deeply into my research topics, not to settle for superficial answers, and constantly seek new and innovative ways to address issues.

With special gratitude, I want to direct my thoughts to Academician Prof. Eugen Rusu, an internationally renowned figure and the initiator of the research topic I worked on in this academic and scientific journey. Academician Prof. Eugen Rusu has been more than a mentor to me; he has been a careful and demanding supervisor who opened the door to remarkable opportunities. Thanks to his support and trust, I had the privilege of becoming a member of the DREAM project (Dynamics of Resources and Technological Advances in Extracting Renewable Energy from the Marine Environment), a project supported by the Executive Agency for Higher Education, Research, Development, and Innovation Funding in Romania - UEFISCDI, with grant number PN-III-P4-ID-PCE-2020-0008.

I also want to highlight the exceptional contribution of the guidance committee, composed of distinguished professors and researchers, such as Prof. habil. Liliana Celia Rusu, Prof. habil. Mihaela Buciumeanu, and Assoc. Prof. Florin Onea. Their expertise and advice were key to successfully completing the research in the doctoral thesis.

Thanks to the members of the public defense committee for analyzing and evaluating the doctoral thesis.

I cannot fail to mention the unique support of my family, who provided unconditional support and stood by me in all stages of this academic journey.

This thesis represents a significant achievement in my engineering career, and I hope it will make valuable contributions to the research in the field of renewable energy. With gratitude and enthusiasm, I thank everyone who has been part of this journey and offered their unwavering support.

Galați,
November 2023

Table of content

Introduction

About 71% of the Earth's surface is covered by seas and oceans. For this reason, the human activities carried out in the marine environment began to be more and more diversified. Nowadays, transportation, tourism, research, fishing, and resource exploitation are all carried out in the seas and oceans. Regardless of a nation's level of development, all these activities offer financial benefits.

As energy demand increases, conventional sources are no longer sufficient. Due to their availability and ability to either regenerate on their own over time or be deemed "inexhaustible," renewable energy sources have received more attention in recent decades. In addition, most conventional energy production methods face a major problem related to the need to reduce CO_2 emissions. Since the beginning of the industrial revolution, when manual labor was replaced by mechanized equipment, emissions of CO_2 have been continuously increasing. The main factor leading to the increase of these emissions is represented by human activity, which includes the burning of fossil fuels, especially for developing countries, which tend to prioritize economic growth over environmental issues and encourage thus conventional energy consumption. Consequently, the exploitation of energy sources has become a very important aspect.

One of the most popular energy sources, particularly on land, is wind energy. Offshore wind farm projects have however arisen in recent years, but due to their expensive installation and maintenance requirements as well as logistical challenges, they have not been widely used. Due to the shrinking amount of land accessible, interest in offshore wind farms has grown significantly over time. This method has numerous benefits, such as less of an adverse effect on the environment, the potential to build more turbines, the absence of constraints on the land's relief, and the application of more sophisticated technologies. Even if offshore wind farms can generate more electricity, onshore wind farms continue to be more profitable from an economic standpoint. Technological advancements like longer blades, bigger turbines, and greater hub heights, as well as being further offshore, which can offer a higher capacity factor, all have an impact on these variations. However, because offshore wind farms must be built and maintained in challenging marine settings and require longer delivery schedules, their costs are far greater. These projects require intricate planning and development, in addition to higher construction and grid connection expenses. The PhD thesis "Studies and research regarding the generation and transmission of energy in the coastal areas of the Black Sea" aims to conduct a thorough analysis of the energy resources in the Black Sea coastal area of Romania, focusing primarily on wind resources. In order to evaluate the feasibility of constructing offshore wind farms in this location, this PhD thesis aims to provide a comprehensive understanding of the energy potential of the region.

The objectives are numerous and interconnected in order to achieve this goal. First, we intend to examine in depth the Black Sea wind resources, with a focus on wind and temperature data, as well as the forecasting capacity of these resources, taking into account the cyclones that occurred during the analyzed period. Simultaneously, the energy potential of Romania's exclusive Black Sea area is assessed by analyzing 9 important sites divided into categories based on distance from the shore. In order to determine whether it would be feasible to build offshore wind farms in this region, a significant part of the research compares the resources of the Black Sea with those of twelve other areas with energy interest. In order to expand the range of technological possibilities for harvesting wind energy for renewable purposes, alternatives to traditional wind turbines are also examined through the simulation of an airborne wind turbine. The technical aspects of wind farm infrastructure are also examined, which includes an analysis of the foundations and towers of offshore wind turbines through the

use of a Spar foundation simulation. To be able to provide an economic perspective on the viability of wind projects in the Black Sea region, a cost analysis is finally performed for the simulation of a wind farm with 100 wind turbines. These interrelated goals work together to create an in-depth comprehension of the Black Sea's energy potential, which serves as the basis for decisions made in this area regarding renewable energy.

The structure of the PhD thesis

Chapter 1 provides a succinct analysis of the current state of research in the field of renewable energy and associated technologies. It explores the progress made in the development, enhancement, and optimization of these technologies. Additionally, it examines studies that contribute to the foundation of the themes addressed in this PhD thesis.

Chapter 2 focuses on the analysis of wind resources in the Black Sea. By identifying and evaluating the cyclones recorded during the period of interest, this chapter aims to advance the understanding of the forecasting capabilities of the ERA5 database.

Chapter 3 conducts a comprehensive evaluation of the energy resources in Romania's exclusive zone in the Black Sea. The analysis focuses on 9 key locations, grouped by their distance from the shore, to gain a detailed perspective of the energy potential in this region and to identify variations and similarities among the analyzed locations.

Chapter 4 brings forth a rigorous comparison of the energy resources in the Black Sea with 12 other regions of renewable energy interest, either under development or already exploited. The purpose of this analysis is to assess the feasibility of offshore wind farm development in the Black Sea in comparison to other regions, contributing to strategic decision-making in the field of renewable energy.

Chapter 5 explores alternative technologies for renewable energy extraction, with a focus on the simulation of an airborne wind turbine with the equivalent power of a conventional 5 MW turbine. This research diversifies the technological options available for efficient wind energy extraction in the Black Sea.

Chapter 6 analyzes the key components of offshore wind farm infrastructure, with an emphasis on the wind turbine towers. This investigation provides essential technical insights and contributes to the development of efficient solutions for constructing and maintaining offshore wind farms in marine environments.

Chapter 7 presents the simulation of a Spar-type wind turbine foundation using the ANSYS AQWA program, offering a detailed analysis of this critical component of offshore wind farm infrastructure.

Chapter 8 conducts a cost analysis for simulating a 500 MW wind farm, providing an economic perspective on the viability of wind projects in the Black Sea.

Chapter 9 summarizes the conclusions drawn in the thesis, highlights the personal contributions made, and suggests directions for future research. Additionally, it presents the scientific papers published during the doctoral studies to underscore the contribution to the field of renewable energy.

1 State of the art

1.1 Transition from onshore to offshore wind energy

The rapid increase in the use of wind energy in recent years has been driven by its recognition as a key component of sustainable development. Wind energy is a renewable energy source that significantly distinguishes itself from traditional fossil fuels, such as gas and coal. The emergence of the first offshore wind farms marked the beginning of a new era in wind energy generation. Although the initial offshore installations were relatively small and experimental, they paved the way for exploring the vast potential of marine winds. Over time, accumulated technology and experience have enabled the development of large-scale offshore wind farms, significantly contributing to global electricity production from renewable sources.

The initial steps in offshore wind energy utilization were cautious and modest, with the installation of a 220 kW turbine in Swedish waters in 1990. This paved the way for a series of experimental projects between 1991 and 1998, testing different turbine models and offshore foundations. Further development brought multi-megawatt wind turbines and the construction of the first commercial wind farms, such as those at Blyth, Middelgrunden, and Yttre Stengrund. Subsequently, projects like Horns Rev and Nysted in Denmark solidified the position of offshore wind energy in the global energy landscape.

One of the main factors supporting the transition from onshore to offshore wind turbines was the negative impact on the environment and visual quality caused by onshore wind farms. Onshore wind turbines occupied vast land spaces and rose in rural or even urban landscapes, often generating controversy and opposition from local communities. Furthermore, the vibrations and noises produced by these turbines could affect the quality of life for nearby residents. Research on the impact of wind energy on the environment and residential communities has produced a series of significant perspectives and findings. Although each study had a distinct approach, there are notable common points in the conducted research.

Several studies focused on assessing the visual and auditory impact of wind farms on residents. Works like those referenced in [1] and [2] investigated how wind turbines affect the quality of life for residents and the level of noise generated by them. These studies highlighted the importance of considering public perception and noise levels in the design and placement of wind farms. Simultaneously, research related to landscape impact assessment, such as that by Jin Guan [3], explored how the construction and operations of wind farms could modify the visual appearance of the areas where they are located. These studies emphasized the need for careful evaluation of visual impact and the development of architectural and landscape integration strategies. However, for a deeper understanding of the visual impact of wind turbines, it is essential to consider the temporal factor of visibility, as suggested by the research of Ian D. Bishop [4]. Bishop's work adds a significant temporal perspective to the assessment of the visual impact of wind turbines.

While research on the visual impact of wind turbines advances and develops, it is important to address other aspects related to wind energy. One of these aspects is the growing concern about the health effects associated with wind turbines, known as "wind turbine syndrome." Although there is no solid scientific evidence supporting a direct link between onshore wind turbines and certain health conditions, this phenomenon has often been discussed and analyzed in public health research. In the work of van Kamp and van den Berg [5], the health effects of the noise generated by wind turbines, including low-frequency sound

and infrasound, were examined. This analysis investigated whether there is solid evidence of negative effects on human health caused by these sound phenomena. The work of Hessler et al. [6] addressed the same issue and raised the crucial question about the effects of wind turbines on human health. These authors critically examined existing studies, questioning the existence of a specific syndrome called "wind turbine syndrome," and attempted to determine whether wind turbines can indeed make people feel sick.

As for offshore wind turbines, they represent a significant advancement in the field of wind energy and have several significant advantages over onshore ones. One of the most notable advantages is their ability to generate more energy. Being located offshore, these wind turbines are exposed to more constant and stronger winds, allowing them to generate larger amounts of electricity compared to onshore turbines.

Moreover, the offshore wind market is in continuous growth. Several countries are investing in the development of offshore wind farms to harness their energy potential. The work referenced in [7] provides an overview of the current situation and future trends in the offshore wind industry in Europe. Similarly, the study referenced in [8] analyzes technological advancements regarding the size and power of wind turbines. This aspect is crucial for increasing production capacity and the energy efficiency of offshore wind farms. On the other hand, the study [9] focuses on innovations in the design and materials used for wind turbine blades.

Regarding design optimization, Chen and Kim [10] explore strategies and methodologies for optimizing the design of offshore wind turbines. These approaches contribute to maximizing efficiency and production capacity.

The conclusions drawn from these works are diverse and do not offer a unified perspective on the impact of wind turbines on human health. Some researchers have argued that there is limited evidence of negative effects on human health caused by the low-frequency noise and infrasound produced by wind turbines. Others have contested the existence of a specific syndrome called "wind turbine syndrome" and have suggested that negative perceptions may be largely related to psychological and subjective factors.

The analysis of the studies presented in this subsection highlights the rapid evolution of offshore wind turbines and the complexity of the field. The studies have covered a wide range of aspects, from wind resource assessment to the technological development of offshore wind turbines, to reliability and efficiency-related issues.

1.2 An overview of offshore energy potential

In the global context of transitioning to sustainable energy sources, research on the exploitation of wind resources has become essential for the development of a sustainable energy future. In recent years, studies related to the use of renewable energy from wind sources have garnered significant attention in the scientific and industrial communities. This research focuses on using data based on reanalysis databases and direct measurements to investigate specific aspects related to wind resources.

Regarding the choice of the best reanalysis database, it should be noted that this decision largely depends on the specific objectives of the research and the geographical region of interest. In the literature, numerous studies have been conducted to assess the potential of offshore wind energy using reanalysis data and in-situ measurements, addressing different regions and methodologies. A common aspect in these studies is the use of reanalysis databases such as ERA5, CFSR, or MERRA to obtain information about winds and meteorological conditions.

For example, the work of Hsiao et al. [11] focused on evaluating the wind energy potential in the Taiwan Strait, using ERA5 and CFSR reanalysis data. This study aimed to accurately assess the energy potential in this specific region. Tahir et al. [12] evaluated ERA-Interim and NCEP-CFSR reanalysis datasets in comparison with in-situ measured wind speeds at the Keti Bandar port in Pakistan. The objective of this study was the validation and comparison of the accuracy of reanalysis data with ground-based measurements. Additionally, the study by Rajat Kanti Samal et al. [13] evaluated wind energy resources using reanalysis data and compared these data with on-site measurements to analyze variations in these resources over time.

In another context, the study by Pedro M M Soares and his team [14] presented a global characterization of offshore wind power density using ERA5 reanalysis data. This study emphasized the importance of resolution and accuracy in the reanalysis of data when assessing wind energy resources globally.

Finally, Boming Liu and colleagues [15] used machine learning algorithms to estimate wind speed on the coast of China using reanalysis data and in-situ data. This study analyzed the potential of wind energy on the coast of China and evaluated the performance of different machine learning algorithms in estimating these resources.

In the context of offshore wind energy, several studies have addressed various aspects related to extreme weather conditions and their implications for wind farms. These research efforts provide a broad perspective on the complexity of meteorological phenomena in offshore environments and the challenges they pose.

A relevant example is the work of Vemuri et al. [16], which focuses on modeling extreme meteorological events in the North Sea and evaluating the sensitivity of physical parameterizations in meteorological models. Although this work makes significant contributions to understanding these phenomena, it underscores the difficulty of finding a unique model configuration that fits all extreme events.

Regarding the assessment of offshore wind turbine behavior in extreme weather conditions, the work referenced in [17] provides valuable contributions by investigating the nonlinearity of waves and the cyclic response of the soil. This research emphasizes the need to consider extreme conditions in the design and operation of offshore wind farms.

In another context, the study by Yang et al. [18] proposes an innovative method for evaluating offshore wind resources by characterizing meteorological regimes. This approach shows that meteorological regimes can significantly influence wind energy production, providing a crucial perspective on the predictability of resources based on meteorological conditions. Moreover, studies have been conducted to assess environmental impact and economic analyses for the development of offshore wind energy in this region [19–21]. The North Sea has been the subject of numerous studies related to the variability of offshore wind resources and the assessment of energy potential [22–25]. These studies covered aspects such as the variability of energy potential, the development of a decision support system, the quantification of offshore wind resources, and a detailed assessment of the energy potential in the coastal area of the North Sea.

Regarding the South China Sea, extensive research has been conducted to evaluate the offshore wind potential in this region of China. These studies examined wind resources and analyzed the feasibility of offshore wind farm projects in the South China Sea area. They also focused on assessing environmental impact and conducted economic analyses to promote the development of offshore wind energy in this region [26–28]. Additionally, in-depth studies have been conducted on the offshore energy potential for the Yellow Sea [29–31] and other regions.

Following these research, potential opportunities for increasing renewable energy production capacity in these regions have been identified, contributing to reducing greenhouse gas emissions and transitioning to cleaner energy sources. Although each area has its unique characteristics and specific challenges, the research conducted so far has laid the groundwork for the efficient development and implementation of offshore wind farms worldwide. With ongoing research and innovation efforts, the enormous potential of offshore wind energy can be fully utilized for a sustainable and clean future.

1.3 Recent developments and perspectives in airborne wind energy systems

Over the past decades, numerous studies have been conducted to analyze and assess the energy potential of high-altitude winds, seeking to understand how this natural resource generated in the upper layers of the atmosphere could significantly contribute to sustainable electricity production. Research by Archer and Caldeira [32] has highlighted that harnessing winds at higher altitudes leads to a significant increase in their power and stability, both onshore and near coastal areas. This observation opens new perspectives for the development of production capacity and the efficiency of wind systems. For instance, in Europe, analyzing winds at variable altitudes up to 500 meters above the ground reveals a doubling of available wind power density 95% of the time compared to fixed-altitude production, specific to conventional wind turbines [33]. Conversely, using a climate model, Marvel et al. [34] concluded that ground-based wind turbines could extract at least 400 TW, while high-altitude wind energy could exceed 1,800 TW. They also emphasized that the global uniform implementation of distributed wind turbines to meet the global demand for primary energy of 18 TW would not significantly impact the global climate.

To exploit this potential, the concept of airborne wind energy has been introduced. The airborne wind turbine, known as the Airborne Wind Turbine (AWT), represents an emerging paradigm in the field of renewable energy production, marking a radical shift from traditional approaches to capturing wind energy.

Among the intensively studied aspects is the analysis and optimization of the performance of these systems. The work of Sommerfeld et al. [35] focuses on evaluating the impact of wind profiles on the performance of AWE systems, using advanced simulations to determine optimal flight trajectories. The obtained data show that optimal operating heights are generally below 400 m, with most AWES operating around 200 m. In the same context, the work of Dief et al. [36] applies system identification algorithms and adaptive control to simulate crosswind flight maneuvers, which are essential for harvesting wind energy.

The aerodynamic optimization of profiles is also an important topic, as shown in the work of Arslan Saleem and Man-Hoe Kim [37]. This work proposes a genetic algorithm to optimize the aerodynamic profiles of blades, thereby improving the performance of the airborne wind turbine.

Volkan Salma and Roland Schmenhl [38] discuss the importance of integrating AWE systems into airspace safely and systematically. This work addresses issues related to the operational authorization of commercial AWE systems and methods for assessing associated risks. This effort contributes to identifying and managing risks that can affect the safety of AWE system operations in airspace.

Additionally, the literature suggests that replacing the tower with a relatively thin cable contributes to reducing the visibility of AWE systems compared to traditional wind turbines. These findings can be correlated with the work of Susana Batel and Patrick Devine-Wright [39], exploring the impact of energy infrastructures on the landscape and local communities.

Through their critical approach, the authors suggest that visual and spatial factors need to be evaluated differently to understand how energy infrastructures, including AWES, affect people's perception of the landscape.

Regarding residents' attitudes toward wind turbines, the study conducted by Ben Hoen and his team [40] provides an interesting perspective. Their study analyzed the attitudes of neighbors of wind projects in the United States and found that, overall, these attitudes are positive, with improvements as residents adapt to the presence of turbines.

Moreover, the work of Megahed [41] examines the issue of evaluating the landscape impact and visual impact of high-altitude wind technologies, including AWE systems. This emphasizes the need to consider spatial and aesthetic characteristics to assess the impact of these technologies on the surrounding environment.

In a landmark study, Johannes Pohl and his colleagues [42] used an integrated approach to analyze the noise impact of wind turbines on residents' stress and annoyance. This study investigated the perception and opinion of individuals exposed to the noise produced by wind turbines and found a correlation between the perception of annoyance and subjective factors such as the perception of justice in the planning process of wind projects.

Another study, conducted by Gundula Hübner and his team [43], compared the perception, annoyance, and stress of residents in the United States, Germany, and Switzerland in areas near wind turbines. This study highlighted a low prevalence of annoyance and stress symptoms related to the noise produced by wind turbines. It also showed that the perception of annoyance was negatively correlated with the perception of justice in wind project development.

1.4 Current perspectives on offshore wind turbine towers and foundations

The marine environment presents a series of unique challenges concerning the construction and operation of offshore wind turbines. Strong marine currents, high waves, and the instability of weather conditions require a rigorous technical approach and innovative design to ensure the optimal functioning of these installations. In this context, the pile and foundation represent key elements of this complex approach.

The offshore wind turbine pile is designed to support the entire structure and maintain it at the appropriate height to capture wind flows. On the other hand, the foundation must provide structural stability and protect the wind turbines from excessive movements or vibrations. In the study by Xiong Liu and his colleagues [44], the complex effects of aerodynamic damping on the loading of the horizontal-axis offshore wind turbine pile are explored. This research provides a detailed perspective on how winds and waves can influence the structural integrity of the pile, contributing to the development of strategies to optimize resistance to these effects. The work of Begum Yurdanur Dagli and colleagues [45] focuses on the dynamic analysis of offshore wind turbine piles using numerical analyses.

One research direction focuses on the corrosion resistance of the offshore wind turbine pile and foundation, given the constant threat posed by the marine environment. In the work developed by Yan et al. [46], corrosion protection strategies for foundations and support structures of offshore wind turbines are examined. However, the work [47] addresses the same topic but specifically focuses on evaluating the performance of different corrosion-resistant coatings used on monopile structures of offshore wind turbines.

Another important research direction in the field of offshore wind energy focuses on the development of monitoring and predictive maintenance systems for wind turbine piles. A notable example is the real-time monitoring system for monopile foundation erosion presented

in the work of Tang and Zhao [48]. The importance of monitoring applies to all types of foundations, and thus, the work of Yolanda Vidal and her team [49] discusses the importance of monitoring jacket structures used for the foundations of offshore wind turbines.

The use of intelligent wireless sensors represents another significant step in the structural monitoring of offshore wind turbines. These sensors provide precise information about the natural frequencies, damping ratios, and modal shapes of the turbines, as illustrated in the work [50]. Wireless sensor technology contributes to more efficient monitoring and early identification of structural issues. As monitoring technologies become increasingly advanced, the work of Vieira et al. [51] discusses an important aspect: the economic impact of implementing these systems on the support structures of offshore wind turbines.

In terms of research in the field of Multi Wind Turbine (MWT) platforms, it focuses on several aspects. One major aspect is the analysis of interactions between wind turbines installed on the same platform [52]. In the work developed by Bashetty and Ozcelik [53], the effect of shadowing interference between wind turbines installed on the same MWT platform is analyzed. Research in this field also focuses on the development of innovative solutions for anchoring and stabilizing these platforms to cope with challenging offshore conditions [54]. This includes the development of advanced anchoring systems and high-performance materials to stabilize platforms in the face of waves and extreme weather conditions. Bae and Kim [55] developed a numerical simulation tool for the coupled dynamic analysis of multiple turbines on a single floating platform. The results showed that defects in one turbine can influence the performance of other turbines and the floating platform, highlighting the importance of coupled dynamic analysis in designing these complex systems.

One of the important materials used in pile construction is composite material. O'Leary and colleagues [56] explore the application of lightweight, fiber-reinforced composite materials in the construction of offshore wind turbine piles. Additionally, Young et al. [57] present a methodology for the design and optimization of composite material wind turbine piles intended for use on offshore floating platforms.

Regarding traditional materials, the work in reference [58] investigates the relative performance of steel and concrete piles for different heights and wind speeds. This analysis highlights the probabilistic characteristics of exceeding the limit state based on wind loads. In contrast, the work [59] focuses on the behavior of pre-stressed concrete wind turbine piles with a circular section.

In terms of anchoring, research is directed towards the development of advanced anchoring methods to ensure the stability and safety of offshore wind turbines, especially in deep water conditions. Technologies such as screw anchor systems or hybrid solutions are subjects of interest, and researchers explore options for optimizing these systems based on the specifics of each location. The work of A.C. Pillai and his team [60] focuses on anchor loads in shallower waters and investigates synthetic and novel solutions for anchoring systems. This research brings innovative alternatives to ensure stability in shallow waters.

Overall, this subchapter has identified promising directions for future development in the field of offshore wind energy, emphasizing the importance of continuous research and innovation to maximize the efficiency, durability, and sustainability of these renewable energy sources in a complex and variable maritime environment.

1.5 A recent evaluation of levelized cost of energy in the offshore wind industry

The levelized cost of energy (LCOE), also known as the cost per unit of electricity generated, synthesizes all the aspects mentioned earlier, focusing on the economic dimension. The fundamental goal of estimating LCOE is to optimize offshore wind farm projects.

Studies, such as those conducted by Castro Santos Laura et al. [61], focusing on cost analysis in specific regions, and the work by Maienza et al. [62], developing a detailed analytical approach to costs for different turbine types, have brought crucial themes to the forefront. They emphasize the importance of the specifics of each project in determining LCOE and the need to consider a wide range of factors, from geographical and technological variables to economic aspects.

A detailed perspective on recent research in the field of offshore wind farm site selection reveals a complex and interconnected landscape of this critical subject. Studies like that of Mytilinou and Kolios [63] adopt a comprehensive approach to site selection, aiming to optimize efficiency across multiple criteria. These contributions are complemented by research such as that conducted by Song et al. [64], discussing multidisciplinary optimization in the design of virtual wind turbine farms. This complex approach is extended by the study of Rodrigues et al. [65], which integrates the optimization of offshore wind farm architectures with electrical infrastructure, highlighting the essential interdependencies between these two aspects.

While the work of Li et al. [66] pursues a statistical and analytical aspect of capacity development in the offshore wind energy industry, focusing on the UK region and incorporating a multi-criteria analysis element into the location selection process, the work of Deveci et al. [67] offers an innovative approach, integrating interval-value methods to define selection criteria.

Another notable aspect emerging from the analysis of the works is the profound relevance of technological specificity and location conditions in the process of choosing the optimal turbine structure and determining the corresponding costs. Studies like that conducted by Myhr et al. [68], comparing various turbine types and analyzing how water depth and distance from the shore influence LCOE, underline the importance of technological adaptation to the specific requirements of each site.

At the same time, it is observed that operation and maintenance costs have a significant impact on the overall value of LCOE in offshore wind farms, as suggested by the work of Hammond and Cooperman [69]. This raises questions about the maintenance and operation strategies adopted in the industry and how these can be optimized to ensure long-term economic performance. One notable achievement of this work is the development of an analytical tool, WOMBAT, which provides a rigorous approach to assessing the costs and benefits of operations and maintenance within wind farms. By identifying and analyzing key factors influencing these costs, the study offers directions and solutions for optimizing economic performance and long-term project sustainability. Additionally, another work contributing to this field is the one conducted by McMorland et al. [70]. providing a conceptual and analytical framework to understand how new technological innovations can influence and be integrated into operation and maintenance strategies.

Moreover, questions arise regarding risk and uncertainty management approaches. The work of Yeter et al. [71] proposes an innovative approach to maintenance planning in offshore wind farms. The authors identify and evaluate potential risks and their impact on wind turbine performance.

1.6 Conclusions

Perspectives on the future of the offshore wind industry are diverse and exciting, with multiple research and innovation directions aimed at contributing to the sustainable development of this sector. Some of these directions include the ongoing development of innovative turbine technologies, aiming for larger, more efficient, and more reliable turbines, and even exploring new concepts such as vertical-axis turbines. Energy storage is a central focus, with research concentrated on advanced batteries, hydrogen storage systems, and thermal storage to manage production fluctuations and ensure a constant supply of electrical energy. The efficiency of operations and maintenance (O&M) is crucial for cost reduction, and research is focusing on the development of strategies and technologies for efficient monitoring and maintenance of installations. Risk management, safety, and expansion to greater depths are key directions, and the development of unified standards and regulations is vital for enhancing industry competitiveness and sustainability. The integration of offshore wind energy with other renewable sources, such as solar and hydropower, can lead to more efficient hybrid systems. Additionally, continuous research on environmental and biodiversity impacts, along with efforts in education and public awareness, is crucial. With these well-defined directions and collaboration among industry stakeholders, the offshore wind sector is poised to play a significant role in renewable energy production and the fight against climate change.

2 Wind and wave energy resource potential in the Black Sea basin

2.1 ERA5 database

Reanalysis, also known as retrospective analysis, is a relatively new field that emerged in 1979 with the use of meteorological data collected during the First Global Atmospheric Research Program's Global Experiment (FGGE) [72].

In the context of climate monitoring, reanalyzed datasets play a fundamental role and are widely recognized for their significant contributions. ECMWF (European Centre for Medium-Range Weather Forecasts) has a long and impressive history in this field, as evidenced in Table 2.1. The latest notable achievement is ERA5, representing the fifth generation.

Table 2.1 Atmospheric resolution for the 5 projects developed by ECMWF [73].

Reanalysis	Period covered	Integrated Forecasting System (IFS)	Resolution
FGGE	1979	-	200 km
ERA-15	1979-1994	-	125 km
ERA-40	1957-2002	23r4	125 km
ERA-Interim	1979-2019	31r2	80 km
ERA5	1950-prezent	43r1	31 km

In the development of ERA5, the starting point consisted of using the Integrated Forecasting System (IFS) Cy41r2, which served as the foundation in the ECMWF's operational medium-range forecasting system between March 8 and November 21, 2016.

Compared to its predecessor, ERA-Interim, ERA5 benefits from a decade of sustained research and development at ECMWF. However, there are still unresolved aspects. Parameters downloaded from the ERA5 database.

The ERA5 database serves as a resource for research in climatology, meteorology, environmental science, and engineering. This database provides a wide range of essential meteorological and climatic parameters, covering a significant period and an extensive geographical region.

Within this PhD thesis, relevant parameters were downloaded and processed from the ERA5 database. This dataset is used to analyze in detail the behavior of the Black Sea, to study its potential in terms of renewable energy and climatological research. Additionally, these parameters are used in this PhD thesis to evaluate essential structural elements of offshore wind turbines, such as the foundation. Furthermore, this information contributes to the analysis of the cost of wind energy production. Through the MATLAB program, these parameters are processed and analyzed to obtain relevant data related to the behavior of the Black Sea and the climatic conditions in this area. This data is essential for assessing the characteristics of the wind turbine, as well as other technical aspects related to wind energy production. Thus, the ERA5 database and the parameters obtained from it play an important role in the research of this PhD thesis. Parameters downloaded from the reanalysis database include sea surface temperature, significant wave height, mean wave period, peak wave period, mean wave

direction, zonal component u10 of the wind speed at 10 meters above ground, meridional component v10 of the wind speed at 10 meters above ground.

Together, the u10 and v10 components form the wind vector at a height of 10 meters, also known as the surface-level wind.

2.2 Characteristics of the Black Sea

The Black Sea, one of the most intriguing and complex marine ecosystems in the world, serves as a fascinating research subject for biologists, oceanographers, and climatologists. This body of water, surrounded by seven countries and connected to the Mediterranean Sea through the Bosporus Strait, possesses a range of unique features that distinguish it from other seas and oceans.

Covering an area of approximately 436,000 square kilometers, the Black Sea ranks as one of the largest inland seas globally. It has an average depth of around 1,200 meters, with its deepest point, known as the Crimean Trench, plunging to a depth of 2,212 meters. The climate of the Black Sea is significantly influenced by its geographical position, with average annual temperatures ranging between 11°C and 17°C, warming during the summer and cooling in the winter.

A distinctive feature of the Black Sea is the seasonal nature of its winds. During the summer, west and northwest winds prevail, bringing cool and dry air from central Europe.

2.3 Climate characteristics of the Black Sea

For the climatic analysis of wind, the average and maximum wind speed values, as well as their directions, were calculated using data provided by ERA5 for a 20-year period (2002–2021). The data analysis and processing were carried out using the MATLAB program.

Figure 2.1 illustrates the spatial distribution of the maximum wind speed at a height of 100 meters in the Black Sea basin. The position in the field of the maximum wind speed is located in the western and southeastern areas of the Black Sea basin. Primarily, low values of this parameter are found on the eastern coast of the Black Sea. At the same time, the coast of Romania stands out as the most well-defined area with high average wind speed values.

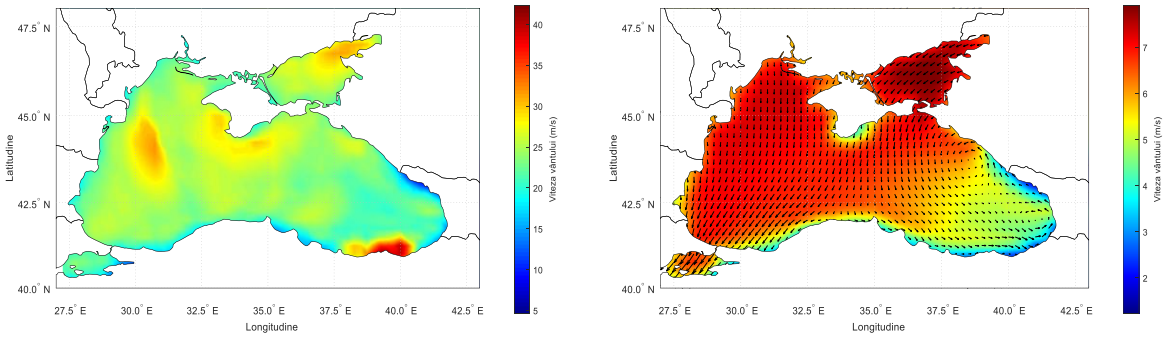

Figure 2.1 The a) maximum; b) average wind speed for the period 2002–2021 at a height of 100 meters.

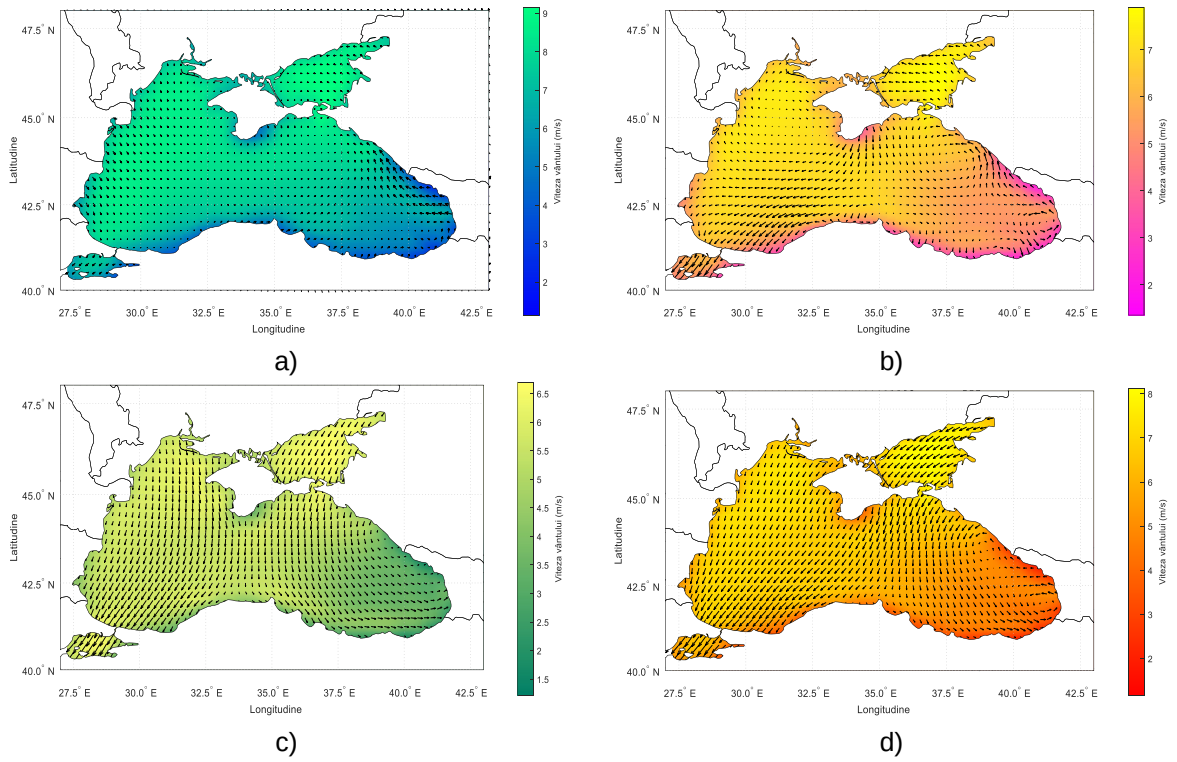

Figure 2.2 The average wind speed at a height of 100 meters during the season: a) winter; b) spring; c) summer; d) autumn for the time interval 2002–2021.

Figure 2.2 depicts the seasonal distributions of wind speed at a height of 100 meters. We observe that, in all cases, the Sea of Azov shows the highest value in the wind distribution. For all seasons, high speeds at the height of 100 meters are encountered above the Sea of Azov and in the western part of the Black Sea basin. It is noteworthy that for spring and summer, the average values in the southern part of the Black Sea decrease considerably, reaching 1.5-2 m/s in certain locations.

Figure 2.3 presents the spatial distribution of the significant wave height for the period 2002-2021. Analyzing this map, it can be observed that the maximum value of this parameter is around 1 meter and is located in the western part of the Black Sea basin. In contrast, the eastern part of the Black Sea presents values ranging from 0.4 to a maximum of 0.78 meters.

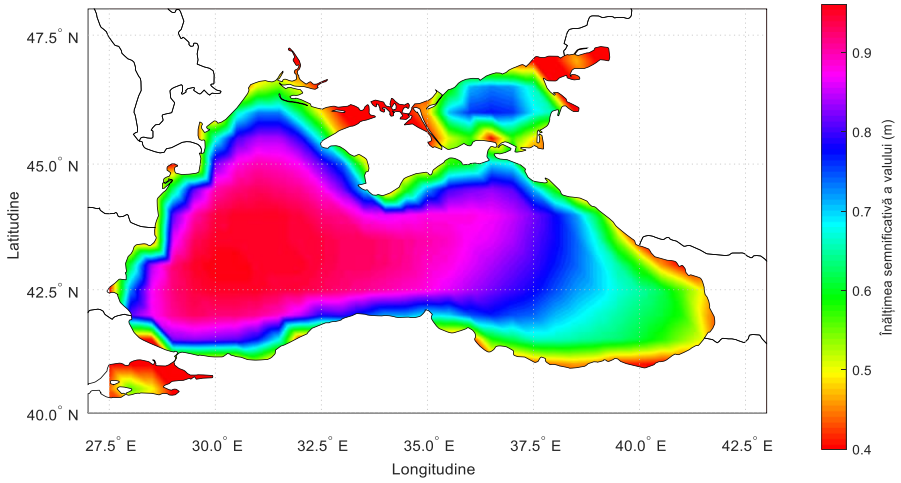

Figure 2.3 The average significant wave height for the time interval 2002-2021.

Figure 2.4 presents the distribution of the mean wave period and the peak wave period in the Black Sea and the Sea of Azov for an extended period, covering the years 2002-2021. The data on this map indicate a varied range of values for the mean wave period, with values ranging from 3 to 4.8 seconds in the Black Sea and a maximum value of 3.2 seconds in the Sea of Azov, located in the northern part of the region.

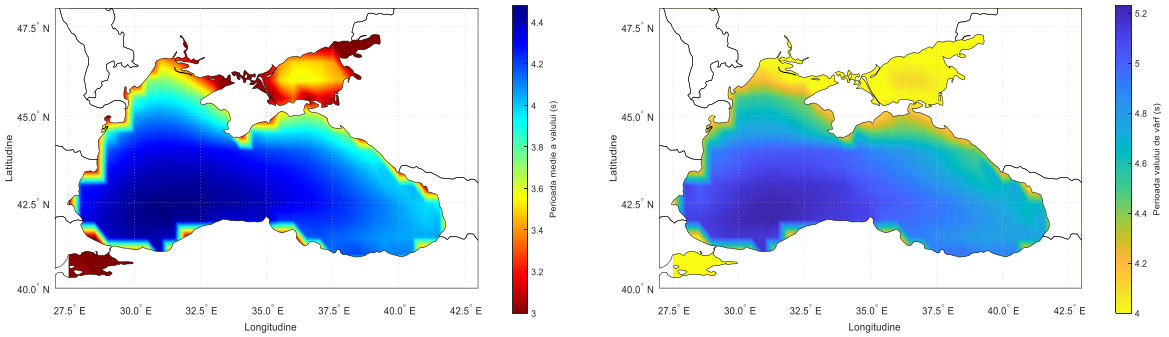

a) b)

Figure 2.4 a) Mean wave period b) Peak wave period for the time period 2002-2021.

The Black Sea, surrounded by a variety of climatic regions, has witnessed exceptional meteorological events throughout its history. Among these events are the Mediterranean tropical cyclones, known as "medicanes."

Over time, the Black Sea has been affected by several notable events similar to medicanes. In Figure 2.5, the position and size of the cyclone that affected the Black Sea on March 21, 2002, are illustrated. This meteorological phenomenon formed in the north-western part of the Black Sea, near the Romanian coast. Using available ERA5 data, the peak moment of this cyclone was identified around 5 AM, when its speed reached a notable maximum. This Ekman spiral exhibited a wind intensity of up to 19.1 m/s, thus classifying this event as a moderate intensity medicane.

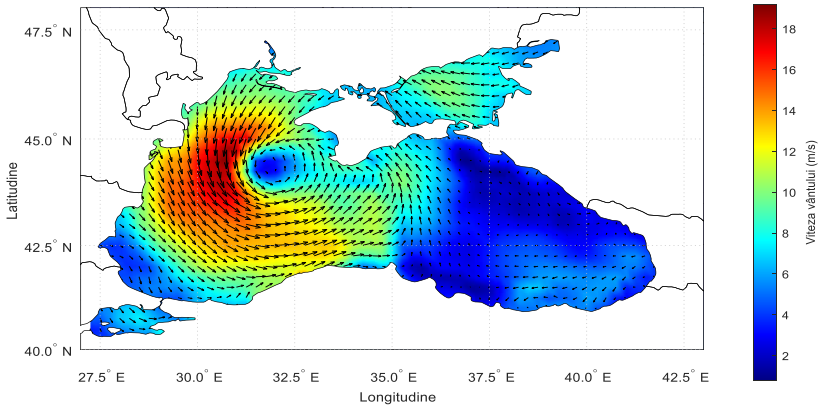

Figure 2.5 The tropical cyclone on March 21, 2002, using ERA5 data.

The cyclonic phenomenon during August 7-11, 2002, represented another notable example of a meteorological event affecting the Black Sea and the Sea of Azov in that year (Figure 2.6). This cyclone had a different trajectory compared to the one discussed earlier, positioning itself in the northern part of the Black Sea and covering an extensive area in this region. Additionally, this meteorological event influenced the entire surface of the Sea of Azov. The peak moment of this cyclone was identified for August 9, around 4 a.m. The maximum

wind speed associated with this event reached 19.2 m/s, similar in intensity to the previously discussed cyclone.

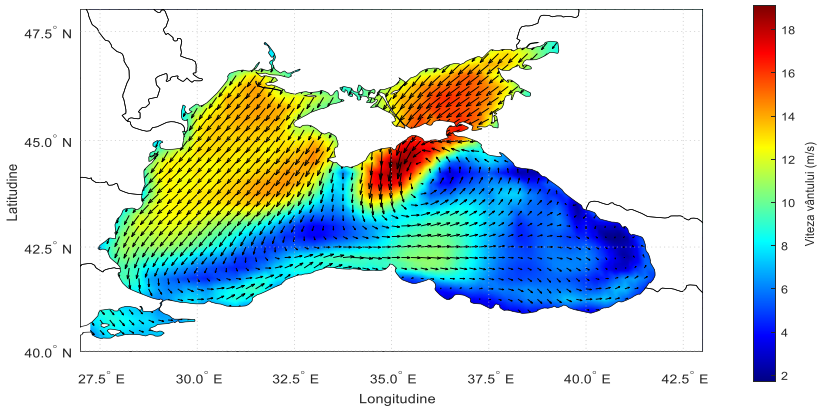

Figure 2.6 Tropical cyclone during August 7-11, 2002, using ERA5 data.

Tropical cyclone impact during the fall of 2005 in the Black Sea was notably observed when an exceptionally intense and unusual tropical cyclone affected the region. The peak moment recorded in the ERA5 database for wind speed was highlighted on the 28th day at 16:00, as depicted in Figure 2.7. Observations reveal a spiraled structure over the southwestern region of the Black Sea, where wind speeds ranged between 14 and 20 m/s.

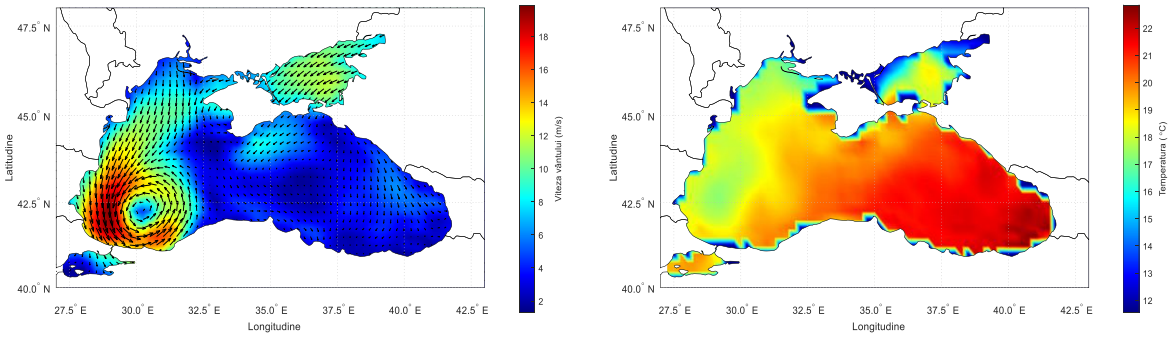

a) b)

Figure 2.7 a) Tropical cyclone; b) sea surface temperature from September 25-29, 2005, using ERA5 data.

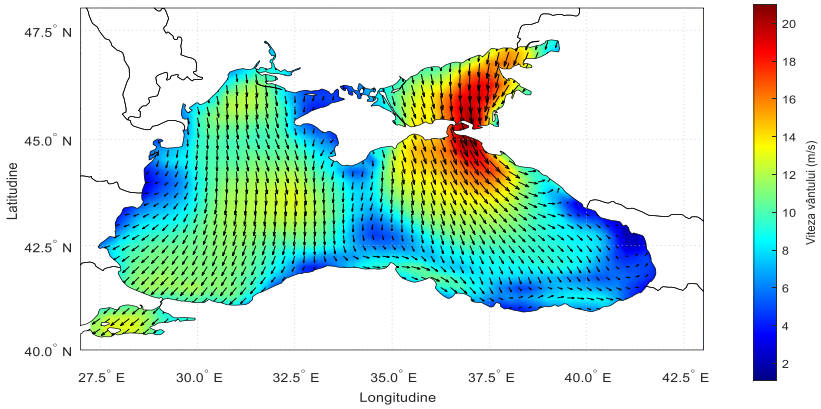

Figure 2.8 The tropical cyclone from August 10-16, 2021, using ERA5 data.

In Figure 2.8, we can observe the last cyclonic event identified, which took place in 2021. According to ERA5 data, the peak moment of this cyclone was identified on August 13, around 19:00, when the wind speed reached a maximum of 21 m/s.

2.4 Conclusions

The Black Sea, a semi-enclosed water body situated between Eastern Europe and Southwest Asia, connected to the Mediterranean Sea through the Bosporus Strait and to the Sea of Azov through the Kerch Strait, plays a crucial role in the ecological, climatic, and economic aspects of the surrounding region. Through a careful analysis of data regarding wind speed, waves, and sea surface temperature across the entire Black Sea basin, as well as the examination of four notable cyclones occurring between 2002 and 2021, a deeper understanding of the atmospheric and oceanographic dynamics of this region has been gained. Within this analysis, specific trends and behavioral patterns of the Black Sea have been observed.

The main conclusion is that the Black Sea is susceptible to significant variations in wind, waves, and water temperature due to the influence of cyclones and other meteorological phenomena. Analyzing the seasonal variations of wind in the Black Sea basin has been a crucial part of the study. Significant variations in winds were observed during different periods of the year. Generally, winds exhibited a seasonal pattern, with periods characterized by intensification and periods of milder winds.

The cyclones described in this chapter presented a diverse range of intensities and trajectories, affecting different regions of the Black Sea and the Sea of Azov. These meteorological events can bring significant changes in local meteorological and oceanographic conditions, including alterations in wind patterns, increases in wave heights, and variations in water temperature. One of these events occurred during September 25-29, 2005, and was well-documented and investigated. This cyclone was characterized by low atmospheric pressure, strong winds, and a significant impact on the marine conditions of the Black Sea. Studying this event provided an opportunity to analyze how Mediterranean tropical cyclones can affect the dynamics of the sea and surrounding coastal regions.

Another important parameter analyzed was the water temperature in the Black Sea. Cyclones had a significant impact on water temperature, causing substantial changes. For instance, during the cyclone in September 2005, the water temperature in the central area of the cyclone dropped significantly, reaching below 17 degrees Celsius, while in the rest of the Black Sea, the water temperature remained above 22 degrees Celsius.

It was also observed that coastal areas and open sea can experience significant variations in wind intensity and speed, with certain regions being more susceptible to cyclone influence. Additionally, water temperature can fluctuate considerably, impacting marine ecosystems and oceanographic processes.

This analysis has contributed to a better understanding of how meteorological phenomena can affect the Black Sea and the importance of monitoring and understanding these changes for the proper management of natural resources and nautical safety in this vital region of Eastern Europe. Moreover, it could contribute to improving weather forecasts and preparedness for extreme weather events in this critical area.

3 Evaluation of wind energy potential in the Black Sea region

3.1 The chosen sites in the Black Sea for the wind energy evaluation

The Exclusive Economic Zone (EEZ) of the Black Sea represents a maritime area surrounding the Black Sea, regulated by international law, providing coastal states with exclusive rights and privileges concerning natural resources and economic activities. The Black Sea has a total of six EEZs, each belonging to the respective coastal states. These include the zones of Bulgaria, Georgia, Romania, Russia, Turkey, and Ukraine.

In this chapter, we will analyze the energy potential for the past, focusing on 9 selected locations within the EEZ of Romania. This strategic area, located in the western part of the Black Sea, has been identified as of interest for studying wind speed. The exact positions of the 9 locations are illustrated in Figure 3.1, and the precise geographical coordinates of these points are presented in Table 3.1.

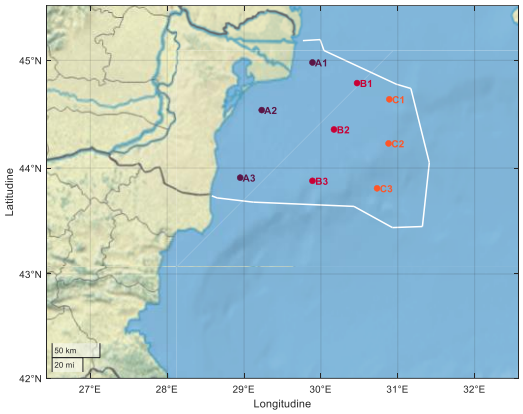

Figure 3.1 The chosen locations for the study of wind in the Black Sea.

Table 3.1 The coordinates of the selected locations of interest.

	Latitude	Longitude	Depth
A1	44° 58' 48"	29° 53' 24"	34 m
A2	44° 32' 24"	29° 13' 48"	26 m
A3	43° 54' 36"	28° 57' 00"	40 m
B1	44° 47' 24"	30° 28' 12"	58 m
B2	44° 21' 36"	30° 10' 12"	78 m
B3	43° 59' 24"	29° 53' 24"	65 m
C1	44° 38' 24"	30° 53' 24"	95 m
C2	44° 13' 48"	30° 52' 48"	173 m
C3	43° 48' 36"	30° 43' 48"	1000 m

According to the United Nations Convention on the Law of the Sea, the Exclusive Economic Zone (EEZ) grants coastal states the right to explore and exploit natural resources, including minerals, energy, and fisheries, as well as to control economic and scientific research activities in this area. This chapter provides a more detailed approach to the analyses initiated

in the works [74,75], with a particular focus on the Exclusive Economic Zones (EEZ) of Romania.

3.2 Selected wind turbines for the study of the Black Sea ZEE

The crisis caused by the COVID-19 pandemic poses an imminent threat to the global economy and the standard of living of communities worldwide. The effects of the COVID-19 pandemic have resulted in significant variations among economic sectors. However, the green energy industry, particularly in the field of renewable wind energy, appears to have been less vulnerable compared to the conventional energy industry, which experienced profound adverse effects due to this pandemic.

3.2.1 Wind turbine components

This form of energy has significant advantages over onshore wind energy, especially due to the stronger and more consistent wind resources available in coastal or offshore areas. To better understand the role of each component of the offshore wind turbine, we can refer to Figure 3.2, which illustrates the constituent parts and provides a more detailed insight below.

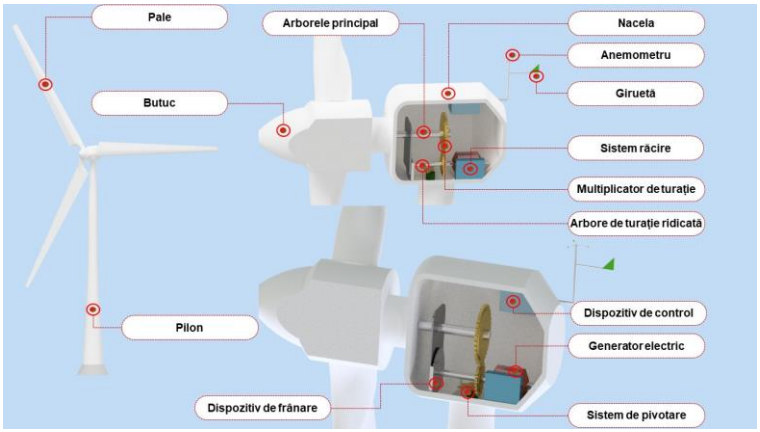

Figure 3.2 Main Components of a Wind Turbine.

3.2.2 Selected wind turbine types

In the context of developing offshore wind potential in the Black Sea, Romania holds a strategically advantageous position. The development and implementation of cutting-edge technological solutions in the offshore wind sector would bring significant economic benefits to the country. Although offshore wind farms have not been constructed in the Black Sea waters to date, thorough studies have been conducted to assess the region's potential for wind energy production. These studies have included wind turbines with capacities ranging from 2 to 4.5 MW, but the technology behind these turbines has evolved rapidly.

The turbines selected for these projects have nominal capacities between 6 and 9.5 MW, and their tower height varies between 92 and 100 meters above sea level. To standardize future calculations and appropriately compare the performance of these turbines, the tower height for all six turbines was approximated at 100 meters above sea level. This provides a common basis for evaluating and comparing the performance of these state-of-the-art technologies.

The power curve of a wind turbine is a crucial characteristic for understanding how it generates electrical energy based on wind speed. The power curve graph indicates the relationship between wind speed and the electrical power generated by the wind turbine. It is an important tool for assessing the performance of a wind turbine and optimizing energy production. The power curves of the selected turbines are presented in Figure 3.3

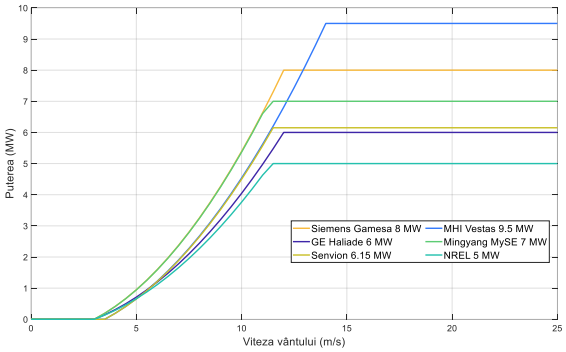

Figure 3.3 Power curves for selected turbines.

To be able to draw the power curve, wind speed and turbine power are required. A quadratic equation is used to obtain this power curve [76].

$$P(U)=\begin{cases} q(U) & U_{cin}<U<U_{rat} \\ P_r & U_{rat}<U<U_{cou} \\ 0 & U\leq U_{cin} \text{ and } U\geq U \end{cases} \quad (3.1)$$

$$q(U)=P_r\frac{U^2-U_{cin}^2}{U_{rat}^2-U_{cin}^2}$$

where: P_r is the nominal power of the turbine, as provided in the technical specifications – in MW, U is the wind speed for which the power is calculated – in m/s, U_{cin} is the cut-in wind speed – in m/s, U_{cou} is the cut-out wind speed – in (m/s), U_{rat} is the wind speed at which the turbine reaches its rated power – in m/s.

3.3 Logarithmic wind profile

The most commonly used equation for determining wind speed at different heights is the Hellmann exponential law. The international standard for the design of offshore wind turbines, IEC 61400-3, developed by the International Electrotechnical Commission (IEC), refers to the initial standard for wind turbine design, IEC 61400-1, which states that wind speed can be calculated using the Hellmann exponential law [77,78]:

$$U(z)=U_{z_{ref}}\left(\frac{z}{z_{ref}}\right)^{\alpha} \quad (3.2)$$

where: U(z) is the average wind speed as a function of height,, $U_{z_{ref}}$ represents the reference wind speed (usually at a height of 10 m), z s the height at which interpolation is desired (in m), z_{ref} is the reference height (10 m), α e is the exponent of the power law, also known as the Hellmann exponent [79,80]; the value of this coefficient is typically estimated at 1/7 (approximately 0.143) [81], evaluating the wind profile under normal meteorological

conditions. However, this value may introduce errors in calculations, especially in the offshore wind domain, specifically in open waters. In such cases, a value of 0.11 is recommended [82] to outline the wind profile under extreme meteorological conditions.

Another formula commonly used in the study of wind speed in Europe is the logarithmical wind profile, also known as the logarithmic wind speed profile. It is an empirical relationship that describes how wind speed varies with height above the Earth's surface in the atmospheric boundary layer [83].

$$U = U_z \frac{\ln\left(\frac{z}{z_0}\right)}{\ln\left(\frac{z_{ref}}{z_0}\right)} \tag{3.3}$$

In this equation U_z (in m/s) represents the reference wind speed (obtained from databases), z_{ref} is the height of 10 m, z is the height at which the calculated wind speed will be obtained (in m/s), and z_0 is the coefficient of roughness of the water surface, with a value of 0.0002 m [84].

3.4 Parameters used in wind energy assessment

Once the wind speed at a certain height is obtained, energy parameters can be calculated. Power density is commonly quantified in watts per square meter (W/m²) or kilowatts per square meter (kW/m²), denoted as P_w. Power density can be calculated using the formula [85,86]:

$$P_w = \frac{1}{2}\rho_{air}(U)^3 \tag{3.4}$$

where: ρ_{air} is the air density with a value of 1,225 kg/m^3, and U is the wind speed interpolated at the desired height in m/s.

One of the energy parameters is the annual electricity production, denoted as AEP (MWh), and is an optimization parameter reported for a specific type of turbine and location [87]:

$$AEP = T \times \int_{cut\text{-}in}^{cut\text{-}out} f(U)P(U)du \tag{3.5}$$

where: T=8.760 h/year is the annual operating time of a turbine. Cut-in corresponds to the wind speed at which the turbine starts operating, and it continues to rotate until reaching the maximum efficiency at the cut-out wind speed [88]. Both parameters have units of m/s. P(U) is the specific power curve of a turbine, f(u) is the Weibull distribution function with the following formula [79–81]:

$$f(U) = \left(\frac{k}{c}\right)\left(\frac{U}{c}\right)^{k-1} \exp\left[-\left(\frac{U}{c}\right)^{k}\right] \tag{3.6}$$

In this formula, k represents the shape parameter (also known as the Weibull slope), which is a dimensionless parameter, c is the scale parameter of the distribution, and U is the wind speed in m/s.

Another parameter that helps evaluate the performance of a wind turbine is the capacity factor denoted as C_f expressed in percentages. It is expressed as the ratio of the total power

over a certain period P to the maximum nominal power P_R. It has the following mathematical expression [89,90]:

$$C_f = \frac{P}{P_R} \tag{3.7}$$

where: C_f is expressed in percentages, P_E is the anticipated electrical power in MW, P_R is the nominal power in MW.

3.5 Wind data processing and analysis for the height of 100 m

For the study, it was initially necessary to interpolate the data obtained from the ERA5 database. The wind speed data is reported at a height of 10 m. To obtain these values, the logarithmic expression of the wind profile is used, which describes the vertical distribution of wind speed, and the height at which the results are calculated is 100 m.

Figure 3.4 presents data on wind speed at a height of 100 m in the western Black Sea, with the nine sites of interest labeled A1, A2, A3, B1, B2, B3, C1, C2, C3. It is divided into three sub-figures, each representing the average and maximum wind speed in those specific locations.

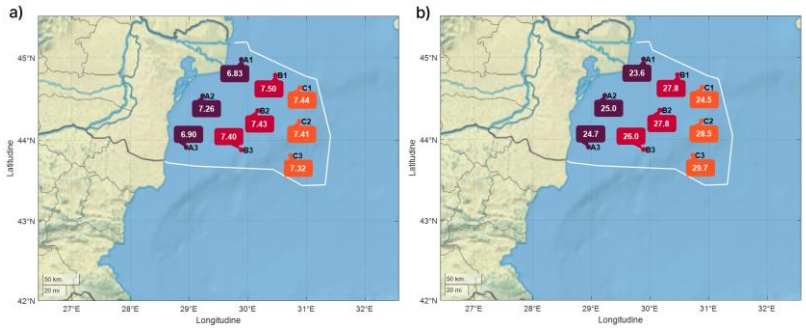

Figure 3.4 a) Average and b) maximum wind speed in m/s at a height of 100 m for the period 2002-2021.

Regarding the average wind speed, site A2 records the highest value of 7.26 m/s, closely followed by the value recorded at site C3, which is located at a greater distance from the western coast of the Black Sea. In the analysis of the maximum, we can observe that the values increase with the distance from the coast, with site C3 recording the highest wind speed value of 29.7 m/s.

Table 3.2 Wind classes interpolated at a height of 100 m.

Wind class	Resource potential	Average wind speed at 100 m α = 0.143 (m/s)	Average wind speed at 100 m α = 0.11 (m/s)
1	Slab	U(z) < 6.1	U(z) < 5.7
2	Marginal	6.1 ≤ U(z) ≤ 7.1	6.1 ≤ U(z) ≤ 6.6
3	Rezonabil	7.1 ≤ U(z) ≤ 7.8	6.6 ≤ U(z) ≤ 7.2
4	Bun	7.8 ≤ U(z) ≤ 8.3	7.2 ≤ U(z) ≤ 7.7
5	Excelent	8.3 ≤ U(z) ≤ 8.9	7.7 ≤ U(z) ≤ 8.2
6	Remarcabil	8.9 ≤ U(z) ≤ 9.7	8.2 ≤ U(z) ≤ 9.0
7	Superb	U(z) > 9.7	U(z) > 9.0

To obtain wind classes at a height of 100 m, Equation 3.2 was used, considering both the Hellmann exponent and the extreme weather exponent (Table 3.2). According to the specialized literature, areas classified as Class 1 are not recommended for wind resource exploitation. It is considered that an area has sufficient wind resources if it is classified as at least Class 2, but there are certain restrictions regarding the tower height.

Figure 3.5 presents the distribution of wind speeds across the 7 classes. It is observed that the predominant class is Class 1, characterized by low wind speeds. This may represent a significant limitation in the development of wind farms in this region. However, there is promising potential in Class 7, representing the best wind resources with high and constant speeds. A detailed analysis shows that Site B1 stands out with results at 26.02% for Class 7.

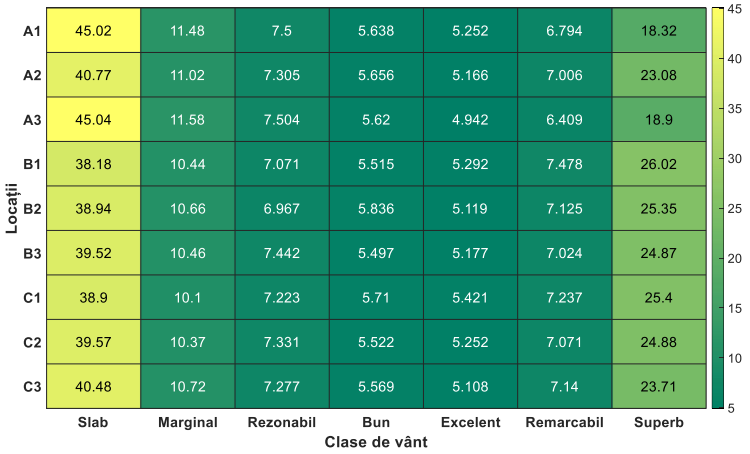

Figure 3.5 Wind speed distribution at 100 m height in % (2002–2021).

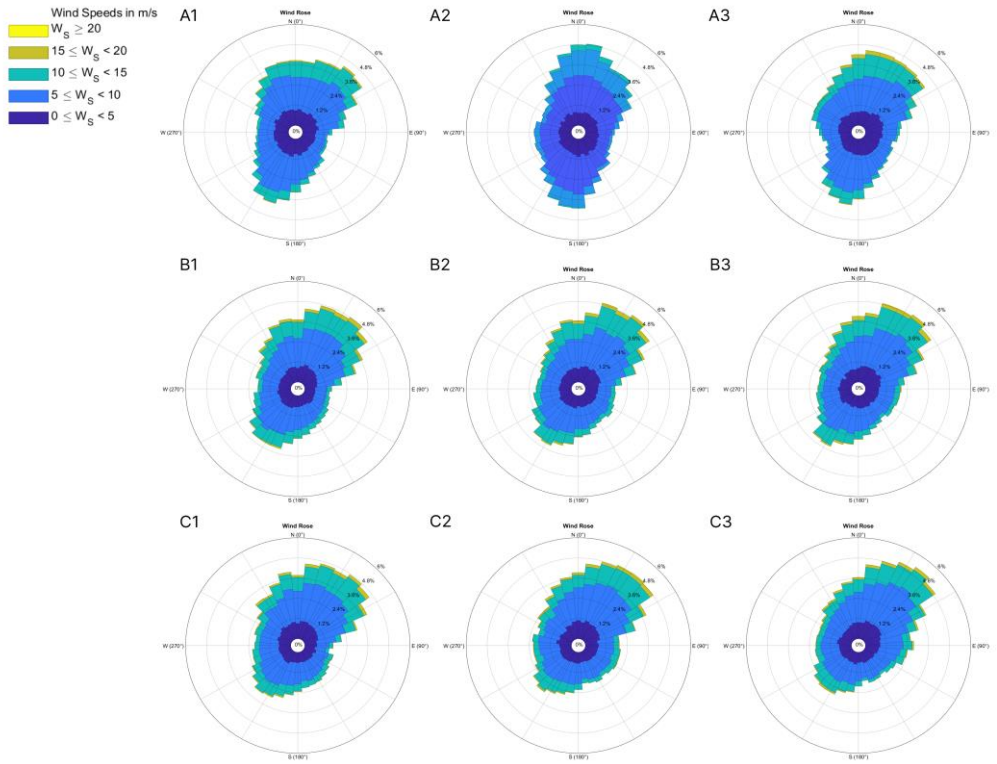

Figure 3.6 Wind rose for the 9 studied locations (2002 – 2021).

Figure 3.6 presents a wind rose for the 9 locations, providing a crucial perspective on the predominant wind direction and speeds in each direction. Observing the wind rose, it can be noted that most locations exhibit a similar profile, with predominant wind directions oriented both northeast (NE) and southwest (SW).

The annual energy production for the 9 selected locations is highlighted in Figure 3.7, using the wind turbines described in subsection 3.2. It can be observed that all 9 locations show similar results regarding wind energy production. Among the 9 locations, Site B1 records the highest values of energy production. For the Siemens Gamesa 8 MW turbine, the average annual production is 28,100 MWh, followed by Site C1 with 27,800 MWh and B2 with 27,600 MWh. These results may be influenced by various factors, such as the average wind speed in each location, specific local characteristics, or turbine configuration.

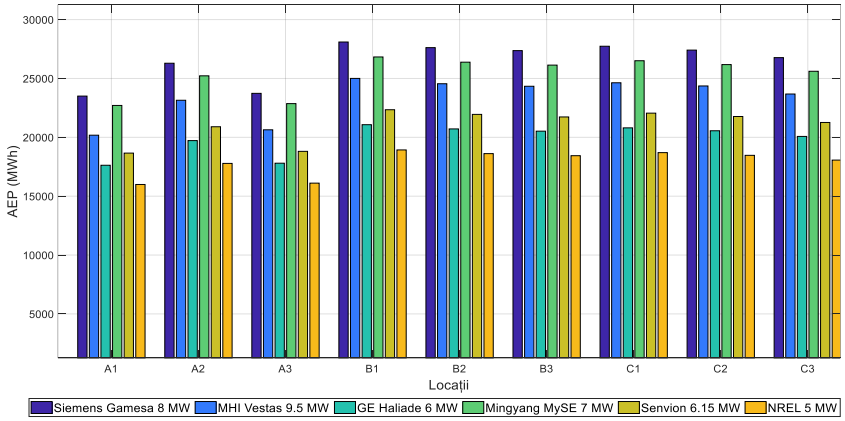

Figure 3.7 Annual energy production for the 9 locations reported for the chosen 6 turbines considering the period 2002 – 2021.

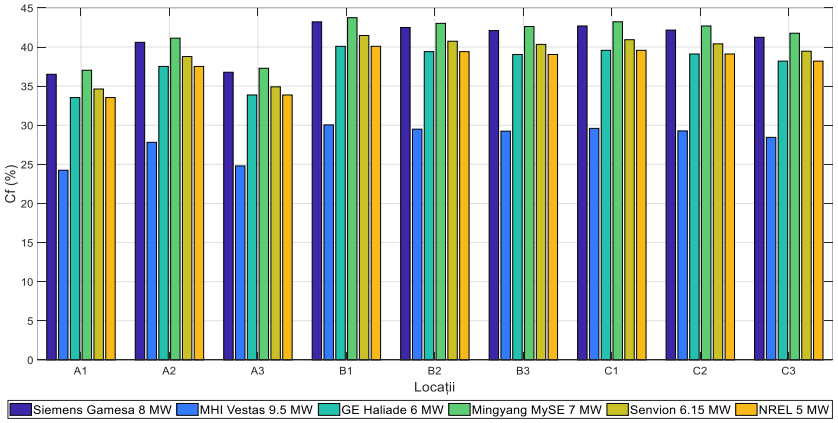

Figure 3.8 Capacity factor for the 9 locations reported for the chosen 6 turbines considering the period 2002 – 2021.

From the analysis of Figure 3.8, we observe that the Mingyang MySE 7 MW turbine records the highest capacity factor. This is mainly due to the fact that this turbine has a low cut-in wind speed required to start generating energy and also a low wind speed required to reach maximum power. These characteristics allow the Mingyang turbine to operate efficiently and produce a higher proportion of its rated power even in variable wind conditions.

Although the MHI Vestas-164-9.5 MW turbine has the highest power, it seems not to be suitable for operation in the chosen area of the Black Sea basin, as it has the lowest capacity factor (approximately 33%), which leads to low AEP values. From the known results, it can be observed that for the turbine with the highest power, the annual energy production is quite low. This is due to the wind speed at which rated power is achieved. In the case of the MHI Vestas-164-9.5 MW turbine, as well as the two turbines from the mentioned study, the rated speeds are higher than 12.5 m/s, which directly affects turbine productivity.

3.6 Conclusions

In this chapter, several reference locations were selected to identify potential suitable projects that could be implemented in this area, as there are currently no operational wind farm projects in the Black Sea. All locations are located near the west coast of the Black Sea, at different distances, but at the same time, all are within the perimeter of the Exclusive Economic Zone of Romania.

Considering the position and climate of the Black Sea, climate change is expected to occur, such as increases and decreases in temperature, which has implications for atmospheric parameters, such as changes in wind speed. Wind resources are directly related to wind speed, and their productivity will be influenced by climate. To understand how these climate changes affect the operation of wind turbines, this chapter focused on the dynamics of wind energy resources. Wind speed data were obtained using the ERA5 reanalysis database, considering a period of approximately 20 years, from January 2002 to December 2021. Each reference location is linked to 6 possible types of turbines (Table 3.2). To identify relevant trends, studies of average and maximum wind speeds, as well as their seasonal variations, were conducted. Furthermore, an evaluation of wind performance is presented.

It was observed that wind speeds are grouped into two major classes, with the most predominant classes being C1 and C7, practically the two extreme classes. Considering the seasonal and monthly variation of the wind, the image of a temperate region was outlined, where there are two opposite seasons, winter and summer, the main cause being the increase or decrease in temperature in these periods. However, there are also two transition seasons in which the months close to those of the mentioned seasons acquire some of their characteristics.

It can also be said that for our area of interest, more advanced wind turbine technologies are not necessary, and turbines such as those from Siemens Gamesa are appropriate. From previous studies regarding the potential of the North Sea [22], the capacity of the Black Sea becomes evident, where wind intensity does not reach the capacity of the North Sea, which is considered the sea with the greatest wind energy potential in Europe, having the largest number of wind farms. However, the Black Sea, which is not yet exploited, could also become a source of energy. Although the onshore wind turbine industry is already used in Romania, there are still no offshore wind farms, although the superior qualities of offshore wind have been demonstrated. In this regard, parameters regarding the performance of wind turbines were analyzed. The obtained results showed remarkable wind resources in these locations. It was also noted that advanced wind turbine technologies are not indicated for these locations, as in the case of high-power turbines such as the MHI Vestas-164-9.5 MW, as they require high wind speeds to reach rated power.

4 Assessment of offshore wind potential in various global regions

After the thorough exploration and analysis of the energy potential of the Black Sea in the previous chapters, we now turn our attention to the global dimension of offshore wind energy. In a world undergoing constant change, with an increasing focus on renewable energy sources, offshore wind energy has become an essential tower in our efforts to shape the planet's energy future.

This chapter builds on our analysis, fitting into the context of the rapid and extensive evolution of the offshore wind energy sector worldwide. The development of wind technologies in the open seas and oceans, along with the ever-increasing production capacity, has transformed this resource into a major player in the fight against climate change and the dependence on fossil fuels.

4.1 Sites of Interest for harvesting wind power worldwide

In the global analysis of wind potential, we have focused on 12 key locations worldwide, each with unique characteristics and considerable potential for wind energy production. In China, we identified an intensively exploited area, demonstrating the country's commitment to wind energy development. Projects such as Huaneng Dafeng, Jiangsu Rudong, and many others already have significant capacity and are under development. This region illustrates China's enormous potential in the field of wind energy.

Near the Caspian Sea, our reference point is near the EnBW Baltic 2 wind farm, showcasing the increased interest in harnessing wind resources in this area. Plans for the Kriegers Flak project with a capacity of 605 MW underscore the growing wind potential in the region.

The Irish Sea stands out with existing wind farms like Walney and future projects. Walney Extension, with a capacity of 659 MW, highlights the importance of this area for wind energy development. With numerous projects in the concept or early design phase, the Irish Sea is a key location for the wind industry.

The Mediterranean Sea draws attention with impressive plans for the Canale di Sicilia, a wind farm with a projected capacity of 2793 MW. This significant initiative underscores the remarkable potential of the region for wind energy production.

In the Adriatic Sea, projects like Romagna 1 and Romagna 2 are evidence of the growing interest in harnessing wind resources. This region enjoys a strategic position and considerable potential for wind infrastructure development.

In the global analysis of wind potential, one of the major points of interest is the North Sea, a region renowned for its extensive development in offshore wind energy. In particular, the Hornsea 2 project stands out as an example of excellence and impressive scale. With an installed capacity of 1,386 MW, Hornsea 2 is the largest offshore wind energy project in the North Sea and, in fact, one of the largest in the world. This impressive initiative not only provides a significant source of clean and sustainable energy but also emphasizes the critical importance of the North Sea region in the global renewable energy industry.

Table 4.1 Coordinates of sites of interest for the global study.

Sites	Location	Latitude (°)	Longitude (°)
P1	Yellow Sea	32° 54' 7.47" N	121° 26' 24.45" E
P2	Taiwan Strait	24° 35' 38.7" N	120° 24' 24.7" E
P3	Arabian Sea	20° 36' 15.3" N	71° 33' 05.3" E
P4	North Sea	53° 53' 6" N	1° 47' 27.6" E
P5	North Sea	53° 15' 55.8" N	1° 22' 45.9" E
P6	Caspian Sea	55° 1' 52.22" N	13° 10' 12.73" E
P7	Irish Sea	54° 1' 1.38" N	3° 35' 30.63" W
P8	Mediterranean Sea	37° 55' 47.9" N	11° 25' 47.9" E
P9	Adriatic Sea	44° 26' 29.85" N	12° 56' 22.91" E
P10	North Atlantic Ocean	41° 4' 51.63" N	70° 44' 16.6" W
P11	Indian Ocean	30° 2' 42.25" S	31°16'49.17" E
P12	Caribbean Sea	32° 54' 7.47" N	121° 26' 24.45" E

In the context of this global analysis, it is important to note that information about the 12 selected locations is systematically and accessibly presented in Table 4.1, and Figure 4.1 complements this information by providing a graphical representation.

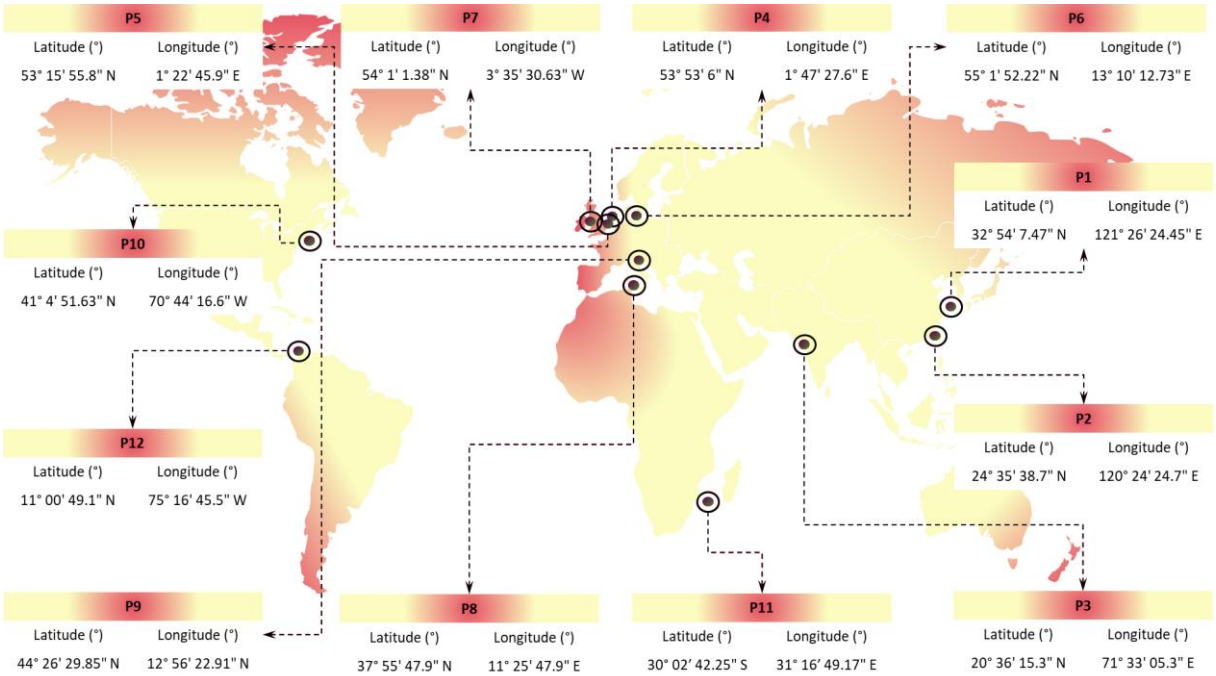

Figure 4.1 Graphical representation of the sites of interest.

4.2 The proposed turbines to be used in the study

In order to obtain a comprehensive and detailed perspective of offshore wind potential, two highly relevant reference turbines were analyzed: Siemens Gamesa SWT-8.0-167 and NREL 5-126, both previously used in the research presented in Chapter 3. The selection of these two turbines was based on pertinent and scientific reasons.

The Siemens Gamesa SWT-8.0-167 turbine was chosen for analysis due to its remarkable performance, which has been carefully documented and validated in the previous chapter. This choice was based on the fact that Siemens Gamesa turbines have demonstrated reliability and efficiency in offshore wind energy production and have been used in numerous major projects worldwide. Therefore, we consider this turbine to be a robust reference for evaluating global wind potential.

On the other hand, the NREL 5-126 turbine was included in the analysis for research and development purposes, as it represents a study turbine used in the industry to investigate and improve technologies and performance in the offshore wind sector. This strategic choice allows us to have extensive and detailed technical data necessary for future analyses and to assess the potential of this type of turbine in various global regions.

Figure 4.2 presents the power curves corresponding exclusively to these two turbines, providing a clear and comparable perspective on their performance in the context of the upcoming development of wind potential.

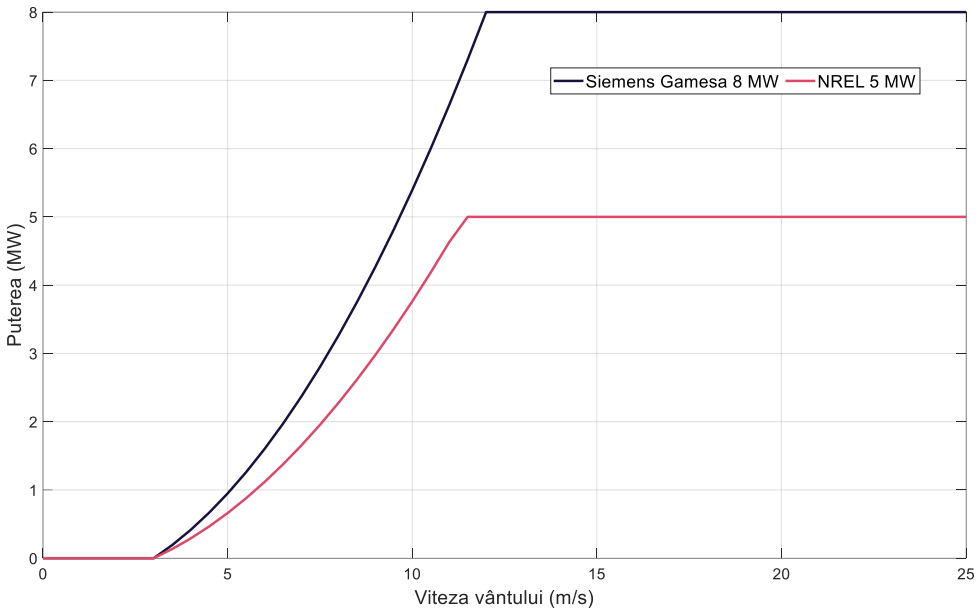

Figure 4.2 Performance of the chosen turbines – power curves.

4.3 Wind data processing and analysis

Figure 4.3 brings to the forefront a detailed analysis of wind speed, organized into wind classes. What can be observed from this figure is that the distribution of these wind classes varies significantly from one location to another, with the only common aspect being the dominance of certain classes. In particular, classes 1 and 7 stand out as predominant in most locations.

However, there are some locations, such as P3 (Arabian Sea), P9 (Adriatic Sea), and P12 (Caribbean Sea), where the predominant speed is in class 1. This suggests that these locations are not ideal for harnessing wind resources, as class 1 is characterized by very low wind speeds, and, according to the analysis, only a small percentage, maximum 30%, is suitable for wind activities. This indicates that these locations are not recommended for placing wind turbines.

On the other hand, there are locations with impressive wind resources, such as those in P4 (North Sea), P5 (North Sea), P6 (Caspian Sea), P7 (Irish Sea), P10 (North Atlantic Ocean), and P11 (Indian Ocean). Among these, P2, P4, and P7 stand out with the highest percentage of wind speeds exceeding 10 m/s.

It is not surprising that these locations coincide with the most energetically exploited ones, where numerous wind farms and wind developments exist in adjacent areas.

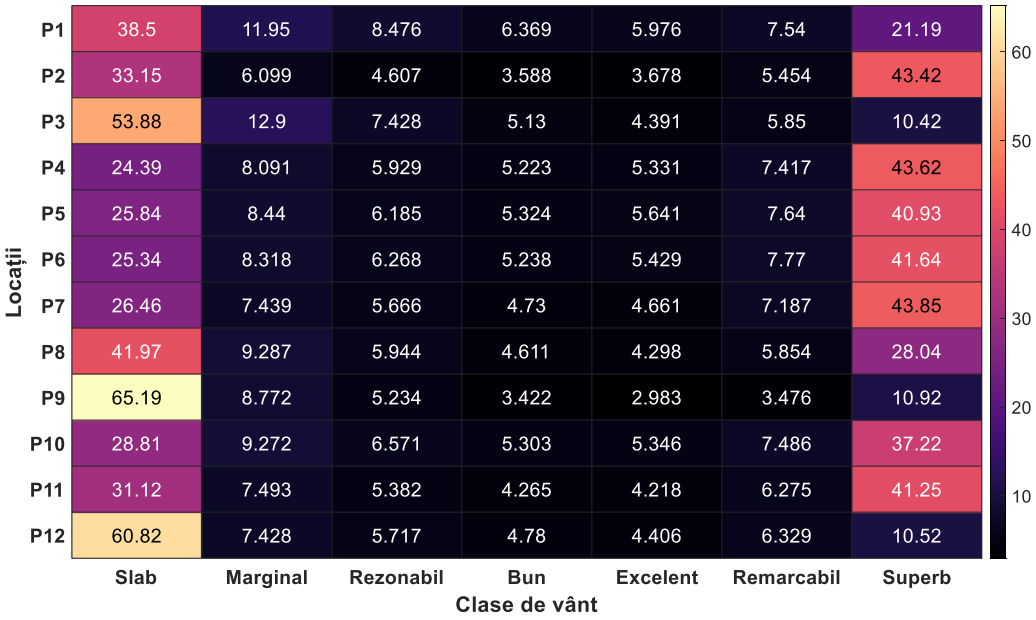

Figure 4.3 Wind classes associated with the 12 locations for the period 2002-2021.

Figure 4.5, depicting the wind rose for the 12 locations, provides an essential perspective on wind behavior in these regions. This type of representation illustrates both the predominant wind direction and the wind speed range in different directions.

A notable location is P2 (Taiwan Strait), which has a predominant wind direction from the NE (northeast) with a frequency of 27%. Wind speeds in this location mostly fall within the range of 10-15 m/s, with 8% exceeding the 15 m/s threshold. This suggests that P2 has significant wind potential and can be a highly efficient wind energy development site. For P11 (Indian Ocean), it is observed that there are predominant directions from both NE and NW (northwest), with wind speeds ranging between 15 and 20 m/s for both directions. This indicates that P11 exhibits a unique behavior with the potential to produce energy consistently, regardless of the wind direction. In contrast, P12 also has a consistent direction from the NE, but the wind intensity in this location is quite low, which may limit its potential for wind energy production. Locations P4, P5, P6, and P7 exhibit similar behaviors, given their proximity. All four locations record significant percentages with wind speeds between 15 and 20 m/s, without having a predominant wind direction. These data suggest that these locations have the potential for wind energy production under favorable conditions.

Overall, even when the wind direction varies, modern wind turbine technologies are equipped with orientation devices that allow adjusting the turbine based on the wind direction. This enables efficient wind energy production in a wide range of conditions, making these locations potential significant sources of renewable energy.

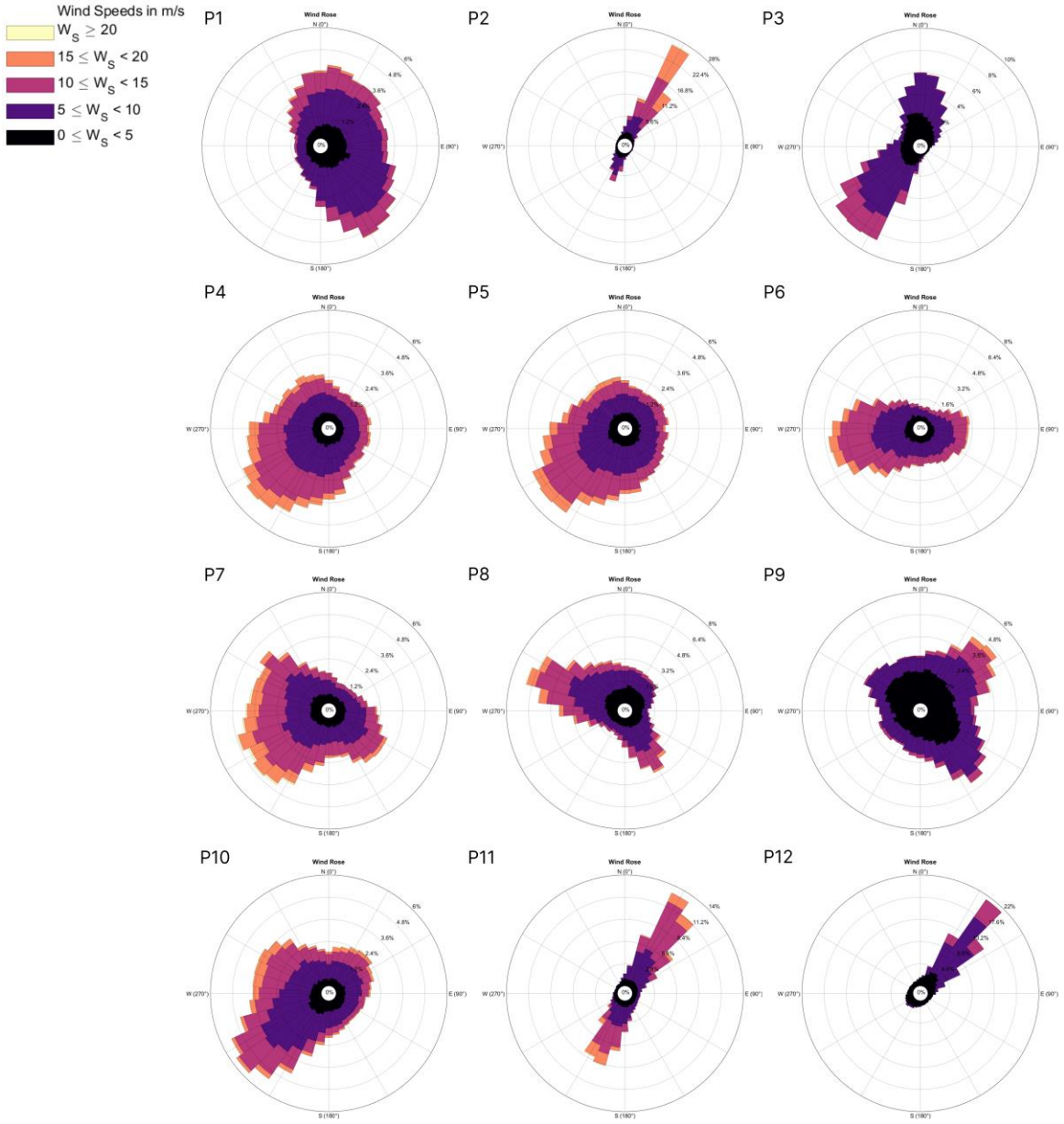

Figure 4.4 Wind rose for the 12 selected locations for the period 2002-2021.

Figure 4.5 confirms the previous finding that P3 and P9 are locations with lower wind speeds, having the lowest AEP values (1.79 TWh and 1.57 TWh, respectively). These values are significantly lower than the AEP recorded for P4 and P7. The most productive locations are predictably those with the best wind classes, as mentioned earlier in Figure 4.5. These locations are also identified in Figure 4.7 as having the highest AEP values.

What is interesting is that, compared to the Siemens Gamesa 8 MW turbine, the productivity of the NREL 5 MW turbine is lower by about a third. This is due to the lower nominal power of the NREL 5 MW turbine. However, the NREL 5 MW turbine has a lower cut-in speed of 11.6 m/s, making it more suitable for low-wind intensity locations.

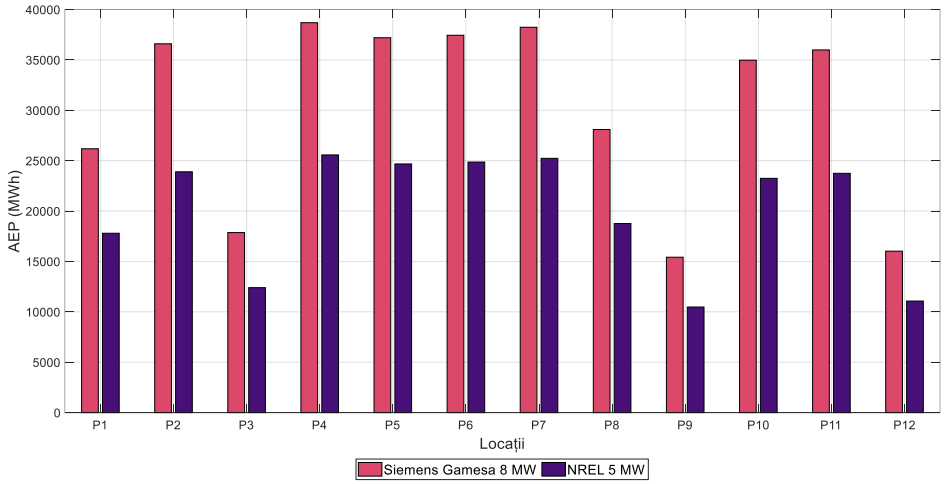

Figure 4.5 Annual energy production for the 12 locations (2002-2021).

To provide a broader context for the observations in Figure 4.6, it can be noted that locations P4 and P7 stand out with the highest capacity factor values. This indicates that these two locations have relatively stable wind speeds situated near or within the range of 12-25 m/s and 11.6-25 m/s, respectively. These favorable conditions allow the turbines to operate nearly consistently at maximum capacity, close to the nominal power of 8 MW (for the Siemens Gamesa turbine) and 5 MW (for the NREL turbine).

In contrast, locations P3, P9, and P12 record the lowest capacity factor values. This is due to the prevalence of wind class 1 in these areas, making wind energy production inefficient as the turbines rarely operate at the capacity required to reach 8 MW or 5 MW power. A notable aspect is that the performance of the NREL 5 MW turbine is better than that of the Siemens Gamesa 8 MW turbine. This is because NREL turbines can reach nominal power at lower wind speeds, making them more efficient under the conditions specified in Figure 4.6.

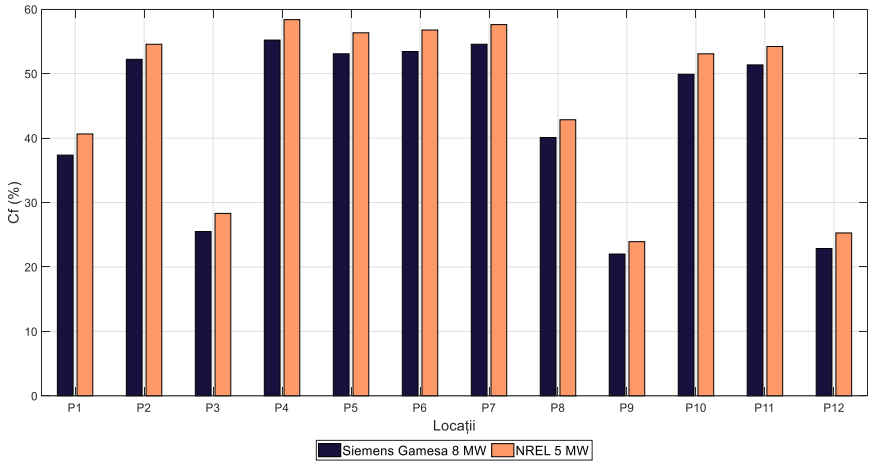

Figure 4.6 Capacity factor for the 12 locations considering the period 2002–2021.

Comparing the results obtained in this chapter with those in Chapter 3, where various locations in the Black Sea were analyzed, a notable similarity in the behavior of the Black Sea with that of locations P1 (Yellow Sea) and P8 (Mediterranean Sea) can be observed. This

comparison provides an interesting perspective on the similarities in wind characteristics across different regions.

All the results obtained in this thesis represent an extension of the research initiated in the work [91]. However, to ensure coherence and relevance within the PhD thesis, it was deemed necessary to modify the analyzed period to obtain a comprehensive perspective on the evolution of the analyzed phenomena.

4.4 Conclusions

In this chapter, the wind energy potential for 12 offshore locations worldwide has been analyzed, all of which are either currently exploited or under development in terms of wind energy. These locations were chosen to represent a variety of wind conditions and potential for renewable energy production. Among these, the Yellow Sea location stands out as one of the most intensively exploited areas, already hosting several operational or in-development wind farms, such as Huaneng Dafeng - Phase 1 - 300 MW, Huaneng Dafeng - Phase 2 - 100 MW, and others. The same level of exploitation intensity is encountered in the North Sea, home to wind farms like Hornsea Project One - 1218 MW, Hornsea Project Two - 1386 MW, and others.

In contrast, less exploited locations, such as those in the Mediterranean Sea and the Adriatic Sea, are areas of interest for future wind farm development, such as Canale di Sicilia with a planned capacity of 2793 MW and the Romagna 1 (120 MW) and Romagna 2 (400 MW) farms. These locations were selected to provide a comprehensive picture of the variation in wind potential globally.

The analysis covered a 20-year period, from January 1, 2002, to December 31, 2021, using data obtained from the ERA5 database. This study revealed that the North Sea is one of the most intensively exploited areas due to its rich wind energy resources. Site P4 proved to have the highest values for both annual energy production and capacity factor, with wind speeds consistently in the range of 12-25 m/s. Point P7, located in the Irish Sea, demonstrated significant potential, with resources similar to those in the North Sea, suggesting that the Irish Sea could play a crucial role in offshore wind energy production. On the other hand, location P9 in the Adriatic Sea showed weaker results in terms of annual energy production and capacity factor, with predominant wind speeds between 0 and 10 m/s. This explains why certain locations are not exploited as intensively as others. However, with the help of appropriate technologies and strategies, the capacity factor can be improved to maximize renewable energy production.

Work [92] focuses on studying the exploitation of offshore wind and solar energy resources in the Mediterranean region. The authors use data from ERA5 reanalysis to assess the potential for renewable energy production in this region over an extended period. Following this analysis, Figure 2 presents the results obtained for wind power density at a height of 100 m for the four seasons. From the figure, values can be extracted as 760 W/m^2 for winter, 600 W/m^2 for spring, 240 W/m^2 for summer, and 450 W/m^2 for autumn. All these values are close to those obtained in this chapter, reported for the Mediterranean Sea location (P8).

Comparing the average speed at a height of 100 m obtained for locations P4, P5, and P7, located in the North Sea and Irish Sea, around the value of 9-9.2 m/s, with the results obtained in the study [93], a notable similarity can be observed. In the mentioned study, the average speed for our locations can be extrapolated from Figure 2, resulting in wind speeds ranging from 9 to 10 m/s, making the results convergent. In another earlier study [22], related to the potential of the North Sea, Figure 3 presented seasonal and monthly variabilities, for

which a seasonal variation of about 0.4 and a monthly variation of around 0.5 were obtained. These values are in line with those obtained in this chapter, showing a difference of about 10-20%.

For the P1 location (Yellow Sea), the power density is approximately 400 W/m^2 in this report, while in Costoya et al.'s work [94], the power density for the same location is shown in Figure 4.a and is approximately 480 W/m^2. We observe that there is, however, a difference of 80 W/m^2 between the two values. This difference could be attributed to several factors, and one of them could be the difference in the analyzed periods. This analysis is reported for the years 2002-2021, while the analyzed period in the mentioned work is between 1986-2005. At the same time, from Figure 4.b, we observe that, for the near future period, the power density in this location decreases, which may indicate a natural variation in wind resources over time.

In conclusion, this chapter shows that, although not all locations have impressive wind energy resources, wind farms can significantly contribute to phasing out conventional energy production. By improving the performance of wind turbines and adapting them to the specific conditions of each location, it is possible to develop efficient wind farms that can generate significant amounts of green energy. This chapter emphasizes the importance of researching and exploring different locations globally to find significant wind energy resources and contribute to the transition to renewable energy sources.

5 Wind power produced by airborne wind turbines

The purpose of this chapter is to provide a comprehensive perspective on wind resources in the Black Sea region by making a direct comparison between wind conditions reported at the standard height of 100 meters, where most offshore wind turbines operate, and those recorded at much higher altitudes, such as 400 meters, where, in the future, Airborne Wind Energy Systems (AWES) generators could be installed. In addition to assessing wind resources, this chapter also takes into account the performance of various wind converters.

This promising technology has the potential to expand access to wind resources available at higher altitudes, where winds are stronger and more consistent. Evaluating wind resources for AWES at altitudes up to 400 meters could provide significant insights into the viability of these systems for offshore wind energy generation in the Black Sea region.

5.1 The fundamentals of functioning of airborne power generation technologies

At higher altitudes, the wind is often stronger and more persistent in most parts of the world. Airborne Wind Energy Systems (AWES) [95] aim to harness this untapped energy potential, which is inaccessible to conventional ground-based wind turbines. The concept of harvesting wind energy using Airborne Wind Turbines (AWT) is new and exciting. The kite's apex is equipped with a turbine, an electric generator, and a power converter. The generated electricity is transmitted to the ground through a medium-voltage cable [96].

The classification refers to Airborne Wind Energy Systems (AWES) based on their interactions with the ground and methods of energy production. These systems are divided into two main categories: Ground-Gen AWES (with Ground Generator) and Fly-Gen AWES (with Flying Generator) (Figure 5.1).

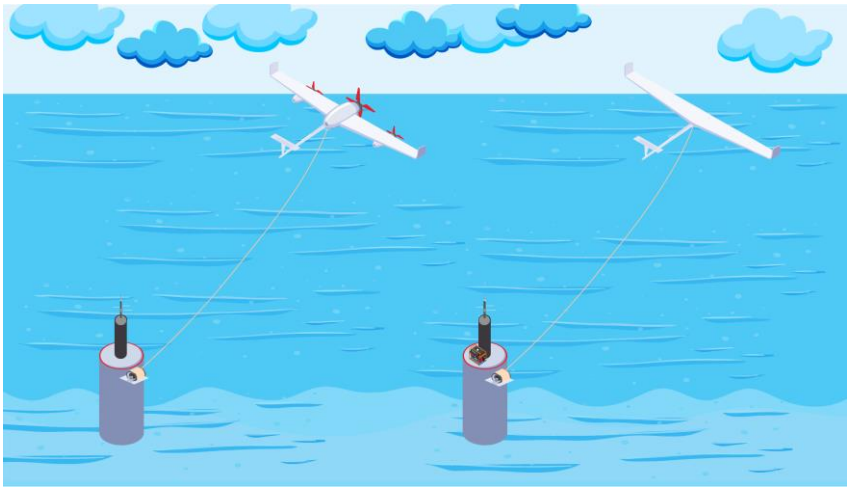

Figure 5.1 Types of AWES systems a) Fly-Gen System; b) Ground-Gen System.

According to Betz's law [97], only the tip of the blade and/or a lightweight turbine are necessary to generate a given amount of electrical energy, as the kite flies at a speed several times faster than the actual wind speed. The AWES concept is highly attractive, considering that 30% of the blade length produces more than half the power of a conventional turbine (Figure 5.3) [97,98].

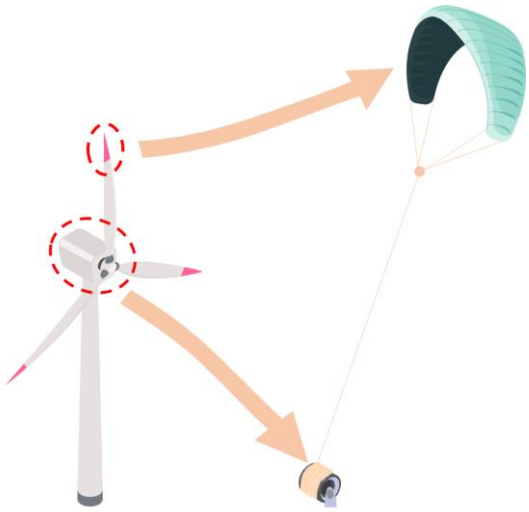

Figure 5.2 The fundamental idea of AWES systems with a ground generator.

5.2 High altitude wind data processing and analysis

Meteorological data was extracted from the ERA5 reanalysis database over a 20-year period (January 2002 – December 2021) to cover the entire Black Sea region and evaluate wind conditions at a height of 100 meters (U100).

However, the concept behind Airborne Wind Energy Systems (AWES) is to operate at much higher altitudes, such as 1000 meters, as seen in the Kite Gen project [99]. Wind speed increases significantly with height, up to the atmospheric boundary layer, and this relationship follows a logarithmic function [100]. Thus, to adapt the initial dataset to the specific operational height of the AWES system, a wind logarithmic profile is applied [101]. This adjustment is necessary to accurately reflect the wind characteristics at the desired height of the AWES system and ensure a precise assessment of the energy generation potential. To obtain the wind speed for the operation of an AWES system, the logarithmic wind profile is again used, but this time using U100 as the reference speed.

$$U_{AWES}=U_{ERA5}\frac{\ln(z_{AWES})-\ln(z_{ERA5})}{\ln(z_{ERA5})-\ln(z_0)} \tag{5.1}$$

Where: U_{AWES} – is the wind speed adjusted for a specific AWES; U_{ERA5} – is the wind speed associated with ERA5 data (U100 in this case); z_{AWES} – is the operating height of an AWES; z_{ERA5} – is the reference height of wind data according to ERA5 (100 m in this case); z_0 is the surface roughness coefficient, with a value of 0.0002 m [102]. It's important to note that while this method may seem less precise for higher atmospheric layers, it is reliable enough to estimate marine wind resources based on the information provided by Schelbergen et al. [103].

For this chapter, only the parameter U100 has been considered for six-hour intervals (00:00:00, 06:00:00, 12:00:00, 18:00:00) of each day to avoid possible uncertainties that may arise when using the logarithmic wind law.

5.3 Airborne wind energy systems

The performance of a specific wind turbine (a three-blade system) can be expressed through a power curve, establishing a direct relationship between the designed power and a specific wind speed. Figure 5.3 illustrates these curves, including a 5 MW wind turbine already analyzed in Chapter 3, and two Airborne Wind Energy Systems (AWES) (500 kW and 5 MW); these three systems will be further considered for evaluation. Based on this information, the wind turbine's performance has already been analyzed for a tower height of 100 m, compared to AWES, where two operating heights will be used (200 and 414 m). It is important to note that, in Weber et al. [100], a clear distinction is made between an AWE with flexible blades and one with rigid blades, while this chapter uses only information related to generic power curves.

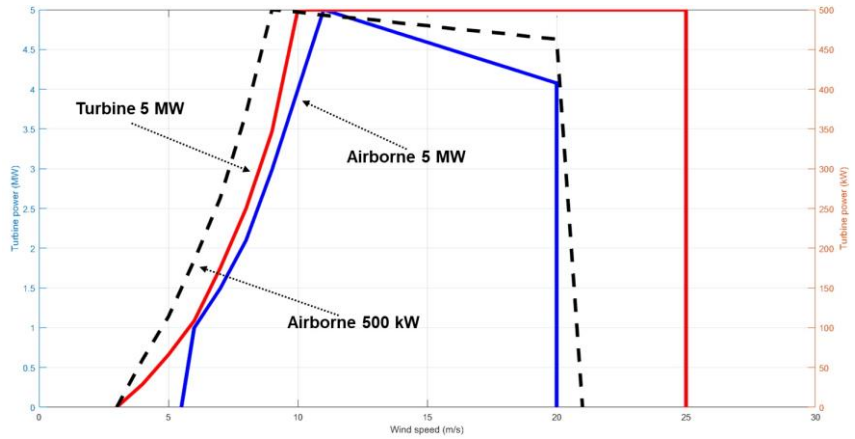

Figure 5.3 Power curves of wind turbines according to Weber et al. [100].

5.4 Results obtained for airborne wind energy systems

An initial overview of the wind resources of the Black Sea is presented in Figure 5.4, showing the spatial distribution of the U500 parameter (average values). As expected, the central and western parts of this region exhibit more consistent values, with significantly higher values displayed for the Sea of Azov (located to the north). For the western coastal area, wind conditions in the range of 6 to 8.2 m/s represent a common trend, especially along the Romanian coastline.

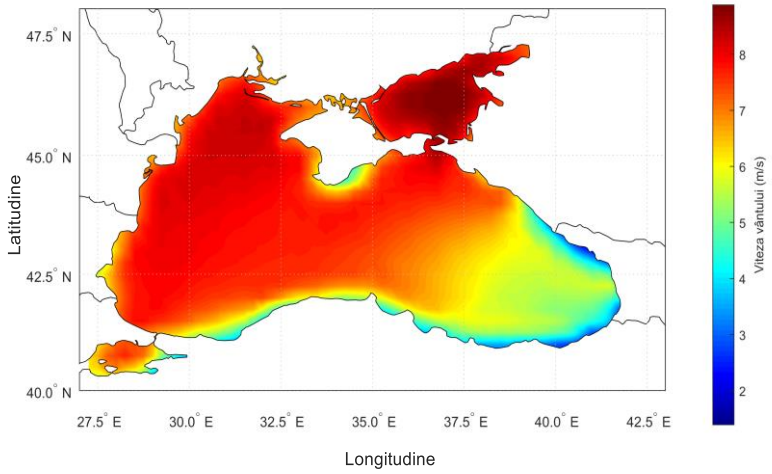

Figure 5.4 Average wind speed at a height of 500 m [104].

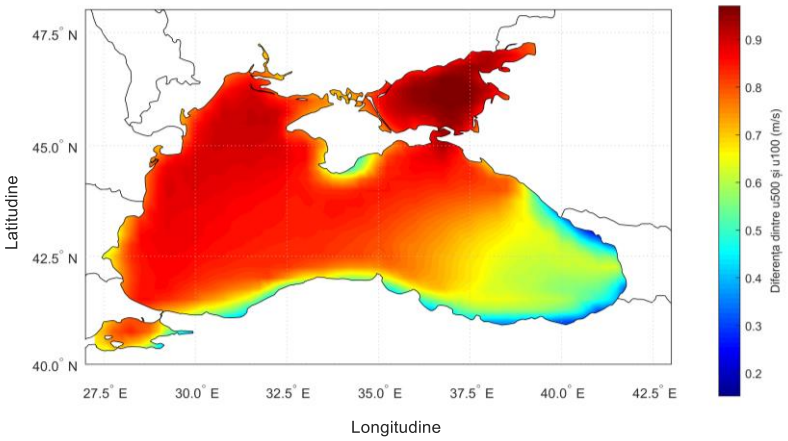

Figure 5.5 Direct comparison between wind conditions associated with reference heights of 100 and 500 m for the time interval 2002 – 2021 (U500 minus U100 — in m/s) [104].

Figure 5.5 represents a detailed analysis of the differences between two distinct wind fields, U500 and U100, throughout the entire dataset. The choice of the U500 parameter for comparison is justified because it represents an average height at which an airborne system can operate, being relevant in the context of exploiting renewable wind resources. By examining the anticipated variations between the two wind fields, it is observed that they fall within the range of 0.3 to approximately 1 m/s.

Figure 5.6 a) provides an initial perspective on the performance of airborne wind energy systems (AWES) by presenting the annual electricity production of a 500 kW system with an average flight altitude of 200 m. This analysis reveals a gradual increase in electricity production, starting from 0.5 GWh in the eastern coastal areas, up to 1.25 GWh in the eastern offshore region. Additionally, values progressively increase to peak at 2.39 GWh in the western sector.

Figure 5.6 b) illustrates the capacity factor of the aforementioned airborne system with a capacity of 500 kW. According to these data, we observe that the maximum values of the capacity factor range between 55% and 58%, with outstanding performances near the Sea of Azov. In the offshore region, situated between 30% and 32.5% on the Black Sea map, more stable values of this factor are noticeable, starting to decrease until reaching a level of 35% near the eastern coast.

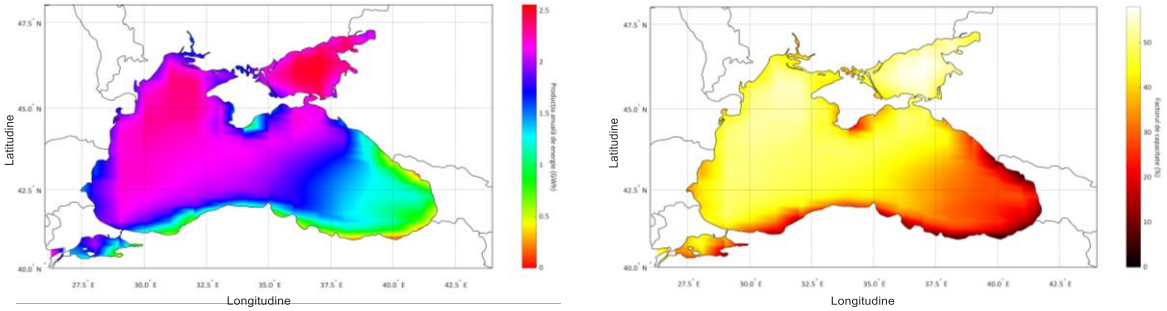

a) b)

Figure 5.6 a) Annual energy production; b) capacity factor (in %) for the estimated 500 kW AWES system under U200 wind conditions for the time interval 2002 – 2021 [104].

The results of the analysis (Figure 5.7) reveal that, for this operational height, the performance of the 5 MW AWES system is substantially lower compared to that of a traditional wind turbine. In the Sea of Azov region, estimates indicate a maximum AEP production of 16.33 GWh. In the Black Sea, electricity production reaches a maximum of 14.34 GWh in the northwest sector, gradually diminishing to 10 GWh in the southwest.

The capacity factor for the Black Sea region exhibits variations ranging from 5% to 33%, depending on the specific region of interest.

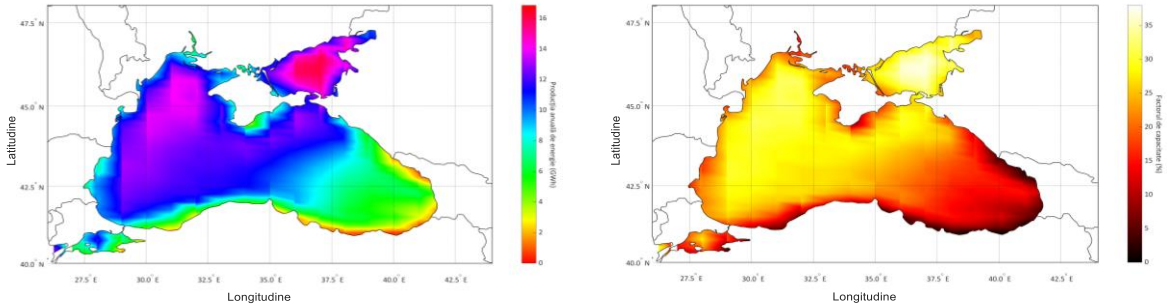

a) b)

Figure 5.7 a) Annual energy production; b) capacity factor (in %) for the estimated 5000 MW AWES system under U200 wind conditions for the time interval 2002 – 2021 [104].

Figure 5.8 highlights the evaluation of the 5 MW AWES system's performance at a reference height of 414 m, presenting results regarding annual electricity production and, respectively, the capacity factor. These data provide a more detailed perspective on the system's performance in various regions. In the case of the Black Sea, significant improvements in AWES performance compared to the 200 m height are also highlighted.

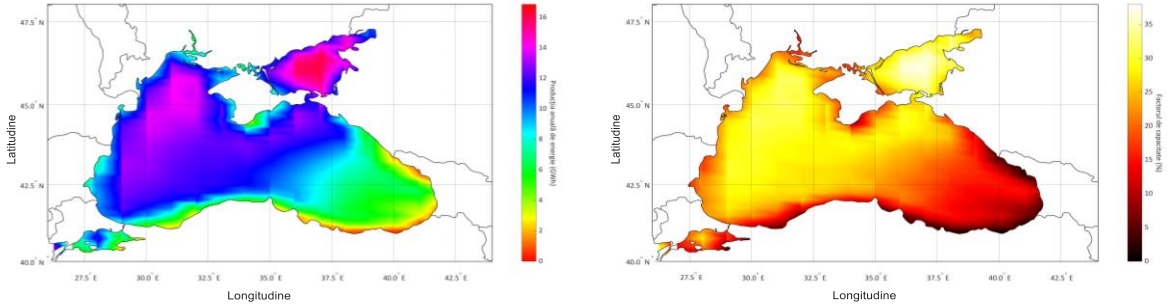

a) b)

Figure 5. 8 a) Annual energy production; b) capacity factor (in %) for the estimated 5000 MW AWES system under U414 wind conditions for the time interval 2002 – 2021[104].

Data validation is essential. According to reference [105], which analyzed wind speeds using in-situ data for three locations in the western Black Sea, the average wind speed for the years 2015–2020 at a height of 2.5 m was 6.7 m/s (which corresponds to approximately 9.3 m/s at a height of 100 m). The results obtained in this study indicated an average wind speed of about 8 m/s for the same location. It is important to note that the ERA5 database seems to underestimate wind speeds, although these differences can be attributed to temporal variations and an irregular wind profile. Nevertheless, these results suggest the possibility of better wind resources than those recorded, which is beneficial for the energy industry.

5.5 Conclusions

In this chapter, a comprehensive overview of the wind energy potential in the Black Sea has been provided, considering different reference heights and wind turbine technologies. The entire study was based on wind data from the last 20 years (2002-2021) extracted from the ERA5 reanalysis project. Overall, this project tends to underestimate regional wind resources, as shown by the comparison with in-situ measurements. Although the Black Sea was the focus of this study, it is noteworthy that the best wind resources were, in fact, found near the Sea of Azov (northern area), regardless of the time interval considered. However, given the current geopolitical situation, it is challenging to anticipate the implications of a renewable energy project for this area.

Regarding wind turbines, all results were presented in terms of spatial maps covering the entire Black Sea, which, to the author's knowledge, can be considered an innovative element for this region. It is important to note that no restrictions were included in these maps (e.g., maritime routes, exclusive zones, etc.). The main element of originality lies in the analysis of airborne wind energy systems (500 kW and 5 MW) since such an analysis has not been conducted previously for this geographic region (either on land or at sea). Based on existing literature, several scenarios were developed where the optimal flight altitude of AWES was defined for two particular heights (200 and 414 m).

From the comparisons of 5 MW systems, it is clear that the traditional wind turbine (with three blades) offers better performance, regardless of the operational heights of AWES. From a direct comparison (using airborne values - U200) of electricity production, a difference of 22% was observed in the western part of the Black Sea and a maximum of 80% in the eastern area. However, similar performance can be expected only if such an AWES can operate at altitudes above 750 m.

Although the operating principles of airborne generators are similar, most AWE systems are still in the early stages of development. To become competitive with traditional wind turbines, these airborne systems need to be able to improve their production capacity. The scalability process must be carefully planned, as the kite's traction force will increase significantly, while the overall characteristics of the airborne generator need to be upgraded. For example, in the work of Dominguez Santana and El-Thalji [106], a 30 kW prototype was scaled up to a 1500 kW version. In this case, the following modifications were identified: the traction force increased from 7.5 to 375 kW; the diameter of the traction cable increased from 2 to 30 mm; and the drum diameter increased from 0.25 to 1.2 m.

6 Analysis of the offshore wind turbine tower's structure

Offshore wind turbine foundations play a crucial role in harnessing wind energy from the open sea. These tall structures are carefully designed and constructed to support the entire wind turbine system, enabling the capture of clean and renewable energy from the strong offshore winds.

The foundation, typically made of steel or concrete, is built in sections, each composed of cylindrical tubes. These sections are manufactured off-site in specialized facilities. Steel foundations are constructed from conical sections of tubular steel welded together in lengths ranging from 30 to 40 meters and then transported to the construction site for assembly. In the case of concrete foundations, molds are used to achieve the desired shape, and the concrete is poured and allowed to set.

The height of onshore wind turbines is greater to exploit the stronger wind speeds. However, the powerful wind speeds in the maritime zone can be harnessed at lower altitudes. Therefore, foundations for offshore wind turbines can be shorter, as the same height is not required to achieve similar wind speeds [107]. Once the foundation sections are fabricated, they are transported to the installation location of the offshore wind farm using specialized vessels. The assembly phase begins once the foundation sections have reached their destination. Large installation vessels equipped with cranes are used to lift and position each foundation section accurately. Alignment is done precisely, and the sections are securely fastened using bolted connections or welding.

6.1 Wind turbine and tower characteristics

The selected turbine for this chapter is the Vestas V112-3 MW, corresponding to IEC Class I. This type of wind turbine has a horizontal axis with wind orientation. The turbine is equipped with a three-blade rotor positioned by a microprocessor-controlled pitch system. The turbine's characteristics are presented in Table 6.1 and Figure 6.1.

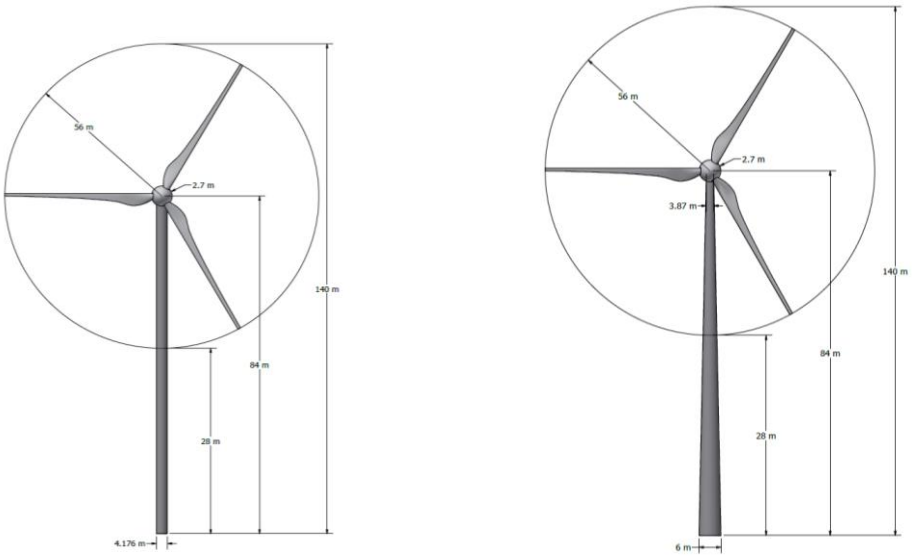

(**a**) (**b**)

Figure 6.1 The 2D model for the wind turbine a) with cylindrical tower; b) with conical tower [108].

Table 6.1 Turbine characteristics.

Properties	Values	
Rated capacity	3 MW	
Wind class	IEC Ia	
Rotor diameter	112 m	
Area	9852 m^2	
Mass (blades, rotor and nacelle)	155 t	
Hub height	84 m	
Material	Steel S355JR	
Tower type	Cylindrical	Conical
Tower diameter	4.176 m	6 m at base 3.87 at top

The material characteristics of the tower from the Vestas V122-3 MW turbine are presented in Table 6.2.

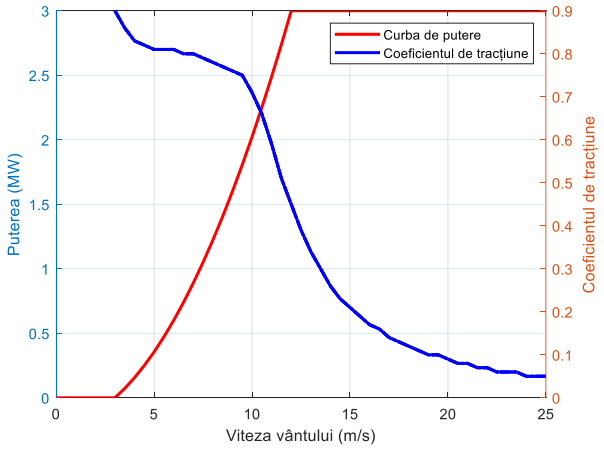

Figure 6.2 Power curve and thrust coefficient of the turbine Vestas V112-3 MW [108].

Table 6.2 Tower material characteristics.

Properties	Values
Young's modulus (E)	$200 \cdot 10^3$ MPa
Density (ρ)	7800 kg/m^3
Poisson's ratio (v)	0.3

6.2 Fundamental presuptions

- The tower was considered to be a cantilevered beam fixed to the structure. At the top, a load equal to the combined mass of the nacelle, blades, and rotor was applied.
- The tower material was assumed to be isotropic and homogeneous. One tower has a constant circular cross-section along its height, while the other has a tapering cross-section from the base to the top, both with relatively small thicknesses of the shell.
- Secondary effects were neglected (such as axial and shear deformations and moment of inertia).
- Distributed aerodynamic loads were caused only by the traction forces.

6.2.1 Load calculations

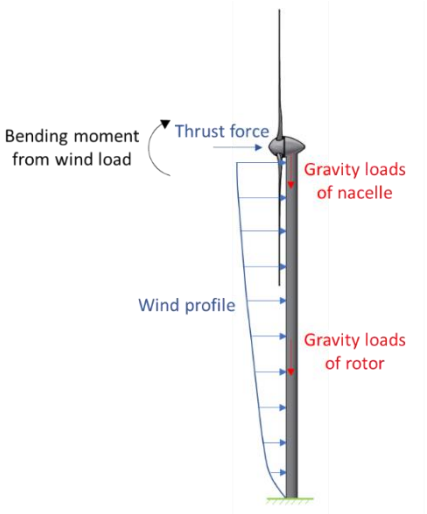

Figure 6.3 The forces and moments acting on the tower [108].

The main loads acting on the tower are gravitational loads and aerodynamic loads resulting from wind action, which can be traction and bearing forces. Aerodynamic loads were grouped into two categories: those acting directly on the tower and those acting on the rotor and transferred further to the upper part of the tower. The forces and moments acting on the turbine are illustrated in Figure 6.3.

6.2.2 Gravitational loads

Gravitational loads are determined by the weight of the supported components, which in this context include the nacelle, rotor, and wind turbine blades. Together, these components have an approximate weight of 155 tons. This gravitational load contributes to the development of compressive stresses on the tower structure.

To illustrate this influence, a simplified model was used, involving placing a mass point at the top of the tower. This mass point effectively represents the point where the total weight of the wind turbine components is concentrated.

6.2.3 Aerodynamic loads

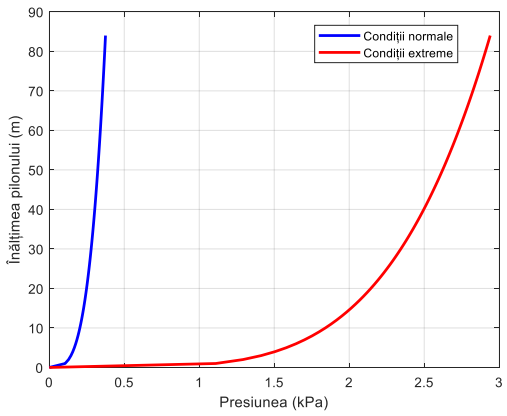

Figure 6.4 The pressure applied along the two towers [108].

$$F_d=\frac{1}{2}\rho_{air}U(z)^2C_dD(z) \tag{6.1}$$

where: ρ_{air} is the air density (having the value of 1.225 kg/m^3), U(z) is the wind velocity at height z (in m/s), C_d is the drag coefficient (this parameter has a value of 0.7), D(z) is the tower diameter at height z (in m).

Wind speed varies along the tower height under normal wind conditions, and it will be calculated using formula 3.2.

For the extreme wind model, wind speed was calculated using the formula below, according to the IEC 61400-1 standard [109]:

$$U_{e50}=1.4\cdot U_{ref} \tag{6.2}$$

Offshore wind turbines are classified based on wind speed and turbulence parameters, according to the IEC standard. In the formula above, U_{e50} is the predicted extreme wind speed with a 50-year return period (in m/s). The chosen turbine belongs to the IEC Ia class, and according to the standard, the reference speed U_{ref} is 50 m/s.

Using the power law wind profile equation, the above equation becomes:

$$U_{(e50)_z}=1.1\cdot U_{ref}\left(\frac{z}{z_{tower}}\right)^{\alpha} \tag{6.3}$$

In addition to the loads imposed by the wind on the tower, the top of the tower was also affected by a series of forces and moments resulting from the wind action on other components of the turbine assembly [110]. The design standard IEC61400-1 [109] defines twenty-two load cases for turbine design, covering all operating conditions from startup to extreme conditions. The typical cases used were those in extreme wind conditions and those in normal operating conditions. The aerodynamic force resulting from the wind action on the rotor can be calculated using the formula [111,112]:

$$F_x=\frac{1}{2}C_T\rho U^2A \tag{6.4}$$

Where: C_T is the thrust coefficient, ρ is the air density (with a value of 1.225 kg/m^3), U is the wind speed in m/s, and A is the area described by the blades in m^2.

6.3 Tower performance analysis and optimization in various black sea locations

Within Chapter 3 of the study dedicated to exploring the potential of renewable wind energy in the Black Sea area, significant results have been outlined. Carefully analyzing the six points of interest, two remarkable locations for wind speed assessment at a height of 100 meters have been identified. Point B1, where the water depth reaches 58 meters, highlighted the highest interpolated values of wind speeds. This emphasizes remarkable potential for harnessing wind energy in this area. At the same time, we chose to consider the location of point C3, characterized by an impressive depth of 1000 meters.

In this phase of the study, the algorithm described in Chapter 3 was carefully implemented for calculating wind speeds at a height of 84 meters.

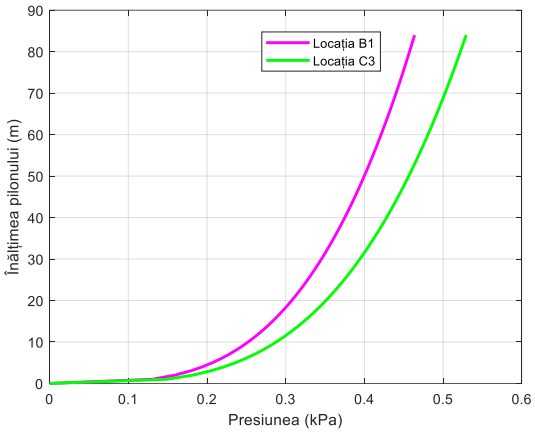

Figure 6.5 Pressure applied along the tower height for the conditions in the Black Sea.

Table 6.3 Information related to the chosen location.

Data	Values	
Location	B1	C3
Longitude (°)	30.47	30.73
Latitude (°)	44.79	43.81
Depth (m)	58	1000
Maximum wind speed at 84 m (m/s)	27.8	29.7
Average wind speed (m/s)	7.5	7.32

As the chosen points have a maximum wind speed value of 27.8 m/s and 29.7 m/s, an attempt was made to reduce the thickness of the tower wall in two steps, by 25% and 50%, for the strength study.

6.4 Results obtained from finite element analysis

The most common method for designing the tower of a wind turbine is the manufacturing of sections between 20 and 30 meters coupled with flanges at both ends and then fixed in place. In this chapter, only the tower sections were considered without simulating the connections. The tower was divided into four sections, three with a length of 20 meters and one with a length of 24 meters. The two towers were modeled as shell structures in ANSYS [113,114], using 8-node elements. The main features are detailed in Tables 6.1 and 6.2. The thicknesses of the two towers are indicated in Table 6.4. The 3D model is presented in Figure 6.6 a) and b).

Table 6.4 Tower wall thickness [108].

Segment	Thickness
Segment 1	50 mm
Segment 2	30 mm
Segment 3	19 mm
Segment 4	19 mm

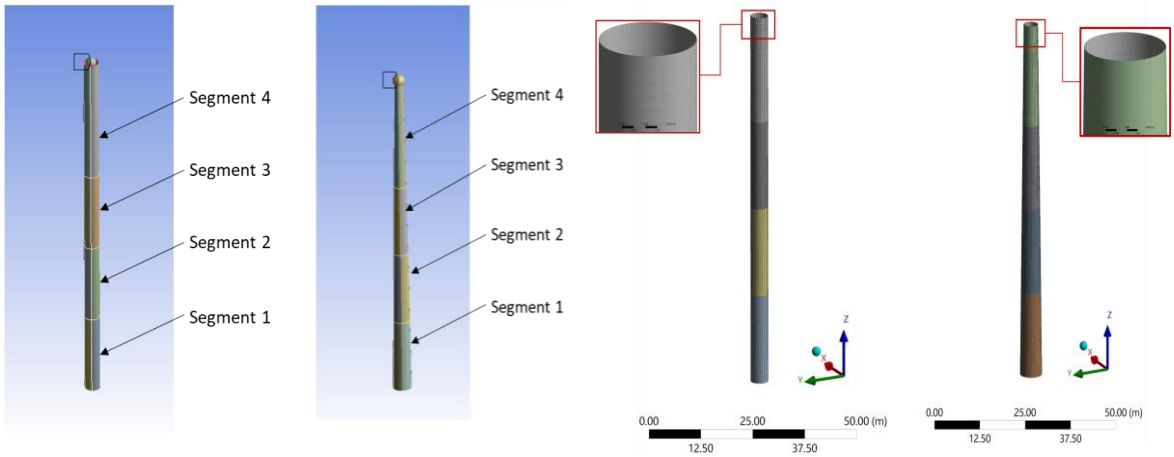

a) cylindrical **b**) conical **c**) cylindrical **d**) conical

Figure 6.6 Tower geometry and mesh of 0.5 m [108].

The mesh was generated using quadrilateral elements because they best reproduce the stress distribution, and the results of finite element analysis depend on the chosen discretization solution. The size of the applied quadrilateral elements was 0.5 m (Figure 6.6 c) and d)).

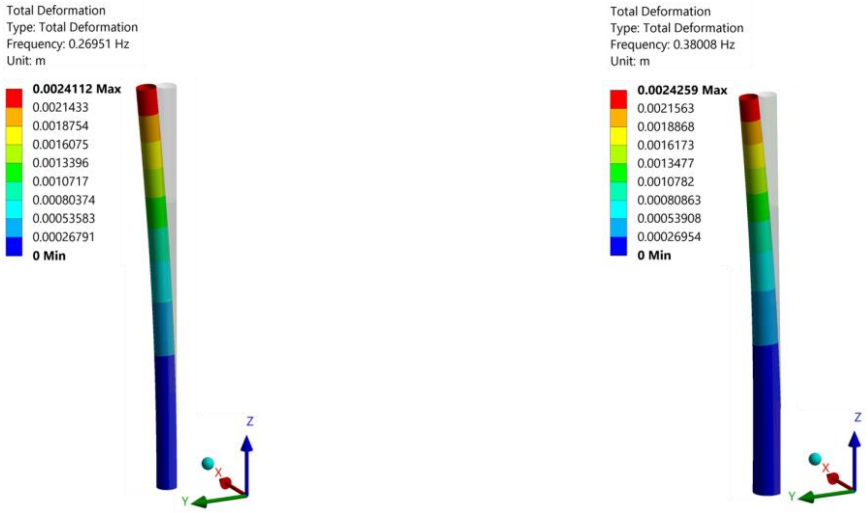

a) cylindrical **b**) conic

Figure 6.7 The first mode of vibration for the two towers [108].

To avoid resonance caused by vibrations, the tower's frequency must differ from harmonic vibrations associated with the rotor. The rotor has a harmonic vibration value between $1P=f_{rot}\cdot S_f$ and $3P=\frac{3\cdot f_{rot}}{S_f}$. The primary excitation frequency of the rotor, caused by the rotor's rotation at a given speed, inducing mass imbalances, is denoted as 1P. The second excitation frequency is caused by the blade passing the tower; this wind turbine has three blades, denoted as 3P. The range of variation of the tower's natural frequency can be expressed by the inequality (6.5). This represents the recommended interval for optimal design [115]:

$$f_{rot}\cdot S_f \leq f_{tower} \leq \frac{3\cdot f_{rot}}{S_f} \tag{6.5}$$

where: S_f is the safety factor for frequency (has the value of 1.05 according to the GL standard [116]), f_{tower} is the first natural frequency of the tower, and f_{rot} is the frequency associated with the rotor. The Vestas V112-3 MW has a rotor rotation speed of 12.8 rpm, corresponding to a frequency of 0.213 Hz.

Thus, the first natural frequency of the tower must be between the values:

$$0.244 \leq f_{tower} \leq 0.640 \tag{6.6}$$

As seen in Figure 6.7, the first vibration mode for the cylindrical structure was 0.269 Hz, and for the conical structure, it was 0.380 Hz. Both values were within the range of 0.224-0.640 Hz.

Figure 6.8 illustrates the two towers deformed under the action of forces and moments in normal and extreme wind conditions. A tower is considered safe when the maximum deformation (denoted as d_{max}) does not exceed the allowable deformation (denoted as $d_{allowable}$). The structure is considered globally stable and out of danger when the following relation is fulfilled [117]:

$$d_{max} \leq d_{allowable} \tag{6.7}$$

The allowable deformation can be calculated using the formula [118]:

$$d_{allowable} = 1{,}25 \cdot \frac{L}{100} \tag{6.8}$$

where L is the tower height and measured in meters.

From the above equations, a value of 1.05 m was obtained for the allowable deformation. The deformations obtained for the two tower geometries were below this value. The cylindrical structure had the maximum deformation at the top of the tower, and its value was approximately 0.44 m, while for the conical structure, the deformation was much smaller, about 0.24 m. These values were much smaller than the allowable deformation, indicating that the structure was sufficiently rigid. The maximum deformation under extreme conditions for the cylindrical tower was 1.6385 m, exceeding the allowable deformation value. This result indicates that the cylindrical structure was not rigid enough for these conditions. The maximum deformation of the conical tower was 0.87261 m.

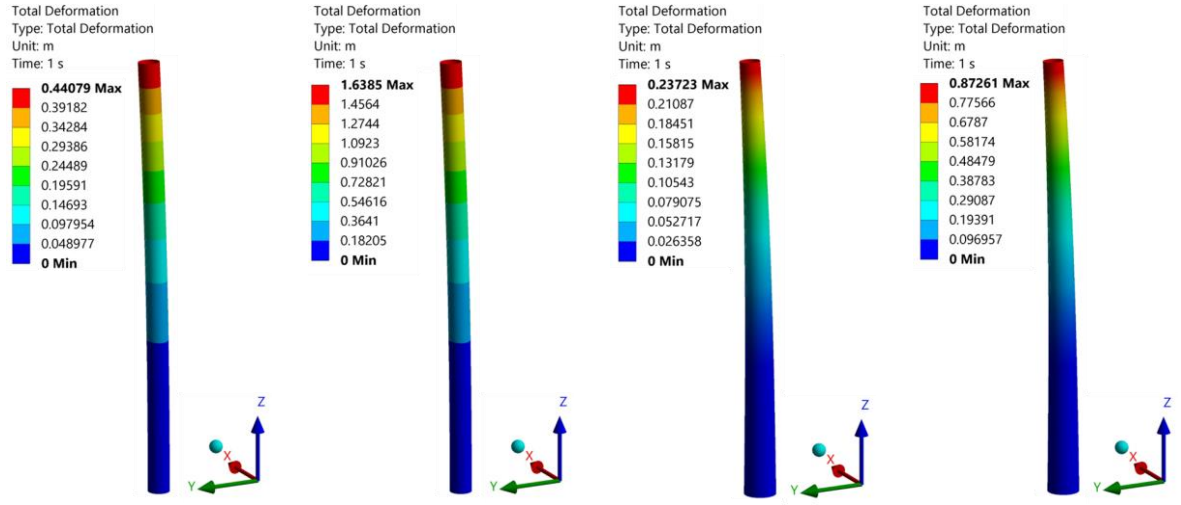

a) cylindrical **b**) cylindrical **c**) conical **d**) conical

Figure 6.8 Total deformation of the tower: a) normal wind conditions; b) extreme wind conditions; c) normal wind conditions; d) extreme wind conditions [108].

The von Mises stress, σ, generated by loads cannot exceed the allowable stress. This can be expressed by the following inequality:

$$\sigma \leq \sigma_{allowable} \tag{6.9}$$

The allowable stress is given by:

$$\sigma_{allowable} = \frac{\sigma_y}{\gamma_m} \tag{6.10}$$

where σ_y is the yield strength and γ_m is the material safety factor.

The yield strength of S355 steel is 335 MPa for thicknesses of 40 mm ≤ t ≤ 63 mm, and for thicknesses of 16 mm ≤ t ≤ 40 mm, the yield strength is 345 MPa. In the case of the chosen tower, the yield strength at the upper thickness was considered to ensure that all desired conditions are met.

The value of the safety factor was 1.1. This value is a minimum compared to those used in practice but serves as a reference value taking into account material instability. For this reason, the values obtained from the calculation may be higher than the actual ones.

Using Equations (6.9) and (6.10), the allowable stress value of 305 MPa was obtained. The von Mises stress values in the case of cylindrical and conical structures under normal operating conditions were 100 MPa and 71.5 MPa, respectively (Figure 6.9). These values are below the allowable stress value. Under extreme conditions, we can observe that the cylindrical tower had a von Mises stress value of 360 MPa; this exceeds the allowed value, indicating that the cylindrical structure was not safe. The conical tower had a von Mises stress of 254 MPa. The conical structure was safe under both normal operating conditions and extreme conditions.

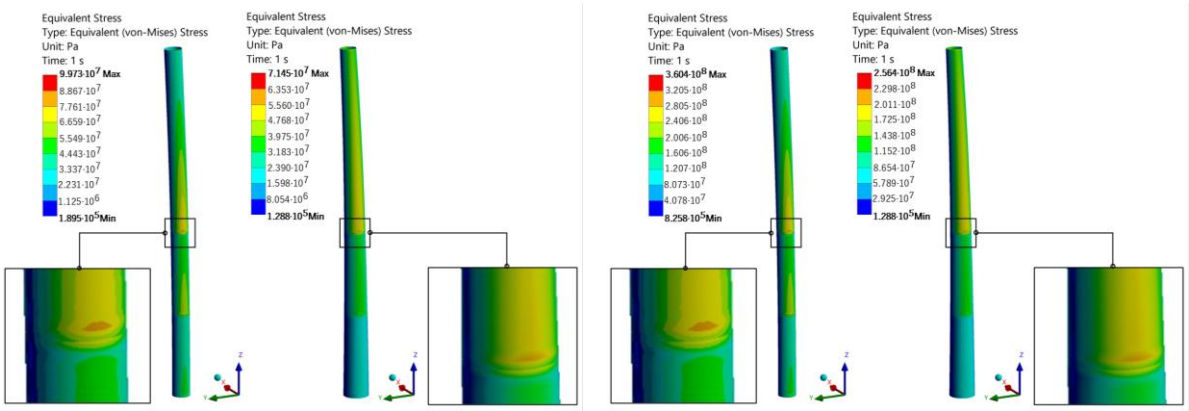

a) cylindrical **b**) conical **c**) cylindrical **d**) conical

Figure 6.9 Von Mises stress in a) normal wind conditions; b) normal wind conditions; c) extreme wind conditions; d) extreme wind conditions [108].

Following the reduction of wall thickness, the total mass of both towers underwent a reduction, accompanied by a decrease in their natural frequencies. Table 6.5 provides an overview of the highlighted trends, where natural frequencies show a decrease as the wall thickness is reduced. Analyzing in detail, we observe that for the first vibration mode, all recorded values for various thicknesses fell within the mentioned range, indicating efficient avoidance of the resonance phenomenon, regardless of the chosen thickness. Additionally, we found that deformations had an upward trend proportional to the reduction of the wall thickness of the tower, but none of the values exceeded the maximum allowable limit of 1.05 m. Regarding von Mises stress, it also showed a clear increase proportional to deformations.

However, none of the obtained values exceeded the allowable limit defined by Equations (6.9) and (6.10).

Table 6.5 The results obtained for the three types of thicknesses.

Type of tower	***Parameters***	***Baseline***	***25% thickness reduction***	***50% thickness reduction***
Cylindrical	Maximum total deformation	0.52311 m	0.69313 m	1.0338 m
	Maximum von Mises stress	117.28 MPa	153.28 MPa	222.50 MPa
	1st natural frequency	0.36082 Hz	0.32099 Hz	0.26951 Hz
Conical	Maximum total deformation	0.27942 m	0.37088 m	0.55414 m
	Maximum von Mises stress	84.03MPa	109.60 MPa	159.50 MPa
	1st natural frequency	0.51194 Hz	0.45413 Hz	0.38008 Hz

6.5 Analysis for a 100 m wind turbine tower

In the absence of specific technical data for a 100-meter tower in operation, we can turn to the information provided in the work [58], which adopted an interesting approach. The authors extrapolated the specifications of the Vestas V-90 turbine, scaling them to a height of 103 meters, and assigned component weights according to the NREL 5 MW turbine (Table 6.6). Additionally, we will extend the comparison to an alternative structure, namely a concrete tower, to highlight the advantages and disadvantages of each option in terms of performance, durability, and environmental impact. Thus, we can obtain a more complete and enriched understanding of the technical and design implications of a 100-meter-tall tower.

Table 6.6 Basic properties of the NREL interpolated turbine for a 103m tower height.

Properties	**Steel tower**	**Concrete tower**
Height	103 m	
Bottom diameter	6 m	8,2 m
Bottom thickness	35 mm	250 mm
Top diameter	3.87 m	4.8 m
Top thickness	25 mm	250 mm

In Table 6.7, the material characteristics used for the construction of the tower are presented. It can be observed that, in this case, two types of materials are considered, with a particular emphasis on precast concrete towers. It is important to note that precast concrete towers are equipped with steel tendons that stretch along their diameter.

Table 6.7 Material Characteristics for Tower Construction[59].

Properties	Steel tower	Concrete tower
Young's modulus (E)	$210 \cdot 10^3$ MPa	$26 \cdot 10^3$ MPa
Density (ρ)	8500 kg/m^3	2450 kg/m^3
Poisson's ratio (v)	0,3	0,2

This aspect is significant because the use of steel tendons in precast concrete towers contributes to the consolidation and strengthening of the tower's structure, thereby increasing

its capacity to withstand the gravitational and compressive loads to which it is subjected. Steel reinforcement is often employed in the construction of towers to ensure the necessary strength and stability in variable loading conditions and challenging environments.

The admissible parameters that must be respected for the prestressed concrete tower are presented in table 6.8.

Table 6.8 Design variables for prestressed concrete tower [119].

Parameter	**Values of concrete tower**
Frequency	$0{,}212 \leq f_{tower} \leq 0{,}606$ Hz
Allowable deformation	1,29 m
Tensile strength	2,4 - 5 MPa
Compressive strength	27.5 MPa

By examining Figure 6.10, we can observe that the deformation in the case of the concrete tower is smaller compared to that of the steel tower. This behavior can be attributed to the significantly larger diameter of the concrete structure compared to the steel one. Additionally, the thickness of the tower wall may contribute to this aspect, considering that the thickness is approximately 7 times greater than that of the steel tower. Moreover, we can observe that, compared to the 84m tower, deformations in the case of the 103m tower increase significantly from 0.25m to 0.41m. This significant difference could be attributed to variations in the thickness of the tower walls and might be similar to the behavior observed in the case of a 25% reduction in wall thickness. Within the concrete tower, we can observe that the maximum stress is located at the bottom of the tower.

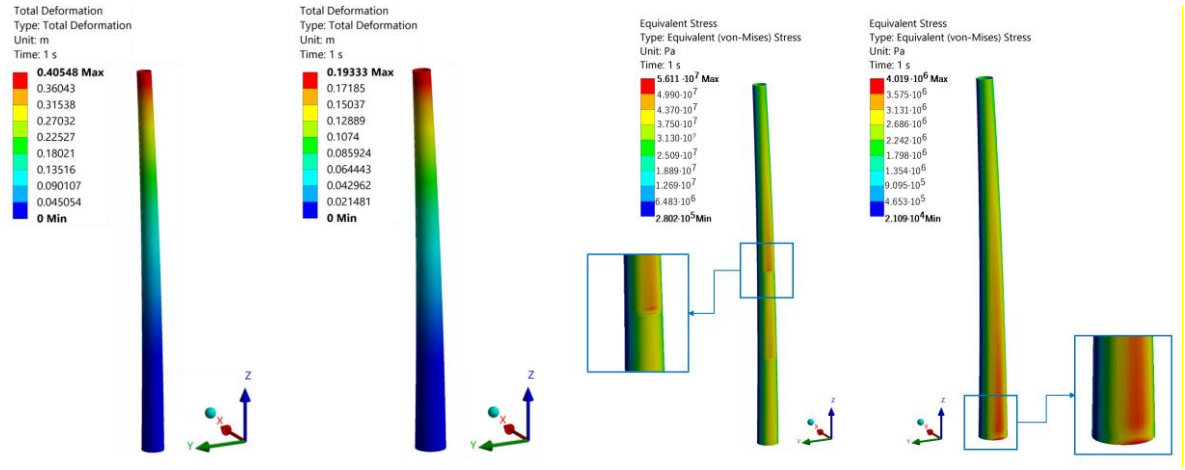

a) steel **b**) concrete **c**) steel **d**) concrete

Figure 6.10 Total Deformation and Von Mises Stresses under the Black Sea Wind - B1.

The results obtained in Figure 6.11 exhibit similarities to those in Figure 6.10, with the note that they reflect an increase determined by the variation in wind speed, which changes intensity in the case of location C3.

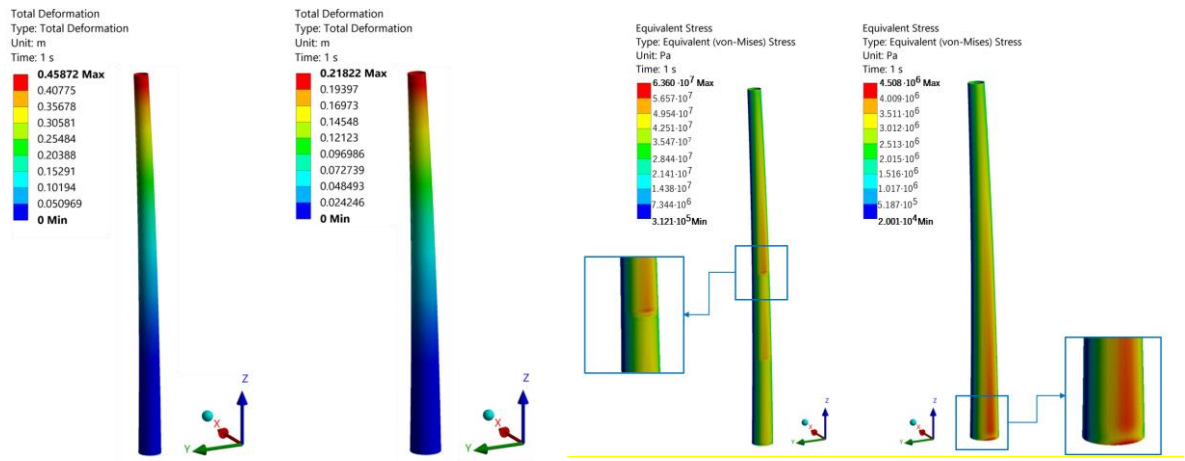

a) steel **b**) concrete **c**) steel **d**) concrete

Figure 6.11 Total Deformation and Von Mises Stresses under the Black Sea Wind - C3.

6.6 Conclusions

This chapter aimed to evaluate two types of towers for a wind turbine: one with a cylindrical shape and the other with a conical shape. Reference parameters were adopted according to the specifications of the Vestas V112-3 MW offshore wind turbine. Based on these data, an adaptation of the conical tower was performed, demonstrating better results compared to the cylindrical tower. Additionally, the possibility of using a concrete tower was explored, with the height interpolated to 103 m, a size increasingly used for offshore renewable energy exploitation. All analyses were conducted using the ANSYS software application.

Following the modal analysis, a mesh size of 0.5 m was adopted, as the difference between the 0.25 m and 0.5 m meshes was nearly imperceptible. The natural frequency for the cylindrical tower was 0.27 Hz, and for the conical tower, it was 0.38 Hz, with both frequencies falling between 0.269 and 0.640 Hz, thereby avoiding the resonance effect.

Within this study, two distinct static analyses were conducted. The first analysis was performed under normal turbine operating conditions, with wind speed up to the cut-off limit of 25 m/s. The second analysis was carried out in a scenario where the turbine was non-functional, and the wind speed reached 50 m/s. Forces acting on the tower in both cases, either under normal conditions or in the fault scenario, were determined by the wind thrust force on the blades, the bending moment of the blades, wind distribution across the tower height, the gravitational force generated by the weight of supported components (nacelle, blades, and rotor), and the weight of the tower itself. In addition to the two mentioned analyses, the specific operating conditions of the Black Sea for two locations already addressed in Chapter 3 were investigated. Furthermore, the possibilities of using a tower taller than 103 m and the prospects of using a material other than steel, specifically concrete, were explored.

Deformations of both towers under normal operating conditions were below the permissible value, being more than 50% lower. In extreme wind conditions, deformations for the conical structure were close to the permissible limit, while those for the cylindrical tower exceeded this limit. The maximum deformations for both towers were located at the top of the tower at a height of 84 m. If we consider a diameter for the cylindrical tower that is equivalent to the conical structure, the deformation obtained had a value of 1.18 m, exceeding the permissible deformation limit. Thus, the conical structure exhibited better resistance than the cylindrical one. The optimal diameter for the structure not to deform below the permissible limit

was 5.2 m (for this diameter, a maximum deformation of 1.02 m was obtained), a difference of 1 m from the diameter chosen for the study.

Von Mises stresses for both towers under normal operating conditions remained below the permissible value, being 305 MPa. The obtained values for the cylindrical and conical towers were 100 and 71.5 MPa, respectively, representing approximately one-fourth and one-third of the permissible stress value. In extreme wind conditions, the cylindrical structure exceeded the permissible value by approximately 55 MPa, while the conical tower remained below this permissible limit. The highest stresses were identified at the junction of the tower sections, particularly in the transition zone from a wall thickness of 30 mm to 19 mm (at a height of 40 m). High stresses were also observed at the junction between sections with a wall thickness of 50 mm and those with a thickness of 30 mm (at a height of 20 m). The fact that stresses were recorded in these zones and not at the bottom of the tower, as would be normal, is due to the design of the two towers without the use of flanges. If we consider the same diameter of 5.2 m for the cylindrical tower, the von Mises stress would remain below the permissible value, recording a value of 287 MPa. An important observation can be made regarding the concrete tower, where the maximum von Mises stresses are in the lower part. This is because the thickness of the tower is constant over the entire height, and the stress values for this case range between 4 and 4.5 MPa, within the permissible limits for this material.

To validate the model presented in this chapter, a comparison was made between the obtained results and the work in [120], where measurements were taken on an 80 m tower wind turbine. This study involved placing sensors at various heights (on four levels, from level 0 to level 3) and recording multiple signal types, such as acceleration, deformation, temperature, and tilt. Additionally, a finite element model was presented in [120], and developed to determine its feasibility and utility in future analyses. The conclusion was that results can be successfully interpreted and calculated using finite element models. From this study, a value close to 0.340 Hz was obtained for the natural frequencies of mode 1. The values obtained in this chapter were 0.361 Hz for the cylindrical tower and 0.512 Hz for the conical one. These differences were determined by the thickness of the shell, which in this analysis was larger than in [120]. However, Table 6.6 revealed a trend of these frequencies to decrease as the wall thickness was reduced. Additionally, the variations are influenced by the diameters chosen for the towers. Considering all these aspects, it can be concluded that the towers had similar frequencies, and the work in [120], can serve as a method to validate the model developed in this analysis. Moreover, in the mentioned study, the maximum stress values under a wind speed of 25 m/s were evaluated, and they were around 70 MPa. In comparison, values for the towers in this chapter were approximately 100 and 65 MPa. These detailed analyses contribute to a better understanding of tower performance in different scenarios and loading conditions.

In the study, a potential direction towards the efficiency of this type of wind turbine was identified, considering its potential location in the Black Sea. In this region, wind speeds do not reach very high levels, but the productivity of such a turbine could reach approximately 45%. It was observed that by thinning the tower wall, the turbine could exhibit adequate mechanical resistance to operate in this location.

7 Floating structure analysis

This chapter presents a detailed analysis of the hydrodynamic characteristics for a spar-type foundation designed to support an offshore wind turbine. The study will be conducted using the ANSYS AQWA program [121], where a model will be generated to include both the foundation and the anchoring system composed of three anchor lines, as well as the export cable.

Data regarding the foundation characteristics can be found in Table 7.1, while the turbine characteristics will be taken from the NREL model used in previous research in the preceding chapters (Table 7.2). It is noteworthy that, although offshore wind turbines have been deployed at depths of up to 150 meters so far, one of the locations of interest for this chapter is associated with a water depth of 1000 meters. This choice is justified by the informative purpose of this study.

Table 7.1 Spar foundation characteristics.

Parameters	**Values**
Diameter	15 m
Height	100 m
Draft	85 m
Displacement	15020.7 m^3
Center of gravity	-59.43 m
Total mass	14698798.37 kg
Number of anchor lines	3

The total mass of the system includes both the weights associated with the structure itself and the fixed and variable ballast.

In this context, the anchor line consists of two main components: chains and polyester cables. A diameter of 239 mm for chains and 160 mm for cables was selected to ensure the necessary strength against the hydrodynamic and mechanical demands of the marine environment [122]. Chains and cables have specific masses of 315 kg/m and 44 kg/m, respectively. Regarding the export cable, it is essential to understand that it does not play a role in ensuring the stability of the structure.

Table 7.2 NREL turbine characteristics of interest for the foundation study [123].

Parameters	**Values**
Rotor mass	110000 kg
Nacelle mass	240000 kg
Tower mass	347460 kg
Center of gravity	60 m

7.1 Types of foundations used in the offshore wind industry

Offshore wind turbine foundations constitute an essential part of the infrastructure required to efficiently harness wind energy off the coasts. These sophisticated and complex structures are designed to firmly support and anchor wind turbines in the tumultuous waters of

the oceans, paving the way for the effective exploitation of wind energy resources offshore. The main types of foundations include monopile foundations (with a single supporting pile), jacket foundations (truss-like structures), tripod foundations, TLP foundations (Tension Leg Platform – vertically pretensioned coupling), semi-submersible foundations, and spar foundations.

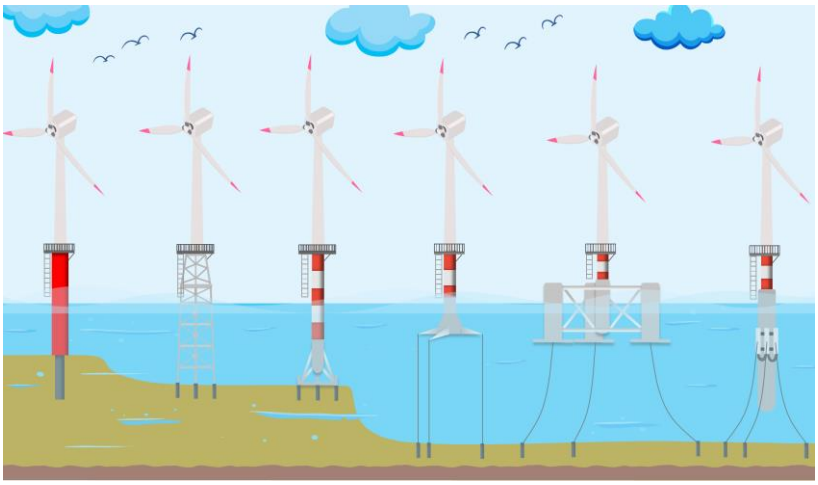

Figure 7.1 Types of Foundations, from left to right: Monopile, Jacket, Tripod, TLP, Semi-submersible, Spar.

7.2 Degrees of freedom for the spar foundation

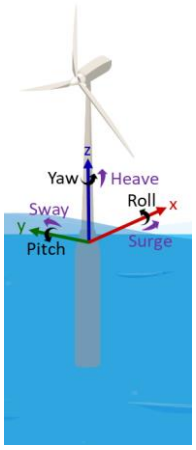

Figure 7.2 The six degrees of freedom for spar foundation.

In the context of floating wind turbines with spar foundation, the concept of 6 degrees of freedom (6-DOF) is crucial to the design and operation of these offshore structures (Figure 7.2). These 6 degrees of freedom describe the foundation's ability to move and rotate in six distinct directions, allowing adaptation to the variable conditions of the ocean. These degrees of freedom include movement along the x-axis (aligned with the wind direction - surge), movement along the y-axis (perpendicular to the wind direction - sway), vertical movement (heave), rotation around the x-axis (roll), rotation around the y-axis (pitch), and rotation around the z-axis (yaw).

The analytical equation in the time domain for floating wind turbines is expressed as follows [124]:

$$(M+A_{\infty})\ddot{x}(t)+\int_0^t h(t-\tau)\dot{x}(\tau)d\tau+Df(\dot{x})+K(x)x=q(t,x,\dot{x}) \tag{7.1}$$

where: M is the mass matrix for the floating spar foundation, A_{∞} represents additional masses as frequency approaches infinity, h(t) is the delay function, reflecting the influence of the motion history on the current state of the wind turbine, D is the nonlinear damping matrix, reflecting the damping forces during the motion of the wind turbine and foundation, K is the restoring stiffness matrix, accounting for the return-to-initial position behavior of the wind turbine and foundation, q is the excitation force vector, including forces generated by incident waves and diffraction, aerodynamic forces of the rotor, wind pressure on the tower, and nonlinear restoring forces, such as those generated by anchoring cables and couples resulting from the structure's motion, $x,\dot{x},\ddot{x}$ represent the position, velocity, and acceleration vectors of the wind turbine origin in the three directions.

7.3 Wave spectrum

The JONSWAP spectrum, developed in the 1970s as part of the Joint North Sea Wave (JONSWAP) project, was designed to address the observed variability of marine waves under different conditions. It is characterized by its distinct mathematical formula, describing the distribution of wave energy in terms of frequency and direction. The JONSWAP spectrum formula is defined as follows [125,126]:

$$S(f,\theta)=\frac{\alpha_{norm}g^2}{f^5}\exp\left(-\frac{5}{4}\left(\frac{f_m}{f}\right)^4\right)\gamma^{\exp\left(-\frac{1}{2}\left(\frac{f}{f_m}-1\right)^2\right)} \tag{7.1}$$

where: $S(f,\theta)$ is the spectral energy density at frequency f and direction θ (In m^2s), α is the normalization coefficient, g is the gravitational acceleration, f_m is the peak frequency of the spectrum (in Hz), γ is the peak enhancement factor.

7.4 Results of the ANSYS foundation simulation

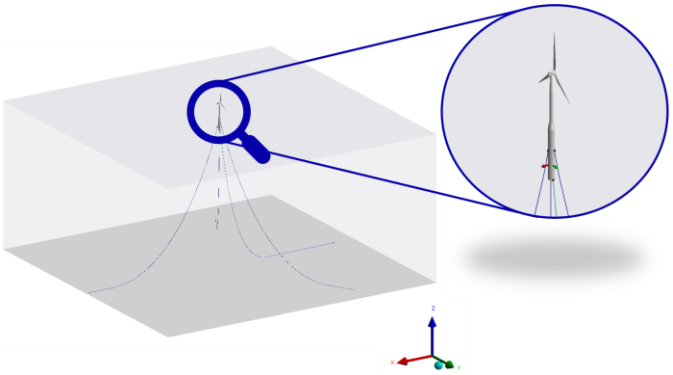

Figure 7.3 Geometry created using ANSYS program.

In this context, the structure is analyzed using diffraction theory. The geometry used for this study is presented in Figure 7.3.

In this chapter, a mesh size of 0.5 meters has been adopted. The total number of panels is 37,233, of which 16,091 are diffraction elements. The results of the discretization generation process are illustrated in Figure 7.4.

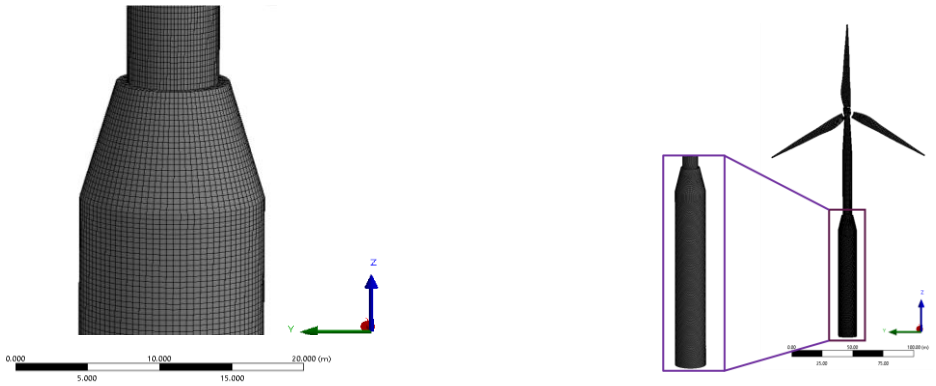

Figure 7.4 Discretization of both the foundation and the turbine created in ANSYS AQWA.

The initial analysis of the spar-type foundation focuses on the diffraction phenomenon. This was performed in the frequency range of ocean waves between 0 and 1.8 rad/s. Figure 7.5 shows that the Response Amplitude Operator (RAO) for longitudinal translation (surge) exhibits a decreasing trend with increasing wave frequency. At the same time, the RAO for vertical translation (heave) and the RAO for pitch oscillation show an increasing trend followed by a decrease.

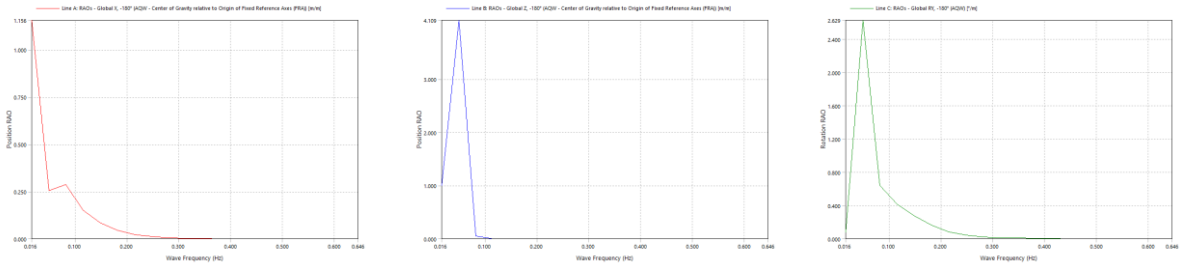

a) b) c)

Figure 7.5 Frequency response function of the a) longitudinal translation; b) vertical translation; c) pitch oscillation.

Comparing the obtained results with those from reference [127], it can be observed that the frequency response function for longitudinal translation oscillation is approximately 1.8, a value close to that obtained in this analysis. Using the mentioned reference as a benchmark, both for the analysis of vertical translation oscillation and for roll oscillation, it is noted that for vertical translation oscillation, the RAO value is a maximum of 7, while roll oscillation presents values of 2.5. It can be concluded that the results are close, although differences exist, which can be attributed to the different dimensions of the structure and the environment in which the foundation operates.

The data presented in Figure 7.6 illustrate the results obtained from evaluating the hydrodynamic forces and moments induced by both incident waves (Froude-Kryloff method) and the direct interaction of the body with the surrounding environment. The excitation force in the longitudinal direction reaches a maximum of 3632 kN, while for the excitation in the vertical direction, it halves, reaching a maximum of 1617 kN. It is observed that the maximum excitation

force in the vertical direction occurs at the lowest frequency, where the wave period is large. For the excitation moment around the x-axis, it reaches its maximum value at a frequency of 0.15 Hz and has a value of approximately 158,600 kNm.

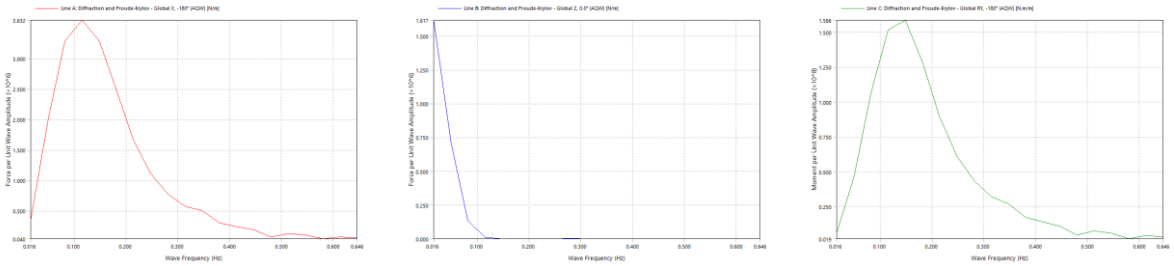

a) b) c)

Figure 7.6 a) Excitation force of the wave in the longitudinal direction; b) excitation force of the wave in the vertical direction; c) excitation moment given by the wave for roll oscillation.

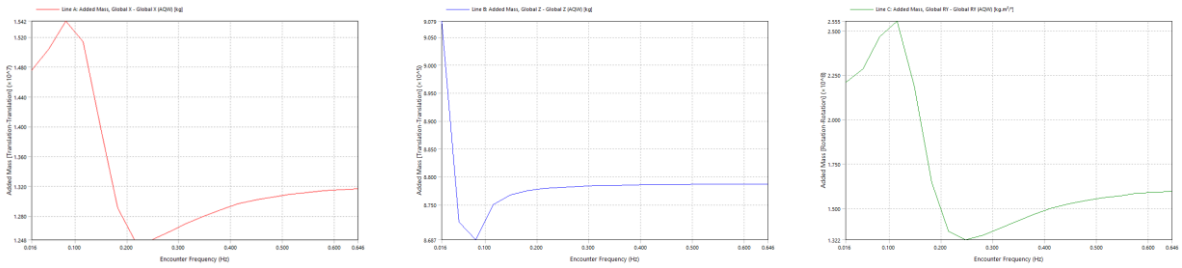

a) b) c)

Figure 7.7 Additional masses for a) surge oscillation; b) heave oscillation; c) pitch oscillation.

The additional masses for the analyzed structure are presented in Figures 7.7 for the three types of movements: surge, heave, and pitch. These additional masses largely depend on the structure's geometry, influencing the fluid particle acceleration on the geometric surface.

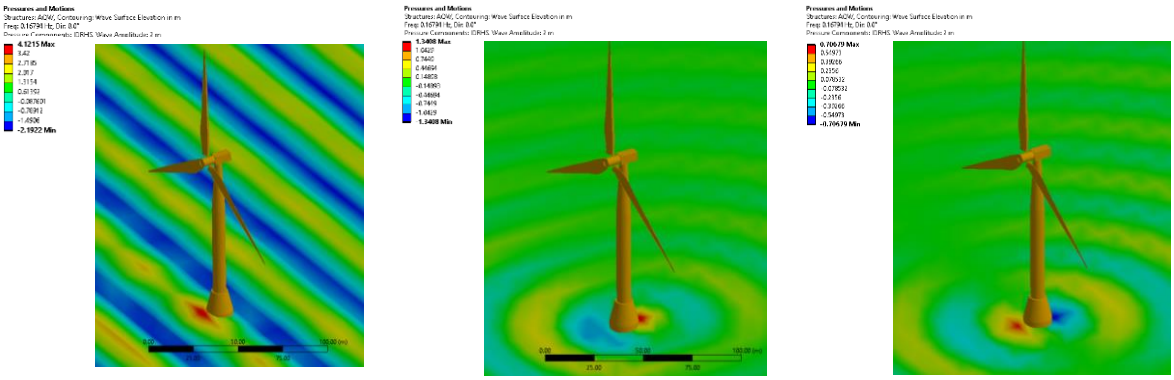

Figure 7.8 Wave height a) considering all components; b) diffraction; c) radiation.

Simulating a wave with an amplitude of 2 m for a wave period of 6 s, equivalent to a frequency of 0.167, the wave height containing all its components was obtained. The simulated wave is of the frontal type. As seen in Figure 7.8, its maximum height is 4.12 m, and the minimum is -2.19 m.

To analyze the hydrodynamic response of the structure along with the anchor lines, a stability analysis was conducted. In this analysis, an irregular wave was simulated using the JONSWAP spectrum, requiring the definition of the significant wave height and wave peak period. For this scenario, a significant wave height of 2 m and a peak period of 6 s were considered, characterizing the wave spectrum adequately. For simulation, a frontal wave direction was chosen. The significant wave height value of 2 meters represents the maximum level recorded for the period between 2002 and 2021, specific to the eastern part of the Black Sea. This value corresponds to a wave period of 6 seconds. As a result of this analysis, it was found that the foundation will vertically displace by 1.531 m, indicating the stability of the foundation under the simulated environmental conditions.

7.5 Conclusions

This chapter presents the hydrodynamic analysis of a spar-type foundation modeled and simulated using the ANSYS AQWA program. Consequently, a detailed geometric model of the foundation and the anchoring system was created. This model also included the three anchor lines and the export cable connecting the foundation to the electrical grid.

According to the analysis results obtained in the ANSYS AQWA simulation, it is observed that the drift force calculated by the near-field method and the far-field method agree, thus reflecting the accuracy of the discretization. Regarding the diffraction phenomenon analysis, it was observed that the frequency response functions for longitudinal displacement, vertical motion, and tilt exhibit specific trends, while for other types of movements (sway, roll, and yaw), significantly lower values are recorded due to the wave orientation at 0°.

Comparing the obtained results with those in the literature, a significant agreement is observed for vertical displacement and roll oscillation, with minor differences due to the different dimensions of the structures and the operating environment. It was also noted that water depth plays a crucial role in determining the frequency response function value.

The additional masses for surge, heave, and pitch movements depend largely on the structure's geometry and are used to assess the sinking risk factors in the offshore wind industry. Comparing the obtained results with literature references, it was observed that the values fall within the specified range for heave motion and are close for the other oscillations. The differences that emerged are largely influenced by the structural variations, as discussed in detail in a previous study [128].

The hydrodynamic response analysis included simulating a frontal-type wave with a significant height of 2 m and a period of 6 s. This analysis demonstrated the stability of the foundation under simulated environmental conditions. In conclusion, the data presented in this chapter illustrate the results obtained from evaluating the hydrodynamic forces and moments induced by the action of incident wave forces and the direct interaction of the structure with the marine environment.

8 Levelized cost of energy for a wind turbine farm

8.1 Levelized cost of energy in the current wind industry

The Levelized Cost of Energy (LCOE) represents the theoretical price at which electricity should be sold to achieve financial breakeven. Therefore, it plays a fundamental role in assessing the economic feasibility of energy projects and provides a standardized method for comparing costs across different energy sources [129,130]. LCOE can be defined as the ratio of the costs of an energy project to its electricity production over its lifespan, usually expressed as [131]:

$$LCOE=\frac{\sum_{i=1}^{T_{project}}(CAPEX_i+OPEX_i)(1+r)^{-i}}{\sum_{i=1}^{T_{proiect}}AEP_i(1+r)^{-i}} \quad (8.1)$$

In this formula, costs are divided into two categories: capital expenditures (CAPEX), covering costs incurred before the project's operation, and operational expenditures (OPEX), encompassing the costs of electricity production and infrastructure maintenance. Annual energy production (AEP) is the primary source of revenue. The project's lifespan is denoted by $T_{project}$, and r is the discount rate.

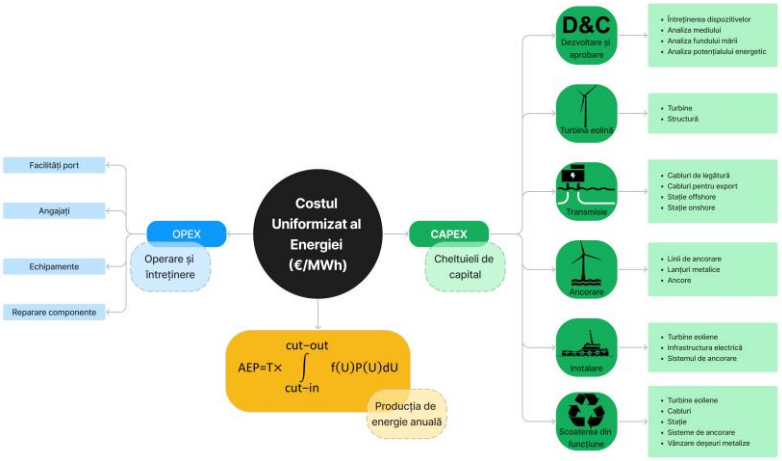

Figure 8.1 Components of the levelized cost of energy.

8.2 Relevant aspects in the levelized cost of energy evaluation

In this context, LCOE values are specific to each project, and the approach in this chapter exemplifies a concrete situation for the Black Sea region. For this simulation, focus is placed on the nine locations identified in Chapter 3, where Siemens Gamesa 8 MW turbines demonstrated optimal performance. These turbines were assigned the capacity to generate a total power of 800 MW.

To provide insight into specific components, considerations related to the distance from the shore will also be discussed. In the Black Sea region, where offshore wind farms do not yet exist, assumptions will be made based on existing legislation in other countries where such projects are already underway. Factors such as visual impact minimization and generated noise levels will be considered. The theoretical visibility limit of turbines is limited to distances

greater than 45 km due to the Earth's curvature. Depending on the country, various regulations are in place, such as the 12 nautical miles (NM) restrictions for North Sea wind farms (e.g., Belgium, the Netherlands, and Scotland) or the 2-kilometer distance from the shore, as in Norway [132], or approximately 11 kilometers in Greece and 12 kilometers in Spain [133].

In addition to the distance from the shore, water depth plays a crucial role in determining the optimal foundation for turbines. Therefore, for each location, a specific foundation type will be chosen according to the indications presented in Table 8.1.

Table 8.1 Depths and distances from the Black Sea coast for the 9 established locations.

Locations	**Depth**	***Distance to shore***	**Foundation type**
A1	34 m	20 km	*Monopile*
A2	26 m	25 km	*Monopile*
A3	40 m	24 km	Jacket
B1	58 m	70 km	Jacke
B2	78 m	70 km	Tension leg
B3	65 m	100 km	Tension leg
C1	95 m	100 km	Semi-submersible
C2	173 m	120 km	Semi-submersible
C3	1000 m	145 km	*Spar*

The last variable addressed in this context is maritime transportation. As shown in Figure 8.2, a significant volume of maritime transport is highlighted, especially in port areas like Constanta in Romania. Overlaying this map with the locations selected in Chapter 3 reveals that locations A3, B1, B2, and B3 are in high-traffic zones, making them unsuitable for wind turbine farm placement to prevent potential maritime incidents.

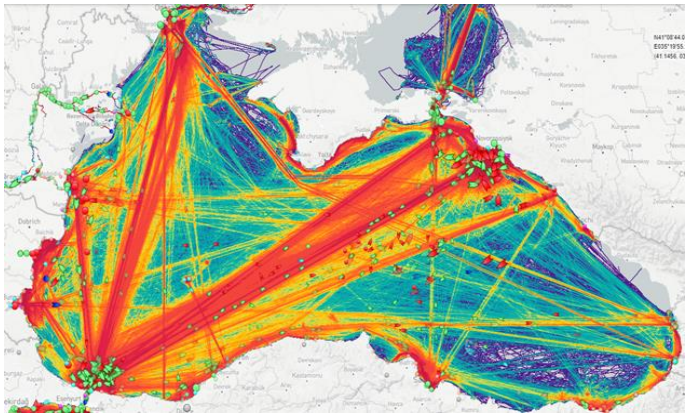

Figure 8.2 Maritime traffic in the Black Sea.

8.2.1 Capital expenditure

- Development and consenting

This stage of the project encompasses environmental studies, seabed surveys, meteorological stations, project management, and development services. According to some authors, this value is estimated at around 4% of the total CAPEX [134]. The total costs for Development and Approval (D&A) are set at approximately 187.2 k€/MW [134].

- Turbine and structure

For offshore wind turbines, the combination of the turbine and substructure represents about 55% of the total CAPEX [134]. Based on data from various sources, the average cost of

a generic wind turbine is estimated to be 950 k€ – 1.6 M€ per MW [135,136]. We will adopt a turbine cost of 1.2 M€ per MW.

For substructures, manufacturing costs will be estimated based on a complexity factor, as presented in reference [137], and an overview is provided in Table 8.2.

Table 8.2 Production cost for different substructure types [137].

Structure type	Material consumption	Material price	Production price	Final price
Monopile	1200 t	1.2 M€	1.2 M€	2.4 M€
Jacket	825 t	0.825 M€	2.355 M€	3.18 M€
Tension leg	521 t	0.521 M€	0.677 M€	1.198 M€
Semi-submersible	2500 t	2.5 M€	5 M€	7.5 M€
Spar	1700 t	1.7 M€	2.04 M€	3.74 M€

- Mooring system

Mooring lines can be made of various materials, such as synthetic cables, chains, or metal cables. Synthetic cables, typically made from polyester or polyethylene, providing strength and durability in the marine environment, are commonly used to connect floating structures to anchors and, consequently, to the seabed.

Determining the length of mooring lines is a crucial aspect of designing these systems. For spar foundations, it is assumed that the length of the mooring line for a depth of 100 meters is 500 meters, with an addition of 150 meters for every additional 100 meters of depth [129]. For semi-submersible foundations, an additional 60 meters is added to these estimates. In both cases, an additional 50 meters of chain is added for each mooring line.

Table 8.3 Estimated price for mooring systems for each foundation type at a depth of 200 m [137].

Structure type	Mooring system component	Anchor type	Number/ length	Final price
Tension leg	Anchors	Suction	3	1.5375 M€
		Catenary Stevpris Mk6	3	0.165 M€
	Mooring Lines	Vertical metal cables	528 m	0.0355 M€
		Catenary metal cables	2130 m	0.0479 M€
		Chains	150 m	0.0188 M€
Semi-submersible	Anchors	Catenary Stevpris Mk5	4	0.456 M€
	Mooring Lines	Metal cables	2840 m	0.1278 M€
		Chains	200 m	0.05 M€
Spar	Anchors	Catenary Stevpris Mk5	3	0.342 M€
	Mooring Lines	Metal cables	1950 m	0.0878 M€
		Chains	150 m	0.0375 M€

- Transmission

The electrical system of an offshore wind farm has evolved significantly over time to adapt to the growing needs of the offshore wind industry. This complex electrical network is essential for the efficient capture and distribution of wind energy into the power grid.

To illustrate the structure of the offshore wind farm, we can frame it in a rectangular scheme, composed of two columns, each having 5 turbines, with a total of 10 rows. In this

arrangement, the offshore substation will be positioned in the center of the farm to facilitate the efficient collection and transmission of generated energy, as illustrated in Figure 8.3.

In this chapter, an estimated distance of 1 km between turbines is adopted, although a more accurate approximation can be obtained by considering 4-10 rotor diameters. Maximizing this distance results in reduced interference between turbines but entails increased operating and capital costs.

To get an idea of the costs involved, we can consider the price of a cable as 0.281 M€/km for a cable with a section of 300 mm^2.

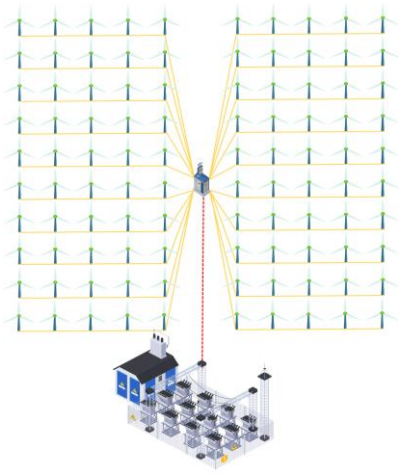

Figure 8.3 Offshore wind farm structure.

Table 8.4 Transmission cost [138].

Parameters	HVAC	HVDC
n_{ex_cables}	3	3
C_{ex_cables} M€/km	2.336	1.168
n_{off_sub}	3	2
C_{off_sub} M€	39	142.75
n_{on_sub}	-	1
C_{on_sub} M€	-	84.35

- Installation

To successfully install the substructures and offshore wind turbines, it is crucial to implement well-planned procedures adapted to the specific maritime environment. In this regard, we focus on two main types of substructures: fixed and floating. Each of these subtypes requires distinct installation approaches [139]. An estimate of the installation costs for turbine foundations is provided in Table 8.5.

Table 8.5 Cost for turbine and foundation installation.

Turbine type	Turbine installation cost	Substructure installation cost
Monopile	0.578 M€/turbine	0.917 M€/turbine
Jacket	0.578 M€/turbine	1.328 M€/turbine
Tension leg	0.768 M€/turbine	0.192 M€/turbine
Semi-submersible	0.644 M€/turbine	0.222 M€/turbine
Spar	0.655 M€/turbine	0.088 M€/turbine

A crucial aspect of the installation process is the use of ships and specialized equipment, adapted to withstand the marine environment and handle the heavy components of both substructures and wind turbines.

For fixed-bottom offshore wind farms, installation costs are estimated at approximately 31 M€, while for floating wind farms, utilizing floating foundations, installation costs are estimated at around 24.54 M€. These estimates reflect variations in cost based on the technology and individual specifications of each offshore wind farm project.

- Decommissioning

The decommissioning process in the context of offshore wind farms is essential to ensure the efficient and safe removal of existing infrastructure at the end of the farm's lifespan. This process involves dismantling and removing various key components, including wind turbines, floating platforms, transition pieces, subsea cables, and the offshore substation. In the decommissioning process, it is assumed that the reverse of the installation process will take place.

Decommissioning costs vary significantly depending on the complexity of the project, specific decommissioning methods, and other factors, often estimated as a percentage of the project's installation costs. These estimates are presented in Table 8.6.

Table 8.6 Decommissioning cost for different substructure types [137].

Structure type	Decommissioning	Material recycling profit	Total
Monopile	0.302 M€	0.238 M€	0.064 M€
Jacket	0.368 M€	0.125 M€	0.244 M€
Tension leg	0.205 M€	0.138 M€	0.067 M€
Semi-submersible	0.193 M€	0.424 M€	-0.231 M€
Spar	0.203 M€	0.311 M€	-0.108 M€

8.2.2 Operation and maintenance

The operations and maintenance (O&M) costs in offshore wind turbine farms involve several essential cost categories, divided into two major groups: fixed costs and variable costs.

As O&M costs are challenging to identify, this subchapter will provide some estimates based on the work [137], presented in Table 8.7. These costs will be grouped into two categories: those reported for fixed foundations and those reported for floating foundations.

Table 8.7 O&M costs [137].

Parameters	Fixed foundation	Floating foundation
Material costs		
Unplanned	5,381 M€	5,372 M€
Basic	0,131 M€	0,131 M€
Planned	1,600 M€	1,600 M€
Labor costs		
Unplanned and basic	4,766 M€	4,766 M€
Planned	0,032 M€	0,032 M€
Equipment costs		
Unplanned and basic	35,165 M€	42,888 M€
Planned	1,456 M€	1,490 M€
Total annual repair costs	48,532 M€	56,280 M€

8.3 Results of implementation in Black Sea areas

Tables 8.8, 8.9, and 8.10 provide the necessary data to analyze the costs associated with locations in the three categories.

It is observed that, in all the tables below, including Table 8.11, the semi-submersible foundation appears to be the costliest option. This conclusion suggests that, although semi-submersible structures may have advantages in terms of stability in deeper water conditions, they may entail significantly higher costs compared to other foundation types, such as monopiles or tension legs, used in other locations.

Table 8.8 CAPEX for locations from category A.

Parameters	***A1***	***A2***	***A3***
Development and consenting (M€)	149.76	149.76	149.76
Turbine (M€)	963.06	963.06	963.06
Substructure (M€)	240.00	240.00	218.00
Anchor (M€)	-	-	-
Transmission (M€)	492.78	509.94	507.07
Installation (M€)	228.04	230.74	271.68
Decommissioning (M€)	0.06	0.06	0.24
CAPEX (M€)	2085.92	2105.79	2222.81

Table 8.9 CAPEX for locations from category B.

Parameters	***B1***	***B2***	***B3***
Development and consenting (M€)	149.76	149.76	149.76
Turbine (M€)	963.06	963.06	963.06
Substructure (M€)	318.00	119.80	119.80
Anchor (M€)	-	176.13	175.47
Transmission (M€)	669.06	669.96	774.49
Installation (M€)	299.36	198.91	310.82
Decommissioning (M€)	0.24	0.07	0.07
CAPEX (M€)	2412.49	2288.71	2504.49

Table 8.10 CAPEX for locations from category C.

Parameters	***C1***	***C2***	***C3***
Development and consenting (M€)	149.76	149.76	149.76
Turbine (M€)	963.06	963.06	963.06
Substructure (M€)	750.00	750.00	374.00
Anchor (M€)	62.65	59.64	1.867.20
Transmission (M€)	775.84	849.43	974.21
Installation (M€)	207.73	221.90	249.49
Decommissioning (M€)	-0.23	-0.23	-0.11
CAPEX (M€)	2926.14	3010.88	4591.18

For the studied wind farm, the total capital cost varies significantly, ranging from 2.085 billion euros to 4.591 billion euros. The lower value is recorded for location A1, which has the shallowest water depth and the closest proximity to the shore, while the higher value is found for location C3, characterized by the farthest distance from the shore and a water depth of 1000 meters.

An important aspect highlighted in Table 8.10 is that decommissioning costs can be negative in specific cases due to the recyclability and reusability of materials and components from wind farms. This emphasizes a commitment to sustainability and can bring significant economic and ecological benefits.

Analyzing Table 8.11, a breakdown of operation and maintenance costs into two main categories is observed: those related to fixed foundations and those related to floating foundations. This classification approach is useful for better understanding the cost structure in offshore wind farms. However, it is important to emphasize some critical aspects and limitations of these data.

Table 8.11 Total OPEX for simulated farms.

Locations	***OPEX (M€)***
A1	970.64
A2	970.64
A3	970.64
B1	970.64
B2	1125.60
B3	1125.60
C1	1125.60
C2	1125.60
C3	1125.60

Analyzing Table 8.12 provides a clear perspective on the levelized cost of energy (LCOE) in the context of offshore wind farms. This measure is essential for evaluating the economic efficiency of projects and considers capital costs, operation and maintenance costs, and annual energy production.

There are significant variations in LCOE between different locations and projects. The lowest LCOE is recorded for the farm located in A2, while the highest LCOE is recorded for C3.

Table 8.12 also presents the results for LCOE with losses, highlighting a significant increase of 38% compared to the LCOE for full production. This indicates the considerable impact of losses on the economic efficiency of projects.

Table 8.12 Total LCOE for simulated farms.

Locations	***LCOE €/MWh***	***LCOE with losses €/MWh***
A1	65.02	89.61
A2	58.50	80.67
A3	67.27	92.75
B1	60.20	83.45
B2	61.81	85.68
B3	66.33	92.27
C1	73.04	101.60
C2	75.46	105.21
C3	106.78	149.32

8.4 Conclusions

In conclusion, this analysis provides a comprehensive perspective on the costs and performance of different types of offshore wind turbines, both fixed to the seabed and floating. However, several aspects requiring further investigation and improvement have been identified. For instance, the costs of anchors should be quantified more accurately, and variables related to anchoring options and soil conditions need to be analyzed in detail. This finding underscores the crucial interdependence between water depth and anchoring costs. Opting for locations with shallower depths can make floating wind technology much more economically attractive, contributing to the long-term sustainability of these projects. Additionally, there is potential for cost savings and scaling effects, especially for mass-produced components such as turbines, anchor lines, and anchors.

It has been observed that water depth has a relatively limited impact on costs, except for those associated with anchoring, which are influenced by the length of anchor lines. However, this influence of water depth on anchor line costs is mitigated by other expenses, such as those related to the anchoring system.

Regarding the Levelized Cost of Energy (LCOE), the analysis has highlighted the paramount importance of energy production and, implicitly, wind resource in comparison to other location-specific aspects such as distance to shore or water depth. Essentially, the estimation of annual energy production has emerged as the key variable determining the cost of energy, emphasizing the importance of precise and location-specific assessments.

In conclusion, this study represents a significant step in understanding the costs and performance of offshore floating wind farms. However, there are clear research needs and a requirement for clarification on certain aspects to obtain more precise estimates and make more informed choices in the development of floating offshore wind farms.

9 Conclusions

9.1 General conclusions

The Black Sea is a semi-enclosed body of water with crucial ecological, climatic, and economic significance in the surrounding region. A detailed analysis of meteorological and oceanographic data, as well as notable events from 2002 to 2021, has revealed the unique characteristics of this region. The main conclusion is that the Black Sea is susceptible to significant variations in wind, waves, and water temperature, influenced by cyclones and other meteorological phenomena. Seasonal variations in wind have been identified as a crucial aspect of the wind resource dynamics in the Black Sea basin, with complex patterns involving periods of intensification and calm.

Cyclones affecting the region have shown a diversity of intensities and trajectories, influencing different regions of the Black Sea and the Sea of Azov. These meteorological events can cause significant changes in local oceanographic and atmospheric conditions, including alterations in wind speed, wave height, and water temperature. The study of the cyclone in September 2005 highlighted the significant impact of Mediterranean tropical cyclones on marine and coastal conditions.

Water temperature, also an important parameter, has been significantly affected by cyclones, leading to substantial changes in the central region of the cyclone. These temperature variations can impact marine ecosystems and oceanographic processes.

Regarding the wind potential in the Black Sea, the analysis of wind speed data has revealed that this region possesses notable wind resources. The selected reference locations have shown annual energy production values in the range of 16,000-28,100 MWh, with promising prospects for the development of offshore wind farms. The results indicate that currently available wind turbine technologies, such as those from Siemens Gamesa, are sufficient for the efficient exploitation of these resources.

Comparing the results with other studies in the field confirms the significant potential of the Black Sea for the development of renewable wind energy. However, it is crucial to monitor climate evolution and wind resources continuously to make informed decisions about the future development of this renewable energy source in this vital region of Eastern Europe.

Although the Black Sea does not boast impressive wind resources at low altitudes, the analysis reveals significant potential for renewable energy generation at higher altitudes. This opens interesting perspectives for the future development of airborne wind energy technologies.

Comparing the performance of a 5 MW AWES system with a conventional wind turbine of the same capacity, it is evident that the airborne system can achieve superior results, especially in the Black Sea region under favorable wind conditions. The choice of operating altitude is crucial for maximizing the efficiency and performance of airborne systems, and the obtained data suggest that the optimal altitude falls within the range of 750-800 m above ground level.

In addition to improved performance, AWES technologies also present advantages in terms of costs. Airborne systems do not require expensive foundations and can be installed in various locations, including areas with deep water depths where conventional wind turbines are not viable. This makes them an attractive option for developing renewable energy infrastructure in the Black Sea region.

While this work focused on assessing the high-altitude wind potential, it is essential to note that the development of AWES technologies is still in the pre-commercial phase, and their widespread implementation requires continuous research and development. However, the obtained results suggest that these technologies have significant potential in the context of transitioning to renewable energy sources in the Black Sea region, contributing to the diversification of the energy sector and the reduction of carbon emissions.

The analysis of the structural elements of wind turbines, with a focus on towers (performed using the ANSYS program), demonstrated the importance of aspects such as shape and material. It was found that, in some cases, modifying the shape and using alternative materials, such as concrete, can lead to improvements in structural and economic performance. This represents a valuable opportunity for the future development of offshore wind technologies.

Furthermore, the analysis of the foundation on which the wind turbine is placed was conducted using the ANSYS AQWA program. The study focused on the hydrodynamic behavior of a spar-type foundation in marine environments, highlighting the importance of factors such as structure geometry, water depth, and their influence on hydrodynamic forces and moments. The results obtained demonstrate the consistency of simulations and the relevance of using the ANSYS AQWA program in such studies. Comparisons with data from the literature confirmed the analysis's coherence and underscored the relevance of the analyzed parameters for assessing the stability and performance of the structure.

Another aspect addressed in the thesis is the evaluation of the efficiency and costs associated with offshore wind technologies, both fixed to the seabed and floating. This analysis brought critical aspects to the forefront, such as adapting structures to withstand extreme wind conditions, optimizing costs based on water depth and energy production, and evaluating the structural robustness of towers.

One of the significant findings of this study was the paramount importance of energy production in determining the Levelized Cost of Energy (LCOE). The results showed that wind turbine performance and wind resources are key factors in establishing the economic efficiency of offshore wind farms.

The impact of water depth on anchoring and transmission costs, with a relatively limited influence on other costs, was also emphasized. This aspect opens new opportunities for regions with greater water depths, highlighting the potential of floating wind energy in these locations.

Regarding structural aspects, the analysis highlighted the advantages of floating structures, such as lower anchoring costs and adaptability to varying depths. However, it was observed that the structural strength of towers is a crucial factor, and their adaptation to specific wind and water depth conditions was necessary to ensure the safety and efficiency of the wind turbine.

This research has provided a comprehensive perspective on the costs and performance of offshore wind technologies and has contributed to a deeper understanding of these crucial aspects. However, there are needs for future research to quantify the uncertainties associated with LCOE estimates and to bring more clarity to cost analyses, especially for locations with greater water depths.

Overall, the PhD thesis underscores the importance of the Black Sea as a significant ecological, climatic, and economic resource in its surrounding region. The extensive analyses have revealed the considerable potential of the region for the development of renewable wind energy, with notable resources, especially at higher altitudes. This perspective suggests that the Black Sea can play a crucial role in diversifying the energy mix, reducing carbon emissions,

and promoting renewable energy sources in Eastern Europe. However, the implementation of these technologies requires continuous research and development, adaptation to specific wind and water depth conditions, and careful monitoring of climate evolution. By exploring these aspects, the Black Sea can become a focal point in the transition to a more sustainable energy and ecological future.

9.2 Original contributions

- Development of a detailed and well-elaborated current state of the art, identifying potential research directions and significant challenges in the field of offshore wind energy.
- Collection, organization, and analysis of wind and wave climate data in the Black Sea for the period 2002–2021, arranged in a logical chronological sequence to provide a comprehensive perspective on the climate of this region. This contributes to understanding the unique characteristics of the Black Sea region and identifying the influences of cyclones and meteorological phenomena on it.
- Investigation of cyclones affecting the Black Sea, analyzing their intensities and trajectories, contributing to understanding the impact of these meteorological events on local oceanographic and atmospheric conditions, as well as studying how the ERA5 database estimates these phenomena.
- Assessment of wind potential in the Black Sea region, identifying promising locations for the development of offshore wind farms, and highlighting existing wind turbine technologies suitable for efficient exploitation of these resources.
- Global-level evaluation and categorization of the Black Sea's energy exploitation potential. By comparing the Black Sea's potential with other globally exploited energy locations, significant conclusions can be drawn regarding its viability and importance.
- Investigation of airborne energy production technologies in the Black Sea region, highlighting the advantages of these technologies in terms of efficiency and costs compared to conventional wind turbines.
- Development of calculation algorithms in the MATLAB program for processing data from the ERA5 database and generating results in graphical format, representing a significant contribution to the analysis and interpretation of meteorological and oceanographic data in the context of this PhD thesis. These algorithms facilitated the extraction of essential information from the ERA5 database, contributing to substantiating conclusions and obtaining relevant research results.
- Analysis of the structural elements of wind turbines, examining aspects such as the shape and material of the towers, and highlighting opportunities to improve the functional and economic performance of these components.
- Development of geometric models using the ANSYS program for evaluating different types of structural designs for wind turbine towers and analyzing them using the ANSYS program. This approach allowed for a detailed analysis of the strength and structural behavior of the towers under different conditions, providing essential data for optimizing and improving these structures to increase the efficiency and safety of offshore wind farms.
- Creation of a detailed geometric model in the ANSYS program for the analysis of the wind turbine foundation and the study of structure diffraction considering the climate of the Black Sea.

- Evaluation of the efficiency and costs of offshore wind technologies in the context of the Black Sea. By using existing data and information, these costs were adapted and personalized to focus on the characteristics of the Black Sea region. Thus, critical factors influencing the efficiency and costs of offshore wind technologies in this region were identified, especially focusing on the impact of water depth and turbine performance on the Levelized Cost of Energy (LCOE).
- Development of adapted auxiliary formulas to generalize and simplify the cost calculation process, especially in the context of integrating these formulas into Chapter 9 to facilitate their application in the calculation model for all types of foundations used.
- Creation of detailed graphical representations that contributed to understanding and illustrating the results obtained throughout the entire research.

9.3 Perspectives

- Modeling and simulation at various depths and evaluating its behavior against irregular waves or wave groups specific to the conditions in the Black Sea for spar-type foundations.
- Investigating the possibility of using other types of foundations, such as semi-submersible foundations or fixed foundations, in the specific context of the offshore environment in the Black Sea through simulations. Performing a comparison of the behavior of these foundation types to assess their advantages and disadvantages in this region.
- Structural analysis of airborne wind energy systems using the ANSYS program.
- Exploring the potential combination of multiple types of renewable energy capture devices, such as wind turbines with solar panels or wind turbines with wave energy capture devices.
- Verifying the accuracy of data from the ERA5 reanalysis database by comparing them with real data and conducting a comparative analysis with other relevant databases.
- Investigating the feasibility of implementing floating solar panels and analyzing the appropriate foundation requirements for their placement in the Black Sea.
- Evaluating the impact on marine biodiversity: Studying the effects of offshore wind farms and other renewable energy extraction systems on the marine environment and ecosystems in the Black Sea.
- Investigating the economic and social impact of developing renewable energy sources in the region, including job creation, infrastructure for local communities, and the impact on energy prices.
- Researching the effects of climate change on wind and solar resources in marine environments.
- Investigating cost optimization solutions for the construction and maintenance of offshore wind farms.
- Analyzing the impact on maritime navigation and safety at sea in the context of developing renewable energy infrastructure.

List of the scientific papers elaborated by the author

A1 Papers published in ISI journals and proceedings

1. Journal: E3S Web Conf.
   Authors: Eugen Rusu, **Alexandra Diaconita**, Alina Raileanu
   Year: 2020, Number of citations according to web of science: **5**
   Title: An assessment of the wind power dynamics in the European coastal environment
2. Journal: Energy Reports, **IF: 5.2, Q2**
   Authors: **Alexandra Diaconita,** Gabriel Andrei, Liliana Rusu
   Year: 2021, Number of citations according to web of science: **7**
   Title: New insights into the wind energy potential of the west Black Sea area based on the North Sea wind farms model
3. Journal: Inventions, **IF: 3.4, Q1**
   Authors: **Alexandra Diaconita**, Liliana Rusu, Gabriel Andrei
   Year: 2021
   Title: A Local Perspective on Wind Energy Potential in Six Reference Sites on the Western Coast of the Black Sea Considering Five Different Types of Wind Turbines
4. Journal: Inventions, **IF: 3.4, Q1**
   Authors: **Alexandra Diaconita**, Gabriel Andrei, Liliana Rusu
   Year: 2022, Number of citations according to web of science: **4**
   Title: Estimation of tower shape effect on stress-strain behavior of wind turbines operating under *offshore* boundary condition
5. Journal: Journal of Marine Science and Engineering, **IF: 2, Q1**
   Authors: Florin Onea, **Alexandra Diaconita**, Daniel Ganea
   Year: 2022
   Title: Assessment of the Black Sea High-Altitude Wind Energy
6. Journal: Energy Reports, IF: 5.2, Q2
   Authors: **Alexandra Diaconita**, Gabriel Andrei, Liliana Rusu
   Year: 2022
   Title: An overview of the *offshore* wind energy potential for twelve significant geographical locations across the globe
7. Journal: Journal of Marine Science and Engineering, **IF: 2**, **Q1**
   Authors: **Alexandra Diaconita**, Gabriel Andrei, Liliana Rusu.
   Year: 2023, Number of citations according to web of science: **4**
   Title: An Evaluation of the Efficiency of the Floating Solar Panels in the Western Black Sea and the Razim-Sinoe Lagunar System

A2 Papers published in BDI journals

1. Journal: MECHANICAL TESTING AND DIAGNOSIS
   Authors: **Alexandra Diaconita**, Florin Onea, Eugen Rusu
   Year: 2019, ISSN 2247-9635
   Title: An evaluation of the wind energy in the North Sea coast
2. Journal: MECHANICAL TESTING AND DIAGNOSIS
   Authors: Daniel Ganea, **Alexandra Diaconita**, Florin Onea
   Year: 2022, ISSN 2247-9635
   Title: Performance assessment of a 5 MW awes generator operating in the black sea western area

A3 Papers published in the volumes of international conferences

1. Conference: 18th ASTR Conference
   Authors: Eugen Rusu, Florin Onea, **Alexandra Diaconita**
   Year: 2023
   Title: Assessment of the solar and wind energy potential related to romanian southern lakes

A4 Papers presented at national conferences with international participation

1. Conference: International Conference on Advances on Clean Energy Research, 15-17 April
   Authors: **Alexandra Diaconita**, Liliana Rusu, Gabriel Andrei
   Year: 2021
   Title: New insights into the wind energy potential of the west Black Sea area based on the North Sea wind farms model
2. Conference: Scientific Conference organized by the Doctoral Schools of "Dunărea de Jos" University of Galați (SCDS-UDJG), 9-10 June
   Authors: **Alexandra Diaconita**, Liliana Rusu, Gabriel Andrei
   Year: 2021
   Title: A perspective on the wind dynamics near the Romanian Black Sea coast based on the forecast climate scenario
3. Conference: International Conference on Advances on Clean Energy Research, 20-22 April
   Authors: **Alexandra Diaconita**, Gabriel Andrei, Liliana Rusu
   Year: 2022
   Title: An overview of the *offshore* wind energy potential for twelve significant geographical locations across the globe
4. Conference: Scientific Conference organized by the Doctoral Schools of "Dunărea de Jos" University of Galați (SCDS-UDJG), 9-10 June
   Authors: **Alexandra Diaconita**, Gabriel Andrei, Eugen Rusu
   Year: 2022
   Title: Inference of the LCOE for a future *offshore* wind farm located in the western area of the Black Sea
5. Conference: Scientific Conference organized by the Doctoral Schools of "Dunărea de Jos" University of Galați (SCDS-UDJG), 9-10 June
   Authors: **Alexandra Diaconita**, Gabriel Andrei, Eugen Rusu
   Year: 2023
   Title: Evaluation and validation using measured data of the global solar radiation model for a site in Romania

A5 Projects

1. Member of the research team for the DREAM project ("Dinamica REsurselor si Avansul tehnologic in extragerea energiei regenerabile din mediul Marin"), supported by the Executive Agency for Higher Education, Research, Development, and Innovation Funding from Romania - UEFISCDI, grant number PN-III-P4-ID-PCE-2020-0008. Link: https://dream.ugal.ro
2. Member of the research team for the project "Soluții avansate pentru utilizarea energiei vântului din bazinul Mării Negre", funded under contract no. 14890/11.05.2022.

References

1. Bakker, R.H.; Bouma, J.; Pedersen; Berg; van den Berg, F. *Project WINDFARMperception Visual and Acoustic Impact of Wind Turbine Farms on Residents*; 2008;
2. Molina-Ruiz, J.; García-Lorenzo, M.L.; Martínez-Sánchez, M.; Gallego, D. Assessment of the Acoustic Impact of Wind Farm Projects: Methodology and Case. *Journal of Geoscience and Environment Protection* **2018**, *06*, 99–110, doi:10.4236/gep.2018.61007.
3. Guan, J. Landscape Visual Impact Evaluation for Onshore Wind Farm: A Case Study. *ISPRS International Journal of Geo-Information* **2022**, *11*, 594, doi:10.3390/ijgi11120594.
4. Bishop, I.D. The Implications for Visual Simulation and Analysis of Temporal Variation in the Visibility of Wind Turbines. *Landscape and Urban Planning* **2019**, *184*, 59–68, doi:10.1016/j.landurbplan.2018.12.004.
5. van Kamp, I.; van den Berg, F. Health Effects Related to Wind Turbine Sound, Including Low-Frequency Sound and Infrasound. *Acoust Aust* **2018**, *46*, 31–57, doi:10.1007/s40857-017-0115-6.
6. Hessler, G.; Leventhall, G.; Schomer, P.; Walker, B. Health Effects from Wind Turbine Low Frequency Noise & Infrasound: Do Wind Turbines Make People Sick? That Is the Issue. **2017**, *51*, 34–44.
7. Soares-Ramos, E.P.P.; de Oliveira-Assis, L.; Sarrias-Mena, R.; Fernández-Ramírez, L.M. Current Status and Future Trends of Offshore Wind Power in Europe. *Energy* **2020**, *202*, 117787, doi:10.1016/j.energy.2020.117787.
8. Bošnjaković, M.; Katinić, M.; Santa, R.; Marić, D. Wind Turbine Technology Trends. *Applied Sciences* **2022**, *12*, 8653, doi:10.3390/app12178653.
9. Brøndsted, P.; Nijssen, R.P.L. Advances in Wind Turbine Blade Design and Materials.; Woodhead Publishing Limited, 2013.
10. Chen, J.; Kim, M.-H. Review of Recent Offshore Wind Turbine Research and Optimization Methodologies in Their Design. *Journal of Marine Science and Engineering* **2022**, *10*, 28, doi:10.3390/jmse10010028.
11. Hsiao, S.-C.; Cheng, C.-T.; Chang, T.-Y.; Chen, W.-B.; Wu, H.-L.; Jang, J.-H.; Lin, L.-Y. Assessment of Offshore Wave Energy Resources in Taiwan Using Long-Term Dynamically Downscaled Winds from a Third-Generation Reanalysis Product. *Energies* **2021**, *14*, 653, doi:10.3390/en14030653.
12. Tahir, Z. ul R.; Sarfraz, M.S.; Asim, M.; Sajid, M.; Imran, S.; Hayat, N. Evaluation of ERA-Interim and NCEP-CFSR Reanalysis Datasets against in-Situ Measured Wind Speed Data for Keti Bandar Port, Pakistan. *Journal of Physics: Conference Series* **2018**, *1102*, 012001, doi:10.1088/1742-6596/1102/1/012001.
13. Samal, R.K. Assessment of Wind Energy Potential Using Reanalysis Data: A Comparison with Mast Measurements. *Journal of Cleaner Production* **2021**, *313*, 127933, doi:10.1016/j.jclepro.2021.127933.
14. Soares, P.M.M.; Lima, D.C.A.; Nogueira, M. Global Offshore Wind Energy Resources Using the New ERA-5 Reanalysis. *Environ. Res. Lett.* **2020**, *15*, 1040a2, doi:10.1088/1748-9326/abb10d.
15. Liu, B.; Ma, X.; Guo, J.; Li, H.; Jin, S.; Ma, Y.; Gong, W. *Assessment of the Wind Energy Resource on the Coast of China Based on Machine Learning Algorithms*; Aerosols/Field Measurements/Troposphere/Chemistry (chemical composition and reactions), 2022;
16. Vemuri, A.; Munters, W.; Buckingham, S.; Helsen, J.; Beeck, J. van Modeling Extreme Weather Events for Offshore Wind in the North Sea: A Sensitivity Analysis to Physics Parameterizations in WRF. *J. Phys.: Conf. Ser.* **2022**, *2265*, 022014, doi:10.1088/1742-6596/2265/2/022014.
17. Wang, S. *Assessment of Offshore Wind Turbines in Extreme Weather Conditions: Wave Nonlinearity Effect, Cyclic Soil Response and Breaking Wave Forcing*; DTU Wind Energy: Roskilde, 2019;

18. Yang, S.; Yuan, H.; Dong, L. Offshore Wind Resource Assessment by Charactering Weather Regimes Based on Self-Organizing Map. *Environmental Research Letters* **2022**, *17*, doi:10.1088/1748-9326/aca2c2.
19. Sobotka, A.; Rowicki, M.; Badyda, K.; Sobotka, P. Regulatory Aspects and Electricity Production Analysis of an Offshore Wind Farm in the Baltic Sea. *Renewable Energy* **2021**, *170*, 315–326, doi:10.1016/j.renene.2021.01.064.
20. Lizuma, L.; Avotniece, Z.; Rupainis, S.; Teilans, A. Assessment of the Present and Future Offshore Wind Power Potential: A Case Study in a Target Territory of the Baltic Sea Near the Latvian Coast. *The Scientific World Journal* **2013**, *2013*, e126428, doi:10.1155/2013/126428.
21. Sobotka, A.; Chmielewski, K.; Rowicki, M.; Dudzińska, J.; Janiak, P.; Badyda, K. Analysis of Offshore Wind Farm Located on Baltic Sea. *E3S Web Conf.* **2019**, *137*, 01049, doi:10.1051/e3sconf/201913701049.
22. Diaconita, A.; Onea, F.; Rusu, E. AN EVALUATION OF THE WIND ENERGY IN THE NORTH SEA COAST. **2019**, *9*, 17–22, doi:10.35219/mtd.2019.1.02.
23. Buatois, A.; Gibescu, M.; Rawn, B.G.; Van der Meijden, M.A.M.M. Analysis of North Sea Offshore Wind Power Variability. *Resources* **2014**, *3*, 454–470, doi:10.3390/resources3020454.
24. Schillings, C.; Wanderer, T.; Cameron, L.; van der Wal, J.T.; Jacquemin, J.; Veum, K. A Decision Support System for Assessing Offshore Wind Energy Potential in the North Sea. *Energy Policy* **2012**, *49*, 541–551, doi:10.1016/j.enpol.2012.06.056.
25. Hasager, C.B.; Barthelmie, R.J.; Christiansen, M.B.; Nielsen, M.; Pryor, S.C. Quantifying Offshore Wind Resources from Satellite Wind Maps: Study Area the North Sea. *Wind Energy* **2006**, *9*, 63–74, doi:10.1002/we.190.
26. Zheng, C.; Zhuang, H.; Li, X.; Li, X. Wind Energy and Wave Energy Resources Assessment in the East China Sea and South China Sea. *Sci. China Technol. Sci.* **2012**, *55*, 163–173, doi:10.1007/s11431-011-4646-z.
27. Tian, Y.; kou, L.; Han, Y.; Yang, X.; Hou, T.; Zhang, W. Evaluation of Offshore Wind Power in the China Sea. *Energy Exploration & Exploitation* **2021**, *39*, 1803–1816, doi:10.1177/0144598721992268.
28. Wen, Y.; Kamranzad, B.; Lin, P. Assessment of Long-Term Offshore Wind Energy Potential in the South and Southeast Coasts of China Based on a 55-Year Dataset. *Energy* **2021**, *224*, 120225, doi:10.1016/j.energy.2021.120225.
29. Jiang, D.; Zhuang, D.; Huang, Y.; Wang, J.; Fu, J. Evaluating the Spatio-Temporal Variation of China's Offshore Wind Resources Based on Remotely Sensed Wind Field Data. *Renewable and Sustainable Energy Reviews* **2013**, *24*, 142–148, doi:10.1016/j.rser.2013.03.058.
30. Liu, H.; Chen, J.; Zhang, J.; Chen, Y.; Wen, Y.; Zhang, X.; Yan, Z.; Li, Q. Study on Atmospheric Stability and Wake Attenuation Constant of Large Offshore Wind Farm in Yellow Sea. *Energies* **2023**, *16*, 2227, doi:10.3390/en16052227.
31. Li, D.; Geyer, B.; Bisling, P. A Model-Based Climatology Analysis of Wind Power Resources at 100-m Height over the Bohai Sea and the Yellow Sea. *Applied Energy* **2016**, *179*, 575–589, doi:10.1016/j.apenergy.2016.07.010.
32. Archer, C.L.; Caldeira, K. Global Assessment of High-Altitude Wind Power. *Energies* **2009**, *2*, 307–319, doi:10.3390/en20200307.
33. Bechtle, P.; Schelbergen, M.; Schmehl, R.; Zillmann, U.; Watson, S. Airborne Wind Energy Resource Analysis. *Renewable Energy* **2019**, *141*, 1103–1116, doi:10.1016/j.renene.2019.03.118.
34. Marvel, K.; Kravitz, B.; Caldeira, K. Geophysical Limits to Global Wind Power. *Nature Climate Change* **2013**, *3*, 118–121.
35. Sommerfeld, M.; Dörenkämper, M.; De Schutter, J.; Crawford, C. Impact of Wind Profiles on Ground-Generation Airborne Wind Energy System Performance. *Wind Energy Science* **2023**, *8*, 1153–1178, doi:10.5194/wes-8-1153-2023.
36. Dief, T.N.; Fechner, U.; Schmehl, R.; Yoshida, S.; Rushdi, M.A. Adaptive Flight Path Control of Airborne Wind Energy Systems. *Energies* **2020**, *13*, 667, doi:10.3390/en13030667.

37. Saleem, A.; Kim, M.-H. Aerodynamic Performance Optimization of an Airfoil-Based Airborne Wind Turbine Using Genetic Algorithm. *Energy* **2020**, *203*, 117841, doi:10.1016/j.energy.2020.117841.
38. Salma, V.; Schmehl, R. Operation Approval for Commercial Airborne Wind Energy Systems. *Energies* **2023**, *16*, 3264, doi:10.3390/en16073264.
39. Batel, S.; Devine-Wright, P. Using a Critical Approach to Unpack the Visual-Spatial Impacts of Energy Infrastructures. In *A critical approach to the social acceptance of renewable energy infrastructures: Going beyond green growth and sustainability*; Batel, S., Rudolph, D., Eds.; Springer International Publishing: Cham, 2021; pp. 43–60 ISBN 978-3-030-73699-6.
40. Hoen, B.; Firestone, J.; Rand, J.; Elliot, D.; Hübner, G.; Pohl, J.; Wiser, R.; Lantz, E.; Haac, T.R.; Kaliski, K. Attitudes of U.S. Wind Turbine Neighbors: Analysis of a Nationwide Survey. *Energy Policy* **2019**, *134*, 110981, doi:10.1016/j.enpol.2019.110981.
41. Megahed, N.A. Landscape and Visual Impact Assessment: Perspectives and Issues with Flying Wind Technologies. *Landscape* **2014**, *3*.
42. Pohl, J.; Gabriel, J.; Hübner, G. Understanding Stress Effects of Wind Turbine Noise – The Integrated Approach. *Energy Policy* **2018**, *112*, 119–128, doi:10.1016/j.enpol.2017.10.007.
43. Hübner, G.; Pohl, J.; Hoen, B.; Firestone, J.; Rand, J.; Elliott, D.; Haac, R. Monitoring Annoyance and Stress Effects of Wind Turbines on Nearby Residents: A Comparison of U.S. and European Samples. *Environment International* **2019**, *132*, 105090, doi:10.1016/j.envint.2019.105090.
44. Liu, X.; Lu, C.; Li, G.; Godbole, A.; Chen, Y. Effects of Aerodynamic Damping on the Tower Load of Offshore Horizontal Axis Wind Turbines. *Applied Energy* **2017**, *204*, 1101–1114, doi:10.1016/j.apenergy.2017.05.024.
45. Dagli, B.Y.; Tuskan, Y.; Gokkus, U. Evaluation of Offshore Wind Turbine Tower Dynamics with Numerical Analysis. *Advances in Civil Engineering* **2018**, *2018*.
46. Yan, G.; Xi-chang, Z.; Yan, L. Anti-Corrosion Protection Strategies for Support Structures and Foundations of Wind Turbines of Offshore Wind Farms. **2009**, doi:10.1109/SUPERGEN.2009.5348091.
47. Marinova, N.; Urbegain, A.; Benguria, P.; Travé, A.; Caracena, R. Evaluation of Anticorrosion Coatings for Offshore Wind Turbine Monopiles for an Optimized and Time-Efficient Coating Application. *Coatings* **2022**, *12*, 384, doi:10.3390/coatings12030384.
48. Tang, D.; Zhao, M. Real-Time Monitoring System for Scour around Monopile Foundation of Offshore Wind Turbine. *J Civil Struct Health Monit* **2021**, *11*, 645–660, doi:10.1007/s13349-020-00467-4.
49. Vidal, Y.; Aquino, G.; Pozo, F.; Gutiérrez-Arias, J.E.M. Structural Health Monitoring for Jacket-Type Offshore Wind Turbines: Experimental Proof of Concept. *Sensors* **2020**, *20*, 1835, doi:10.3390/s20071835.
50. Rolfes, R.; Zerbst, S.; Haake, G.; Reetz, J.; Lynch, J.P. Integral SHM-System for Offshore Wind Turbines Using Smart Wireless Sensors.; DEStech Publications Inc. Stanford, CA, USA, 2007; Vol. 200, pp. 11–13.
51. Vieira, M.; Snyder, B.; Henriques, E.; White, C.; Reis, L. Economic Viability of Implementing Structural Health Monitoring Systems on the Support Structures of Bottom-Fixed Offshore Wind. *Energies* **2023**, *16*, 4885.
52. Lefranc, M.; Torud, A. Three Wind Turbines on One Floating Unit, Feasibility, Design and Cost.; OTC, 2011; p. OTC-21485.
53. Bashetty, S.; Ozcelik, S. Design and Stability Analysis of an Offshore Floating Multi-Turbine Platform. In Proceedings of the 2020 IEEE Green Technologies Conference(GreenTech); April 2020; pp. 184–189.
54. Zambrano, T.; MacCready, T.; Kiceniuk Jr, T.; Roddier, D.G.; Cermelli, C.A. Dynamic Modeling of Deepwater Offshore Wind Turbine Structures in Gulf of Mexico Storm Conditions.; 2006; Vol. 47462, pp. 629–634.
55. Bae, Y.H.; Kim, M.H. Coupled Dynamic Analysis of Multiple Wind Turbines on a Large Single Floater. *Ocean Engineering* **2014**, *92*, 175–187, doi:10.1016/j.oceaneng.2014.10.001.

56. O'Leary, K.; Pakrashi, V.; Kelliher, D. Optimization of Composite Material Tower for Offshore Wind Turbine Structures. *Renewable Energy* **2019**, *140*, 928–942.
57. Young, A.C.; Goupee, A.J.; Dagher, H.J.; Viselli, A.M. Methodology for Optimizing Composite Towers for Use on Floating Wind Turbines. *Journal of renewable and sustainable energy* **2017**, *9*, 33305.
58. Quilligan, A.; O'Connor, A.; Pakrashi, V. Fragility Analysis of Steel and Concrete Wind Turbine Towers. *Engineering structures* **2012**, *36*, 270–282.
59. de Lana, J.A.; Júnior, P.A.A.M.; Magalhães, C.A.; Magalhães, A.L.M.A.; de Andrade Junior, A.C.; de Barros Ribeiro, M.S. Behavior Study of Prestressed Concrete Wind-Turbine Tower in Circular Cross-Section. *Engineering Structures* **2021**, *227*, 111403, doi:10.1016/j.engstruct.2020.111403.
60. Pillai, A.C.; Gordelier, T.J.; Thies, P.R.; Cuthill, D.; Johanning, L. Anchor Loads for Shallow Water Mooring of a 15 MW Floating Wind Turbine—Part II: Synthetic and Novel Mooring Systems. *Ocean Engineering* **2022**, *266*, 112619, doi:10.1016/j.oceaneng.2022.112619.
61. Laura, C.-S.; Vicente, D.-C. Life-Cycle Cost Analysis of Floating Offshore Wind Farms. *Renewable Energy* **2014**, *66*, 41–48, doi:10.1016/j.renene.2013.12.002.
62. Maienza, C.; Avossa, A.M.; Ricciardelli, F.; Coiro, D.; Troise, G.; Georgakis, C.T. A Life Cycle Cost Model for Floating Offshore Wind Farms. *Applied Energy* **2020**, *266*, 114716, doi:10.1016/j.apenergy.2020.114716.
63. Mytilinou, V.; Kolios, A.J. A Multi-Objective Optimisation Approach Applied to Offshore Wind Farm Location Selection. *J. Ocean Eng. Mar. Energy* **2017**, *3*, 265–284, doi:10.1007/s40722-017-0092-8.
64. Song, D.; Xu, S.; Huang, L.; Xia, E.; Huang, C.; Yang, J.; Hu, Y.; Fang, F. Multi-Site and Multi-Objective Optimization for Wind Turbines Based on the Design of Virtual Representative Wind Farm. *Energy* **2022**, *252*, 123995, doi:10.1016/j.energy.2022.123995.
65. Rodrigues, S.; Restrepo, C.; Katsouris, G.; Teixeira Pinto, R.; Soleimanzadeh, M.; Bosman, P.; Bauer, P. A Multi-Objective Optimization Framework for Offshore Wind Farm Layouts and Electric Infrastructures. *Energies* **2016**, *9*, 216, doi:10.3390/en9030216.
66. Li, Z.; Tian, G.; El-Shafay, A.S. Statistical-Analytical Study on World Development Trend in Offshore Wind Energy Production Capacity Focusing on Great Britain with the Aim of MCDA Based Offshore Wind Farm Siting. *Journal of Cleaner Production* **2022**, *363*, 132326, doi:10.1016/j.jclepro.2022.132326.
67. Deveci, M.; Özcan, E.; John, R.; Covrig, C.-F.; Pamucar, D. A Study on Offshore Wind Farm Siting Criteria Using a Novel Interval-Valued Fuzzy-Rough Based Delphi Method. *Journal of Environmental Management* **2020**, *270*, 110916, doi:10.1016/j.jenvman.2020.110916.
68. Myhr, A.; Bjerkseter, C.; Ågotnes, A.; Nygaard, T.A. Levelised Cost of Energy for Offshore Floating Wind Turbines in a Lifecycle Perspective. *Renewable Energy* **2014**, *66*, 714–728, doi:10.1016/j.renene.2014.01.017.
69. Hammond, R.; Cooperman, A. *Windfarm Operations and Maintenance Cost-Benefit Analysis Tool (WOMBAT)*; 2022; p. NREL/TP-5000-83712, 1894867, MainId:84485;
70. McMorland, J.; Flannigan, C.; Carroll, J.; Collu, M.; McMillan, D.; Leithead, W.; Coraddu, A. A Review of Operations and Maintenance Modelling with Considerations for Novel Wind Turbine Concepts. *Renewable and Sustainable Energy Reviews* **2022**, *165*, 112581, doi:10.1016/j.rser.2022.112581.
71. Yeter, B.; Garbatov, Y.; Guedes Soares, C. Risk-Based Maintenance Planning of Offshore Wind Turbine Farms. *Reliability Engineering & System Safety* **2020**, *202*, 107062, doi:10.1016/j.ress.2020.107062.
72. Gleixner, S.; Demissie, T.; Diro, G.T. Did ERA5 Improve Temperature and Precipitation Reanalysis over East Africa? *Atmosphere* **2020**, *11*, 996.
73. Hoffmann, L.; Günther, G.; Li, D.; Stein, O.; Wu, X.; Griessbach, S.; Heng, Y.; Konopka, P.; Müller, R.; Vogel, B. From ERA-Interim to ERA5: The Considerable Impact of ECMWF's next-Generation Reanalysis on Lagrangian Transport Simulations. *Atmospheric Chemistry and Physics* **2019**, *19*, 3097–3124.

74. Diaconita, A.I.; Rusu, L.; Andrei, G. A Local Perspective on Wind Energy Potential in Six Reference Sites on the Western Coast of the Black Sea Considering Five Different Types of Wind Turbines. *Inventions* **2021**, *6*, doi:10.3390/inventions6030044.
75. Diaconita, A.; Andrei, G.; Rusu, L. New Insights into the Wind Energy Potential of the West Black Sea Area Based on the North Sea Wind Farms Model. *Energy Reports* **2021**, *7*, 112–118, doi:10.1016/j.egyr.2021.06.018.
76. Diaf, S.; Notton, G.; Belhamel, M.; Haddadi, M.; Louche, A. Design and Techno-Economical Optimization for Hybrid PV/Wind System under Various Meteorological Conditions. *Applied Energy* **2008**, *85*, 968–987, doi:https://doi.org/10.1016/j.apenergy.2008.02.012.
77. Masri, S.; Mohamad, N.; Hafeez, M. *Wind Speed Analysis at Nibong Tebal*; 2012; p. 4; ISBN 978-1-4673-2468-7.
78. Bauelos-Ruedas, F.; Angeles-Camacho, C.; Sebastin Methodologies Used in the Extrapolation of Wind Speed Data at Different Heights and Its Impact in the Wind Energy Resource Assessment in a Region. *Wind Farm - Technical Regulations, Potential Estimation and Siting Assessment* **2011**, doi:10.5772/20669.
79. Manwell, J.F.; McGowan, J.G.; Rogers, A.L. *Wind Energy Explained: Theory, Design and Application*; Wiley: Chichester, United Kingdom, 2009;
80. Hellmann, G. Über Die Bewegung Der Luft in Den Untersten Schichten Der Atmosphäre. *Meteoral. Z.* **1916**, *34*, 273.
81. Albani, A.; Ibrahim, M.Z. Wind Energy Potential and Power Law Indexes Assessment for Selected Near-Coastal Sites in Malaysia. *Energies* **2017**, *10*, doi:10.3390/en10030307.
82. American Bureau of Shipping (ABS) *Guide for Building and Classing Offshore Wind Turbine Installation*; Houston, TX, USA, 2014;
83. Liu, Y.; Chen, D.; Yi, Q.; Li, S. Wind Profiles and Wave Spectra for Potential Wind Farms in South China Sea. Part I: Wind Speed Profile Model. *Energies* **2017**, *10*, doi:10.3390/en10010125.
84. Jarraud, M. Guide to Meteorological Instruments and Methods of Observation (WMO-No. 8). *World Meteorological Organisation: Geneva, Switzerland* **2008**, *29*.
85. Hussain, I.; Haider, A.; Ullah, Z.; Russo, M.; Casolino, G.M.; Azeem, B. Comparative Analysis of Eight Numerical Methods Using Weibull Distribution to Estimate Wind Power Density for Coastal Areas in Pakistan. *Energies 2023, Vol. 16, Page 1515* **2023**, *16*, 1515, doi:10.3390/EN16031515.
86. Carreno-Madinabeitia, S.; Ibarra-Berastegi, G.; Sáenz, J.; Ulazia, A. Long-Term Changes in Offshore Wind Power Density and Wind Turbine Capacity Factor in the Iberian Peninsula (1900–2010). *Energy* **2021**, *226*, 120364, doi:10.1016/J.ENERGY.2021.120364.
87. Song, D.; Zheng, S.; Yang, S.; Yang, J.; Dong, M.; Su, M.; Joo, Y.H. Annual Energy Production Estimation for Variable-Speed Wind Turbine at High-Altitude Site. *Journal of Modern Power Systems and Clean Energy* **2020**, 1–4, doi:10.35833/MPCE.2019.000240.
88. Afungchui, D.; Aban, C.E. Analysis of Wind Regimes for Energy Estimation in Bamenda, of the North West Region of Cameroon, Based on the Weibull Distribution. *Revue des Energies Renouvelables* **2014**, *17*, 137–147.
89. Gul, M.; Tai, N.; Huang, W.; Nadeem, M.H.; Yu, M. Assessment of Wind Power Potential and Economic Analysis at Hyderabad in Pakistan: Powering to Local Communities Using Wind Power. *Sustainability* **2019**, *11*, 1391.
90. Chang, T.P.; Liu, F.J.; Ko, H.H.; Cheng, S.P.; Sun, L.C.; Kuo, S.C. Comparative Analysis on Power Curve Models of Wind Turbine Generator in Estimating Capacity Factor. *Energy* **2014**, *73*, 88–95, doi:10.1016/J.ENERGY.2014.05.091.
91. Diaconita, A.I.; Andrei, G.; Rusu, L. An Overview of the Offshore Wind Energy Potential for Twelve Significant Geographical Locations across the Globe. *Energy Reports* **2022**, *8*, doi:10.1016/j.egyr.2022.10.193.
92. Soukissian, T.H.; Karathanasi, F.E.; Zaragkas, D.K. Exploiting Offshore Wind and Solar Resources in the Mediterranean Using ERA5 Reanalysis Data. *Energy Conversion and Management* **2021**, *237*, 114092, doi:10.1016/j.enconman.2021.114092.

93. Hasager, C.B.; Hahmann, A.N.; Ahsbahs, T.; Karagali, I.; Sile, T.; Badger, M.; Mann, J. Europe's Offshore Winds Assessed with Synthetic Aperture Radar, ASCAT and WRF. *Wind Energy Science* **2020**, *5*, 375–390, doi:10.5194/wes-5-375-2020.
94. Costoya, X.; deCastro, M.; Carvalho, D.; Feng, Z.; Gómez-Gesteira, M. Climate Change Impacts on the Future Offshore Wind Energy Resource in China. *Renewable Energy* **2021**, *175*, 731–747, doi:10.1016/j.renene.2021.05.001.
95. Aeroelastic Analysis of a Large Airborne Wind Turbine | Journal of Guidance, Control, and Dynamics Available online: https://arc.aiaa.org/doi/10.2514/1.G001663 (accessed on 12 August 2023).
96. Kolar, J.W.; Friedli, T.; Krismer, F.; Looser, A.; Schweizer, M.; Friedemann, R.A.; Steimer, P.K.; Bevirt, J.B. Conceptualization and Multiobjective Optimization of the Electric System of an Airborne Wind Turbine. *IEEE Journal of Emerging and Selected Topics in Power Electronics* **2013**, *1*, 73–103, doi:10.1109/JESTPE.2013.2269672.
97. De Lellis, M.; Reginatto, R.; Saraiva, R.; Trofino, A. The Betz Limit Applied to Airborne Wind Energy. *Renewable Energy* **2018**, *127*, 32–40, doi:10.1016/j.renene.2018.04.034.
98. Diehl, M. Airborne Wind Energy: Basic Concepts and Physical Foundations. In *Airborne Wind Energy*; Ahrens, U., Diehl, M., Schmehl, R., Eds.; Green Energy and Technology; Springer: Berlin, Heidelberg, 2013; pp. 3–22 ISBN 978-3-642-39965-7.
99. Kite Gen Available online: http://www.kitegen.com/pages/technology.html (accessed on 11 August 2023).
100. Weber, J.; Marquis, M.; Cooperman, A.; Draxl, C.; Hammond, R.; Jonkman, J.; Lemke, A.; Lopez, A.; Mudafort, R.; Optis, M.; et al. Airborne Wind Energy. *Renewable Energy* **2021**.
101. Onea, F.; Rusu, L. Evaluation of Some State-Of-The-Art Wind Technologies in the Nearshore of the Black Sea. *Energies* **2018**, *11*, 2452, doi:10.3390/en11092452.
102. He, Y.; Fu, J.; Chan, P.W.; Li, Q.; Shu, Z.; Zhou, K. Reduced Sea-Surface Roughness Length at a Coastal Site. *Atmosphere* **2021**, *12*, 991, doi:10.3390/atmos12080991.
103. Schelbergen, M.; Kalverla, P.C.; Schmehl, R.; Watson, S.J. Clustering Wind Profile Shapes to Estimate Airborne Wind Energy Production. *Wind Energy Science* **2020**, *5*, 1097–1120, doi:10.5194/wes-5-1097-2020.
104. Onea, F.; Diaconita, A.; Ganea, D. Assessment of the Black Sea High-Altitude Wind Energy. *Journal of Marine Science and Engineering* **2022**, *10*, 1463, doi:10.3390/jmse10101463.
105. Inventions | Free Full-Text | An Analysis of the Wind Parameters in the Western Side of the Black Sea Available online: https://www.mdpi.com/2411-5134/7/1/21 (accessed on 10 August 2023).
106. Santana, D.A.D.; El-Thalji, I. Scalability and Compatibility Analyses of Airborne Wind Technology for Maritime Transport. *IOP Conf. Ser.: Mater. Sci. Eng.* **2019**, *700*, 012064, doi:10.1088/1757-899X/700/1/012064.
107. Green, R.; Vasilakos, N. The Economics of Offshore Wind. *Energy Policy* **2011**, *39*, 496–502, doi:10.1016/j.enpol.2010.10.011.
108. Diaconita, A.; Andrei, G.; Rusu, E. Estimation of the Tower Shape Effect on the Stress-Strain Behavior of Wind Turbines Operating under Offshore Boundary Conditions. *Inventions* **2022**, *7*, 11, doi:10.3390/inventions7010011.
109. Commission, I.E. Wind Turbines—Part 1: Design Requirements. Tech. Doc. IEC 61400-1. *International Electrotechnical Commission* **2005**.
110. Hsu, Y.; Wu, W.-F.; Chang, Y.-C. Reliability Analysis of Wind Turbine Towers. *Procedia Engineering* **2014**, *79*, 218–224.
111. Li, X.L.; Ren, L.M. Finite Element Analysis of Wind Turbine Tower. In Proceedings of the Applied Mechanics and Materials; Trans Tech Publ, 2013; Vol. 351, pp. 825–828.
112. Liu, H.; Yang, S.; Tian, W.; Zhao, M.; Yuan, X.; Xu, B. Vibration Reduction Strategy for Offshore Wind Turbines. *Applied Sciences* **2020**, *10*, 6091.
113. Stolarski, T.; Nakasone, Y.; Yoshimoto, S. *Engineering Analysis with ANSYS Software*; Butterworth-Heinemann, 2018; ISBN 978-0-08-102165-1.

114. Lee, H.-H. *Finite Element Simulations with ANSYS Workbench 18*; SDC Publications, 2018; ISBN 978-1-63057-173-3.
115. Gentils, T.; Wang, L.; Kolios, A. Integrated Structural Optimisation of Offshore Wind Turbine Support Structures Based on Finite Element Analysis and Genetic Algorithm. *Applied energy* **2017**, *199*, 187–204.
116. Lloyd, G.; Hamburg, G. Guideline for the Certification of Wind Turbines. *July 1st* **2010**.
117. Wang, L.; Kolios, A.; Luengo, M.M.; Liu, X. Structural Optimisation of Wind Turbine Towers Based on Finite Element Analysis and Genetic Algorithm. *Wind Energy Science Discussions* **2016**, 1–26.
118. Nicholson, J.C. *Design of Wind Turbine Tower and Foundation Systems: Optimization Approach*; The University of Iowa, 2011; ISBN 1-124-74329-4.
119. Ma, H.; Meng, R. Optimization Design of Prestressed Concrete Wind-Turbine Tower. *Sci. China Technol. Sci.* **2014**, *57*, 414–422, doi:10.1007/s11431-013-5442-8.
120. Rebelo, C.; Veljkovic, M.; Simões da Silva, L.; Simões, R.; Henriques, J. Structural Monitoring of a Wind Turbine Steel Tower—Part I: System Description and Calibration. *Wind and Structures* **2012**, *15*, 285.
121. Ansys, A. AQWA User's Manual. *AQWA: Canonsburg, PA, USA* **2020**.
122. InterMoor Available online: https://acteon.com/moorings-anchors/intermoor/ (accessed on 24 October 2023).
123. Jonkman, J.; Butterfield, S.; Musial, W.; Scott, G. *Definition of a 5-MW Reference Wind Turbine for Offshore System Development*; National Renewable Energy Lab.(NREL), Golden, CO (United States), 2009;
124. Crudu, L. Aplicatii Teoretice Si Experimentale in Industria Offshore. *Editura Fundatiei Universitare "Dunarea de Jos"–Galati* **2015**.
125. Isherwood, R.M. Technical Note: A Revised Parameterisation of the Jonswap Spectrum. *Applied Ocean Research* **1987**, *9*, 47–50, doi:10.1016/0141-1187(87)90030-7.
126. Torsethaugen, K. Two Peak Wave Spectrum Model. *Proceedings of the International Conference on Offshore Mechanics and Arctic Engineering - OMAE* **1993**, *2*, 175–180.
127. Yue, M.; Liu, Q.; Li, C.; Ding, Q.; Cheng, S.; Zhu, H. Effects of Heave Plate on Dynamic Response of Floating Wind Turbine Spar Platform under the Coupling Effect of Wind and Wave. *Ocean Engineering* **2020**, *201*, 107103, doi:10.1016/j.oceaneng.2020.107103.
128. Adiputra, R.; Fauzi, F.N.; Firdaus, N.; Suyanto, E.M.; Kasharjanto, A.; Puryantini, N.; Erwandi, E.; Rasgianti, R.; Prabowo, A.R. Roundness and Slenderness Effects on the Dynamic Characteristics of Spar-Type Floating Offshore Wind Turbine. *Curved and Layered Structures* **2023**, *10*, doi:10.1515/cls-2022-0213.
129. Martinez, A.; Iglesias, G. Mapping of the Levelised Cost of Energy for Floating Offshore Wind in the European Atlantic. *Renewable and Sustainable Energy Reviews* **2022**, *154*, 111889, doi:10.1016/j.rser.2021.111889.
130. Kumar, R.; Stallard, T.; Stansby, P.K. Large-Scale Offshore Wind Energy Installation in Northwest India: Assessment of Wind Resource Using Weather Research and Forecasting and Levelized Cost of Energy. *Wind Energy* **2021**, *24*, 174–192, doi:10.1002/we.2566.
131. Bruck, M.; Sandborn, P.; Goudarzi, N. A Levelized Cost of Energy (LCOE) Model for Wind Farms That Include Power Purchase Agreements (PPAs). *Renewable Energy* **2018**, *122*, 131–139, doi:10.1016/j.renene.2017.12.100.
132. SEANSE Planning Criteria for Offshore Wind Energy - North Sea Region Overview. **2019**.
133. Melissas, D.; Vasilakos, N. An Optimal Strategy for Initiating and Efficiently Developing the Floating Offshore Wind Energy Sector in Greece. **2022**.
134. Johnston, B.; Foley, A.; Doran, J.; Littler, T. Levelised Cost of Energy, A Challenge for Offshore Wind. *Renewable Energy* **2020**, *160*, 876–885, doi:10.1016/j.renene.2020.06.030.
135. He, Q.; Chen, H.; Lin, Z.; Dai, X.; Huang, Y.; Cai, W. A Cost-Based Life-Cycle Pricing Model for Offshore Wind Power Plants within China's Carbon Trading Scheme. *Energy Reports* **2022**, *8*, 147–155, doi:10.1016/j.egyr.2022.08.101.

136. Wind Farm Costs – Guide to an Offshore Wind Farm.
137. Bjerkseter, C.; Ågotnes, A. Levelised Costs of Energy for Offshore Floating Wind Turbine Concepts. **2013**.
138. Martinez, A.; Iglesias, G. Multi-Parameter Analysis and Mapping of the Levelised Cost of Energy from Floating Offshore Wind in the Mediterranean Sea. *Energy Conversion and Management* **2021**, *243*, 114416, doi:10.1016/j.enconman.2021.114416.
139. Mostafaeipour, A. Feasibility Study of Offshore Wind Turbine Installation in Iran Compared with the World. *Renewable and Sustainable Energy Reviews* **2010**, *14*, 1722–1743, doi:10.1016/j.rser.2010.03.032.